Molecular mechanism of drug and nascent peptide-dependent ribosome stalling

BY

HARIPRIYA RAMU
B.Pharmacy, The Tamil Nadu Dr. M.G.R. Medical University, 2001
M.S., University of Illinois at Chicago, 2005

DISSERTATION

Submitted as partial fulfillment of requirements for the degree of
Doctor of Philosophy in Pharmacognosy in the Graduate
College of the University of Illinois at Chicago, 2011

Chicago, Illinois

Defense Committee:

Alexander Mankin, Chair and Advisor
Michael Federle
Nancy Freitag, Microbiology and Immunology
Susan Liebman, Biological Sciences
Arnon Lavie, Biochemistry and Molecular Genetics

ACKNOWLEDGEMENTS

I would like to thank my advisor, Dr. Alexander Mankin, whose wonderful guidance and support was instrumental in helping me achieve my goals. I would also like to thank Dr. Nora Vazquez-Laslop for her guidance and extremely helpful discussions on my project. I am grateful to Dorota Klepacki, Dipti Panchal and Anna Ochabowicz who helped me with some of the experiments, and to Sai Lakshmi Subramanian for helping me carry out bioinformatic analysis. I am most thankful to the members of the lab, Jacqueline LaMarre, Krishna Kannan and Pulkit Gupta, especially for their invaluable help towards the completion of my dissertation.

HR

TABLE OF CONTENTS

CHAPTER **PAGE**

TABLE OF CONTENTS (continued)

CHAPTER **PAGE**

LIST OF TABLES

TABLE **PAGE**

LIST OF FIGURES

FIGURE **PAGE**

TABLE OF FIGURES (continued)

FIGURE **PAGE**

LIST OF ABBREVIATIONS

Amp^R	Ampicillin resistant
Erm	Erythromycin resistance methyltransferase
Kan^S	Kanamycin sensitive
MLS_B	Macrolide, lincosamide and streptogramin B
NPET	Nascent polypeptide exit tunnel
PCR	Polymerase chain reaction
PTC	Peptidyltransferase center
rRNA	Ribosomal RNA
r-proteins	Ribosomal proteins
SD	Shine-Dalgarno
tRNA	Transfer RNA
uORF	Upstream open reading frame

SUMMARY

The goal of this work was to characterize the molecular mechanism of drug and nascent peptide-dependent ribosome stalling, which is involved in the regulation of antibiotic resistance genes. Such genes confer resistance to macrolide, lincosamide and streptogramin B antibiotics (MLS_B) and are activated only upon exposure to the macrolide antibiotic. The *ermC* methyltransferase was the first MLS_B gene to be characterized in detail. Extensive analysis of *ermC* regulation has shown that it is regulated by ribosome stalling that occurs during translation of a short, upstream open reading frame (uORF), which encodes a peptide, ErmCL. Such ribosome stalling requires the presence of an inducing antibiotic, such as erythromycin. Translation arrest depends on the sequence of ErmCL as well as the structure of the inducing antibiotic. However, details of the molecular mechanism that underlies translation arrest remained unclear.

Similar to *ermC*, many other MLS_B resistance genes are believed to be regulated by programmed ribosome stalling, though solid evidence is lacking. To gain insight into the mechanism of ribosome stalling, we analyzed upstream regions of various MLS_B resistance genes to identify putative regulatory ORFs. About 30% of the identified genes were found to have uORFs. Comparison of the sequences of the putative peptides encoded by the uORFs revealed that many of them contain common motifs. Based on this, the peptides were grouped into specific classes. Ribosome stalling mediated by peptides belonging to different classes was analyzed experimentally. Representative leader ORFs from each group were translated *in vitro* in the presence or absence of antibiotic. Subsequent primer extension inhibition analysis demonstrated the occurrence of antibiotic-mediated ribosome stalling

during translation of 14 out of 16 tested leader ORFs. The resulting stalled ribosome complexes (SRCs) were found to occur within the conserved sequence motifs in each group of peptides.

Among the leader ORFs that caused strong ribosome stalling, the role of the nascent peptide sequence in translation arrest was investigated in detail for *ermAL1*, *ermBL* and *ermDL* ORFs, which belong to different sequence classes. By alanine scanning, it was determined that the sequence of the four C-terminal amino acids of the nascent peptide is critical for ribosome stalling at *ermAL1* and *ermBL* ORFs, similar to *ermCL*. In case of *ermDL*, the key amino acids were scattered throughout the nascent peptide.

Further analysis of the *ermAL1*-SRC, *ermBL*-SRC and *ermCL*-SRC showed that the identity of the leader ORF codon located in the A-site of the ribosome is highly significant for formation of the stalled complex in case of the first two but not the third leader ORF. Detailed mutational analysis of the stalling peptides encoded in these leader ORFs revealed that the nascent peptide residue located two positions away from the C-terminal peptide residue (-2 position) of the SRC affects the properties of the A-site of the ribosomal catalytic site. When glycine is encoded in the -2 position, the ribosome is in a versatile state, where peptide bond formation can occur with any of the natural amino acids. When alanine is encoded in the -2 position, the A-site is in a selective state, where peptide bond formation can occur only with certain amino acids. The other amino acids serve as poor peptide acceptors and are thus conducive to ribosome stalling. When phenylalanine is encoded in the -2 position, ribosome stalling occurs irrespective of the identity of the A-site codon.

The role of the antibiotic in formation of the SRC was investigated by testing the effect of a variety of MLS_B antibiotics on translation of *ermAL1*, *ermBL* and *ermDL* ORFs. The requirements for ribosome stalling at *ermAL1* were similar to that of *ermCL*, in that, stalling is dependent on the presence and structure of the C3-cladinose sugar attached to the lactone ring of macrolide antibiotics. The same sugar is however dispensable for ribosome stalling at *ermBL* and *ermDL* ORFs; therefore, ketolide antibiotics which were considered non-inducers of some *erm* genes could support SRC formation at *ermBL* and *ermDL* ORFs. 16-membered macrolides, lincosamides and streptogramins B did not cause significant ribosome stalling at any of the leader ORFs. Therefore, antibiotic requirement is different for different stalling scenarios and apparently the structure of the inducing antibiotic has to properly correlate with the sequence of the stalling nascent peptide.

In an attempt to identify ribosomal sensors that recognize the stalling peptide and inducing antibiotics, a number of 23S rRNA nucleotides located in the vicinity of the nascent peptide were mutated and the effects of mutations on ribosome stalling was analyzed *in vitro*. Ribosome stalling controlled by peptides ErmAL1 and ErmCL was abolished by mutations of the rRNA residues U1782 as well as A2062 and A2503 identified previously. Based on this, a signal relay pathway communicating information from the tunnel to the PTC could be envisaged. However, none of the tested rRNA mutations affected formation of SRCs at *ermBL* and *ermDL* ORFs. This result suggests that ErmBL and ErmDL nascent peptides may communicate with the PTC through a pathway different from that activated by ErmAL1 and ErmCL regulatory peptides. Such a pathway could involve the peptidyl-tRNA itself.

Overall, this work revealed that programmed translation arrest occurs during translation of a wide variety of leader ORFs. Important fundamental principles regarding the mechanism of translation arrest were revealed. Specifically, the control of the properties of the PTC A-site by the nascent peptide was discovered which illuminated the molecular mechanism of programmed translation arrest. Our findings could also reveal how nascent peptides that do not require a cofactor molecule can mediate translation arrest. Ultimately, the fundamental ability of the ribosome to respond to specific nascent peptide sequences appears to be a carefully orchestrated mechanism that is carefully exploited by the cell in regulating gene expression.

I. INTRODUCTION

The ribosome is the macromolecular machine that catalyzes the polymerization of amino acids into polypeptides, based on the genetic instructions encoded in messenger RNA. The ribosome interacts with a multitude of ligands and factors to carry out its function. It is composed of two subunits, large and small, which are built of RNA and proteins. Ribosomal RNA accounts for 60% of the weight of the ribosome and plays the central role in protein synthesis. Thus, the peptidyltransferase center of the ribosome (PTC), which is responsible for catalysis of peptide bond formation, is composed only of ribosomal RNA suggesting that the ribosome is actually a ribozyme.

As the catalysis of peptide bond formation between amino acids occurs at the PTC at the interface side of the large ribosomal subunit, the nascent peptide is threaded through a passageway in the large subunit before exiting the ribosome. This path can be viewed in crystallographic and cryo-electron microscopic reconstructions as a hollow space that is enclosed mostly by rRNA. Since virtually all cellular proteins pass through this so-called nascent peptide exit tunnel (NPET), the NPET is usually considered to be neutral to the sequence of the peptide, which would indeed give the tunnel the ability to allow any kind of peptide sequence to pass through it without complications. However, it is now becoming apparent that the tunnel in fact has some bearing on the passage of certain nascent peptides. These nascent peptide sequences, when still within the ribosome have the ability to affect elongation or termination of translation, inducing stalling of the ribosome on its mRNA. This suggests that the NPET may be able to ‘sense’ the nature of the nascent peptide and communicate information to the PTC, causing translation arrest.

This remarkable ability of the ribosome to sense and respond to the nascent peptide sequence is utilized by the cell in regulating the expression of various genes. Examples include genes involved in protein targeting (*yidC2*, *secA*), amino acid metabolism (*tna*) and antibiotic resistance (*ermC*, *ermA*, *ermB*, *ermD*). The expression of these genes is induced only when triggered by a cellular deficiency in the regulated biological process. In case of the antibiotic resistance genes, gene expression is induced when cells are exposed to specific antibiotics. All of these genes are preceded by a shorter, upstream ORF, during the translation of which, the ribosome stalls at a particular codon in response to the cellular signal. This results in isomerization of downstream mRNA structure, causing increased expression of the regulated gene.

The sequence of the peptide encoded in the upstream ORF is critical for ribosome stalling. The residues of the peptide that are most important for stalling are located within the ribosomal exit tunnel, when translation is halted. Intriguingly, most of these regulatory peptides bear no resemblance to each other in terms of structure. Yet, the ribosome has the acuity to sense the unique stalling signal contained within each peptide, by possibly using RNA and protein sensors located in the wall of the NPET. The signal has to then be communicated to the catalytic center, for the appropriate ribosomal response, which requires an arrest of translation. In spite of the significance of this phenomenon, the mechanistic details of ribosome stalling remain unknown. Therefore, in this work, we extensively characterized the stalled ribosome complexes formed at a variety of regulatory leader ORFs to gain further insight into the molecular mechanism of programmed ribosome stalling.

II. LITERATURE REVIEW

A. Introduction

The ribosome uses genetic information encoded in messenger RNAs to polymerize amino acids into polypeptides. Peptide bond formation takes place in the peptidyltransferase center (PTC) located at the interface side of the large ribosomal subunit. As the polypeptide is synthesized, it enters the nascent peptide exit tunnel (NPET) which begins near the PTC, passes through the entire body of the large subunit, and finally emerges at the back of the subunit, on the solvent side [1-3] (Figure 1). In contrast to the original view that the NPET is a passive passage, it is now recognized as a functionally important part of the ribosome.

X-ray structures have revealed the size, shape and composition of the NPET. According to the 2.4 Å resolution structure of the 50S subunit of the archaeon *Haloarcula marismortui* [2, 4], the length of the tunnel is about 100 Å, and its diameter averages ~15 Å. The NPET has two constrictions, one at approximately 25 Å [5] from the entrance and the other at a similar distance from the exit. The constricted portion near the tunnel entrance has a diameter of about 10 Å. Since a protein alpha-helix can barely fit into the tunnel, tertiary folding of the peptide within the ribosome is unlikely. However, there is some experimental evidence that suggests that nascent peptides may acquire specific conformations within the ribosome, at a location near the PTC [6].

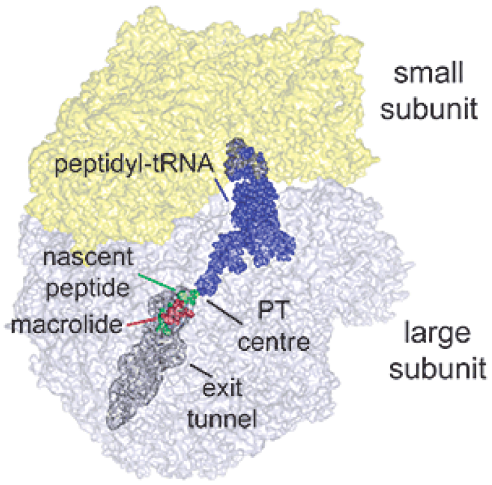

Figure 1. The nascent polypeptide exit tunnel. The small (yellow) and large ribosomal subunits (pale blue) are shown in semi-transparent surface representation [7]. Nascent peptides exit the ribosome through a tunnel (grey). The shape of the exit tunnel was extracted from [2, 3]. The RNA moiety of peptidyl-tRNA is shown in dark blue. The hypothetical position of a 9-amino acid long nascent peptide (green) in the tunnel and the position of erythromycin (red) are shown.

The tunnel walls are paved mainly by nucleotide residues belonging to domains I-V of 23S rRNA, though there are contributions from ribosomal proteins L4, L22 and L39e ('e' indicates archaeal protein that is not found in bacteria and has only a eukaryotic homolog). The components of the tunnel wall are in general polar and non-charged, thereby making the tunnel a suitable, non-sticky conduit for any kind of peptide that passes through it [4]. This could thus explain how the ribosome is equipped to easily translate a great variety of polypeptides encoded in all the genomes. However, in spite of the apparent non-sticky nature of the tunnel, there is now strong evidence that the ribosomal tunnel is capable of sensing the structure of the nascent peptide. In the presence of certain cellular cues, the ribosome is able to functionally respond to specific regulatory nascent peptide sequences, resulting in a temporary arrest of translation. Such 'stalling' of the ribosome at certain regulatory ORFs is involved in control of expression of downstream genes. Examples of bacterial genes

regulated by nascent peptide-dependent ribosome stalling include *secA* [8], genes of the *tna* operon [9], *erm* [10-12], *cat*, *cmlA* [13], *tet(L)* [14] and *tet(M)* [15]. In eukaryotes, genes regulated by uORFs include *Xbp1u* [16], *CPA1* [17], *arg* [18], *AdoMet* [19, 20], reviewed in [21]). In the following sections, we will summarize the main findings about ribosome stalling-mediated regulation of several of these genes.

B. Regulation of *secA* by ribosome stalling

The SecA protein is an ATPase that forms a part of the Sec translocase system which is involved in protein secretion [22]. Expression of *secA* in *Escherichia coli* is regulated by the 170-codon *secM* ORF located immediately upstream of *secA* (Figure 2). While the ribosome binding site (RBS) of *secM* is accessible, the RBS of *secA* is sequestered in the secondary structure of the mRNA. The ribosome that initiates translation of *secM* smoothly polymerizes the first 165 amino acids until the Gly165 codon enters the ribosomal P-site. At this point, the ribosome pauses. If the secretion machinery is active it will 'pull' the N-terminus of the SecM nascent peptide, which has already emerged from the exit tunnel, and cause the release of the ribosome from the paused state; in this case, no activation of *secA* expression occurs. However, under suboptimal secretion conditions, the ribosome remains stalled for an extended time at codon 165 of *secM*. Presence of the stalled ribosome induces a conformational switch of mRNA, which favors translation of the *secA* gene [8, 23].

A

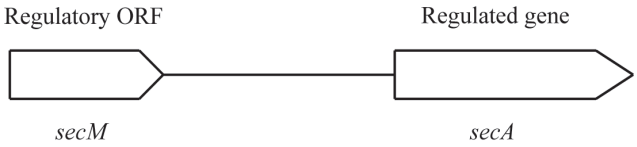

B

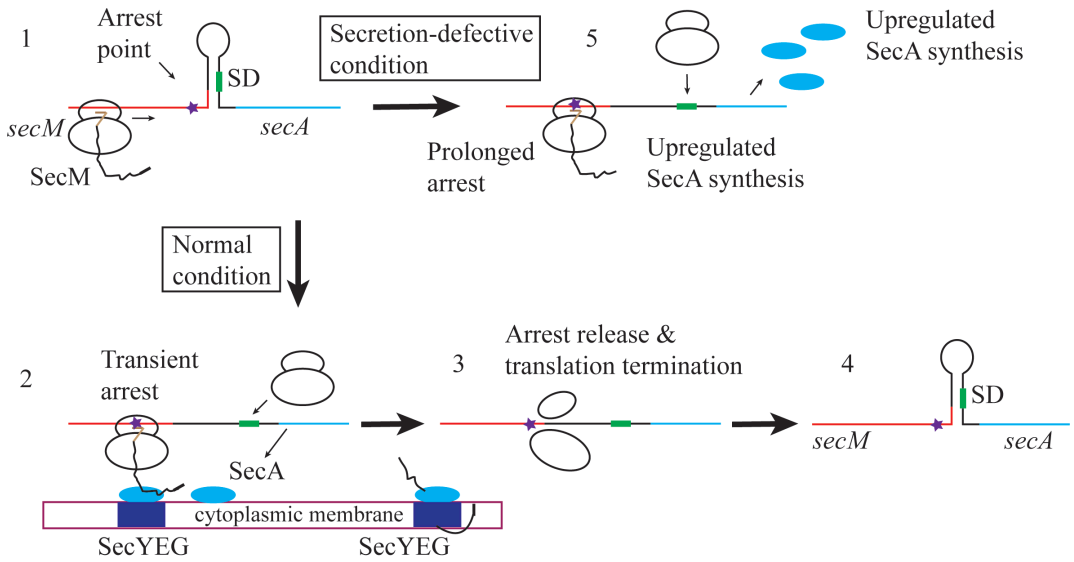

C

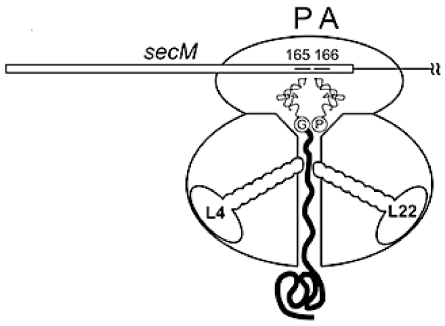

Figure 2. Translational regulation of *secA*. A. The *secA* gene is regulated by a uORF encoding a 170 aa long peptide, SecM. B. Regulation of *secA* [24] (1). Ground state of the *secM-secA* mRNA. The SD sequence of *secA* is sequestered in mRNA secondary structure. (2) During polymerization of the SecM peptide, the ribosome stalls transiently on the mRNA. This causes a change in the mRNA secondary structure making the SD sequence of *secA* accessible, resulting in *secA* translation. (3) The ribosome dissociates subsequently and (4) the mRNA returns to its ground state. (5) During a secretion defect in the cell, the arrest of the ribosome is prolonged thus upregulating SecA synthesis. C. Stalled ribosome complex (SRC) formed at the *secM* ORF [7]. In the SRC, the codons located in the ribosomal P and A sites are indicated by numbers. The tRNAs present in the P and A sites are shown as ribbons and the amino acids positioned in the PTC are circled. Nascent peptide is indicated by a thick, black line.

Stalling of the ribosome at the *secM* ORF is dictated by the sequence of the C-terminal segment of the nascent polypeptide F_{150}XXXXWIXXXXGIRAG$_{165}$. Critical for stalling are the identities of the five C-terminal amino acids, GIRAG$_{165}$, as well as that of F_{150}, W_{155} and I_{156}; the spacing between the essential residues is also important [8, 25]. Secondly, the identity of the A-site proline codon is most important – mutation of this codon to alanine abolishes stalling. Yet, in the stalled complex, the SecM nascent peptide is esterified to $tRNA^{Gly}$ located in the ribosomal P-site [26-28]. In approximately half the amount of these stalled complexes, Pro-$tRNA^{Pro}$ is present in the A-site of the SRC, suggesting that it somehow contributes to stalling in spite of not being incorporated into the nascent peptide [28]. But, in the remaining complexes, Pro-$tRNA^{Pro}$ is not observed in the A-site, perhaps due to limiting amounts of $tRNA_2^{Pro}$ in the cell, under conditions of SecM-overexpression [26]. This makes it unclear if the presence of Pro-$tRNA^{Pro}$ in the A-site is essential for formation of a stable, stalled complex. Proline is known to serve as a poor acceptor of the nascent peptide [29]. This may explain why a proline codon has been selected evolutionarily to be positioned in the A-site of the *secM*-SRC, making it most conducive to support SRC formation, compared to the other amino acids.

When the stalling sequence of the SecM nascent peptide is synthesized by the ribosome, it adopts a special compact conformation in the exit tunnel [30] which is likely required for engaging the appropriate tunnel sensory elements. The stalling signal, whose nature is currently unknown, is then communicated to the PTC [31].

C. Regulation of *tna* by ribosome stalling

Activation of tryptophan catabolizing gene *tnaA* and the permease *tnaB* encoded in the *E. coli tna* operon depends on formation of a stalled ribosome complex at the leader

regulatory ORF, *tnaC* (Figure 3) [9, 32]. When tryptophan concentration in the cell is high, the ribosome halts translation at the last sense codon of *tnaC*. The stalled ribosome blocks access of the transcription termination factor Rho to its recognition site, thus allowing continuation of transcription of the downstream genes [33]. Stalling of the ribosome at the *tnaC* ORF is nascent peptide-dependent. Similar to SecM, both the nature of the critical amino acid residues and the spacing between them are important. The essential residues of the TnaC stalling sequence, $W_{12}XXXD_{16}XXXXXXXP_{24}$, are at the C-terminal segment of the 24-amino acid long nascent peptide esterified to $tRNA^{Pro}$ in the P-site of the stalled ribosome. Formation of the stalled complex depends on binding of a tryptophan molecule to a ribosomal site whose precise location remains unknown [32, 34, 35]. In the *tnaC* ORF of *E. coli*, the Pro_{24} codon, at which stalling takes place, constitutes the last sense codon. Therefore, in the *E.coli tnaC*-stalled ribosome complex (SRC), it is the peptide release activity of the PTC that is inhibited rather than peptide bond formation. However, in *Proteus vulgaris*, the Pro codon at which stalling occurs is followed by two additional sense codons, indicating that similar to SecM, TnaC is capable of arresting translation elongation as well (Cruz-Vera et. al. 2009).

A

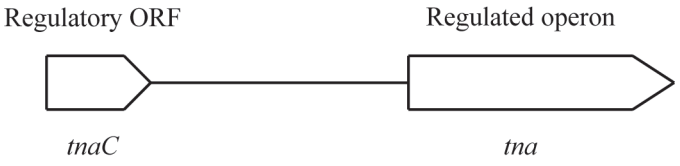

B

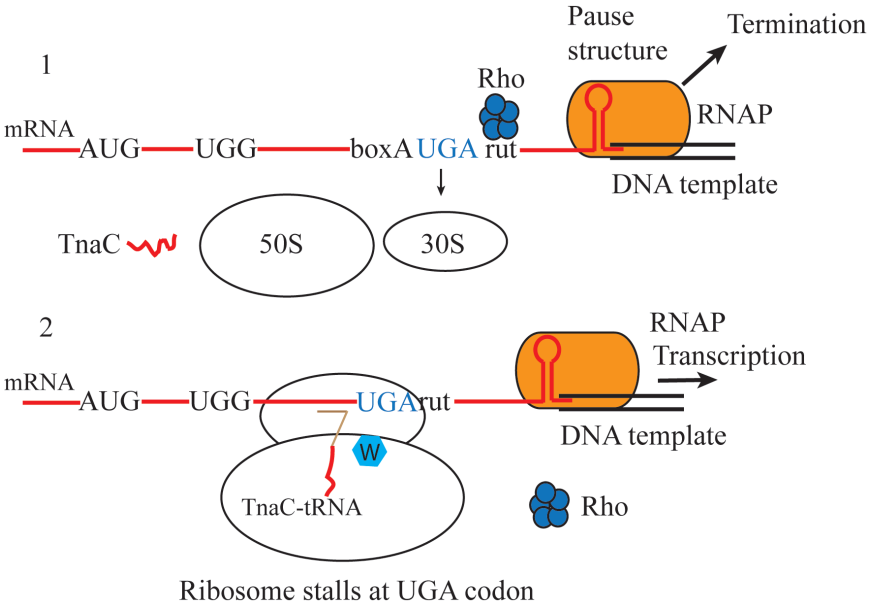

C

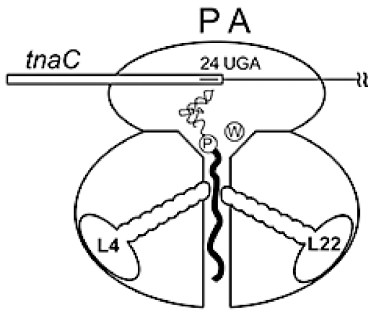

Figure 3. Regulation of the *tnaA* operon by transcriptional attenuation. A. The *tna* operon is regulated by a uORF encoding a 24 amino acid peptide, TnaC. B. In the absence of inducing levels of tryptophan, the ribosome dissociates on encountering stop codon of *tnaC*. Rho factor has access to its binding site and causes transcription termination. (2) In presence of inducing levels of tryptophan, the ribosome stalls at the stop codon preventing access of transcription termination site to Rho factor. Transcription of *tnaA* and *tnaB* continues [36]. C. Stalled ribosome complex (SRC) formed at the *tnaC* ORF [7]. In the SRC, the codons located in the ribosomal P and A sites are indicated by numbers. The tRNA present in the P site is shown as ribbon and the amino acid positioned in the PTC is circled. Nascent peptide is indicated by a thick, black line. The binding site of tryptophan (W) is not known.

D. Regulation of *ermC* by ribosome stalling

Erm-type methyltransferase enzymes modify A2058 in 23S rRNA located in the binding site of macrolide, lincosamide and streptogramin B-type antibiotics (MLS_B). N_6 mono and di-methylation of A2058 prevents binding of these drugs and results in MLS_B resistance [37]. The best-studied example of this class of enzymes is ErmC. Expression of *ermC* in *Staphylococcus aureus* and other bacteria is induced by macrolide antibiotics and is controlled by a 19-codon leader ORF, *ermCL*, located 60 bp upstream of *ermC* [38, 39] (the leader ORF is named similar to the main resistance gene of the operon followed by the suffix 'L' for leader) (Figure 4).

A

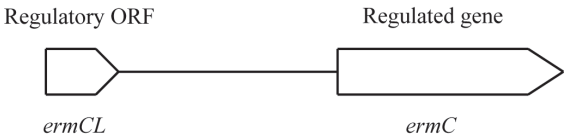

B

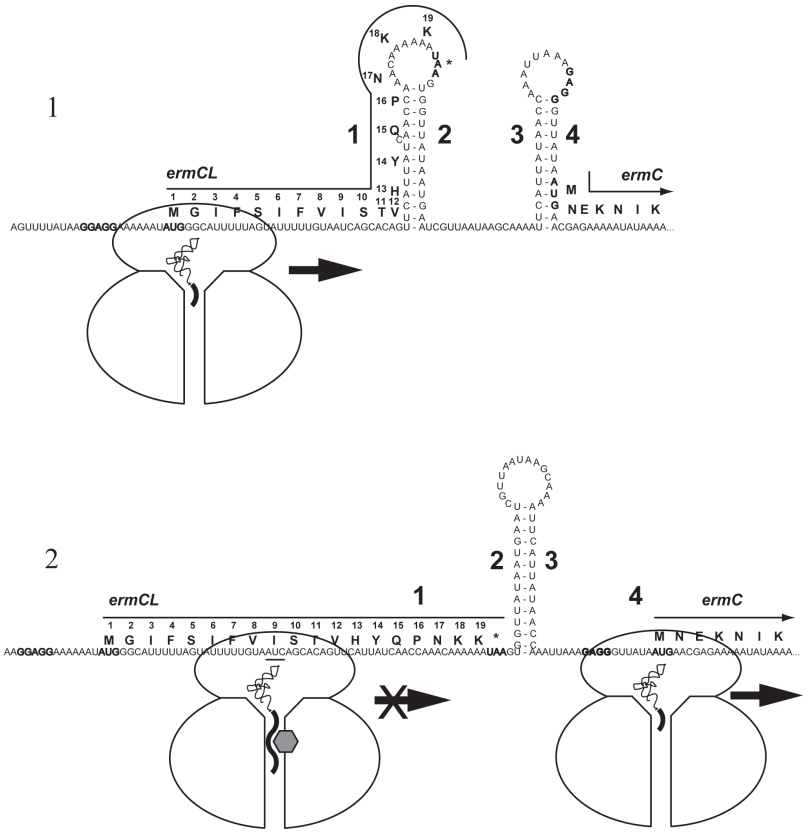

C

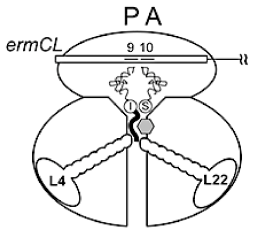

Figure 4. Regulation of *ermC* by translation attenuation. A. The *ermC* gene is regulated by ErmCL [7]. B. Regulation of *ermC* [7]. (1) In the absence of inducing antibiotic, the RBS of *ermC* is sequestered in mRNA secondary structure. The leader ORF (*ermCL*) is translated. (2) In the presence of inducing antibiotic (gray hexagon), drug-bound ribosome stalls at *ermCL*-codon 9. This causes a change in mRNA conformation, increasing translation of *ermC*. C. The SRC formed at the *ermCL* ORF [7]. Codons located in the P and A sites are indicated by numbers. The tRNAs are shown as ribbons and the amino acids positioned in the PTC are circled. Nascent peptide is indicated by a thick, black line.

In the absence of inducing antibiotics, *ermCL* is constitutively translated while translation of *ermC* is attenuated because its RBS is sequestered in a stem-loop structure. For activation of *ermC* expression, the structure of the mRNA regulatory region must be rearranged into an alternative, 'induced' conformation in which the translation initiation region of *ermC* is released. Such rearrangement may occur when the ribosome sequesters strand 1 of the first hairpin, which will allow strand 2 to re-pair with strand 3 and liberate strand 4 which contains the *ermC* RBS. It has been shown that the ribosome unwinds mRNA at a distance of approximately eight nucleotides downstream from the P-site codon [40]. Therefore, the induced conformation of the mRNA is favored when the ribosome is positioned at codons 9 through 17 of *ermCL*. During unimpeded translation, the ribosome polymerizes 10-20 amino acids per second [41] which means that it would need less than a second to transit this mRNA segment. This short time interval could be insufficient for switching the conformation of mRNA and initiating translation of *ermC*. Hence, halting the ribosome for a longer period of time at the appropriate position on the *ermCL* ORF is probably critical for the induction of *ermC* expression. Such stalling occurs in the presence of an inducing antibiotic (erythromycin or a similar drug) and critically depends on the sequence of the ErmCL nascent peptide [10, 42]. Since the work described in this work is more closely related to ribosome stalling at *ermCL*, we will discuss it in more detail.

1. Role of the nascent peptide in formation of the stalled ribosome complex at the *ermCL* ORF

In the presence of the inducing antibiotic, the ribosome stalls at the ninth codon of the *ermCL* ORF [12, 43, 44] (Figure 4). In the stalled complex, $tRNA^{Ile}$, positioned in the ribosomal P-site, is esterified with the nine amino acid long nascent peptide,

fMGIFSIFVI$_9$ [12]. Amino acid substitutions within the IFVI sequence dramatically decrease the efficiency of SRC formation, indicating that the C-terminal segment of the nascent peptide is essential for ribosomal stalling [12, 45, 46] and is likely critically involved in pivotal interactions with the sensory elements of the exit tunnel. While polymerization of the IFVI amino acid sequence of ErmCL is a prerequisite for the formation of the SRC, reaching the ninth codon of the *ermCL* ORF is not an easy task for the drug-bound ribosome. Erythromycin and other 14 and 15-membered macrolides are presumed to interfere with protein synthesis by promoting peptidyl-tRNA drop-off at the early rounds of translation [47, 48]. The loss of peptidyl-tRNA is most prominent when the nascent peptide reaches a length of six to eight amino acid residues [49, 50]. Therefore, only a fraction of the antibiotic-bound ribosomes that start translation of the *ermCL* ORF have a chance to reach the ninth codon and complete assembly of the IFVI$_9$ stalling sequence. Moving the IFVI segment farther away from the N-terminus of the peptide would hence be expected to further decrease the chances of the ribosome to complete translation of the IFVI stalling sequence. Indeed, adding one, two or three Ala codons at the beginning of the *ermCL* ORF prior to the IFVI-coding sequence impedes formation of the SRC [12]. Unexpectedly, Bechhofer and co-workers reported erythromycin-dependent SRC formation when eight additional codons were inserted upstream from the IFVI-coding sequence of *ermCL* [46]; this observation could be reconciled with the mechanism of erythromycin action if it is assumed that specific long amino acid sequences could be polymerized by the erythromycin-bound ribosome. This possibility has been recently demonstrated in our laboratory (Kannan, Vazquez-Laslop and Mankin, in preparation).

If premature peptidyl-tRNA drop-off interferes with drug-dependent SRC formation, one would expect that moving the critical stalling sequence closer to the N-terminus of the ErmCL peptide would increase the fraction of the ribosomes that can complete the assembly of the IFVI sequence and form the SRC. Paradoxically, however, deleting one, two or three non-essential *ermCL* codons that precede the IFVI-coding sequence progressively reduces the efficiency of SRC formation [12, 44, 46]. Thus, drug-dependent stalling calls not only for the presence of a specific amino acid sequence at the C-terminus of the nascent peptide, but also that the nascent peptide reaches a certain length. Such length requirement suggests that the peptide must engage not only the PTC-proximal site(s), but also more distant sensory elements of the tunnel for the stalled complex to form.

2. The role of the antibiotic in formation of the *ermCL*-SRC

The presence of the antibiotic is critical for stalling of the ribosome at *ermCL* and, thus, for *ermC* induction. Although methylation of A2058 confers resistance to three groups of antibiotics (MLS_B) whose binding sites overlap in the exit tunnel of the ribosome, only 14 and 15-membered lactone ring macrolides efficiently activate *ermC* expression [44, 51, 52]. The ability of antibiotics to induce ribosome stalling depends on the structure of the drug (Figure 5) and is determined by the mode of binding and the mechanism of antibiotic action.

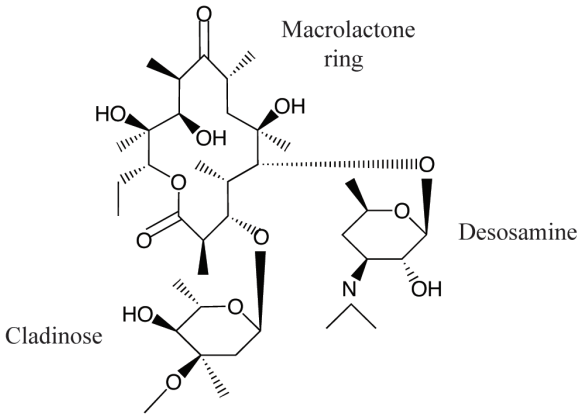

Figure 5. Structure of the macrolide, erythromycin. Erythromycin contains a 14-membered macrolactone ring. The cladinose sugar, attached at the C3 position, is essential for ribosome stalling at the *ermCL* ORF. Erythromycin also contains a desosamine sugar in the C5 position.

Importantly, the function of the antibiotic as a stalling co-effector is clearly different from its function as an inhibitor of translation. For example, lack of the C3-cladinose, which does not prevent macrolides from inhibiting protein synthesis [53, 54], cripples the inducing efficiency of these drugs [55, 56]. Not only the replacement of cladinose sugar with other groups of similar size, but also small alterations in the structure of the cladinose residue have a profound effect on the drug's activity as an *erm* inducer or stalling cofactor [52, 53, 57]. In the structure of the nine amino acid long-ErmCL nascent peptide modeled into the erythromycin-bound 50S ribosome (Figure 6), the critical IFVI segment of the peptide is positioned in virtual contact with the cladinose moiety of the antibiotic [12].

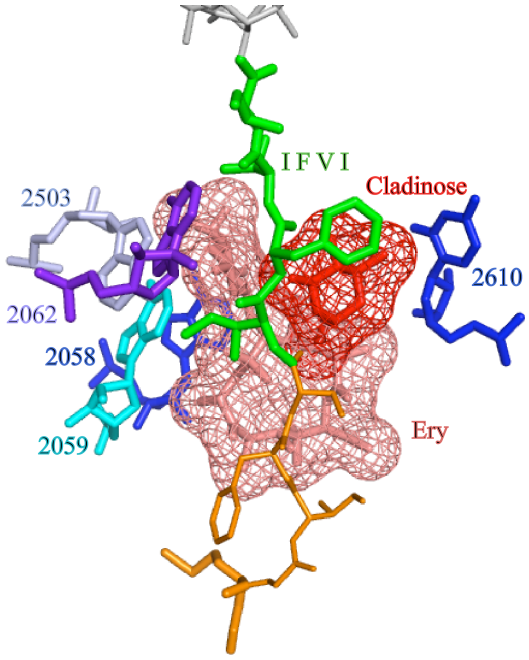

Figure 6. Structure of ErmCL nascent peptide modeled into the erythromycin-bound ribosome. The ErmCL nascent peptide is shown as sticks, with the N-terminus colored orange and the critical IFVI sequence of the C-terminus colored green. The CCA end of peptidyl-tRNA is indicated in grey. Erythromycin (Ery) is shown as salmon-colored sticks and mesh, with the C3-cladinose colored red. rRNA residues that are important for sensing the nascent peptide or the antibiotic are shown [57, 58].

This suggests that precise interactions between the C3-cladinose and the nascent peptide may be important for inducing SRC formation. Mutations in *ermCL* differentially affect induction by structurally different antibiotics, suggesting that interactions of the nascent peptide with dissimilar antibiotics could be different. For example, induction of *ermC* by the 14-membered macrolides erythromycin and megalomycin is similarly affected by *ermCL* mutations [44]. The same mutations however, have a different effect on induction by the lincosamide, celesticetin.

One of the central questions about the role of the antibiotic in ribosome stalling is whether the molecule serves as a mere steric block or if its structural features directly contribute to SRC formation, by establishing specific atomic contacts with the ribosome and

the nascent peptide. The precise structural requirement in terms of the cladinose side chain of macrolides and its close proximity to the critical IFVI segment of ErmCL strongly argue in favor of the latter possibility [12]. Thus, it was shown that mutation of an rRNA nucleotide, C2610, significantly reduces erythromycin-dependent *lacZ* induction and ErmCL-SRC formation [57]. This nucleotide is positioned in the wall of ribosomal exit tunnel, in direct contact with the 3''-methyl group of the cladinose (Figure 6). C2610 does not appear to come into direct contact with the peptide, and is more likely to be a part of the ribosome sensory system used to detect structure of the inducing antibiotic.

Two other rRNA nucleotides, A2058 and A2059, form a part of the macrolide binding site in the ribosomal exit tunnel (Figure 6). These nucleotides are therefore also ideally positioned to act as antibiotic sensors. These residues form an adenine stack with m^2A2503, whose mutation to G, abolished *ermCL*-SRC formation [59]. The post-transcriptional modification carried by A2503 (methylation of the C2 atom) is essential for *ermC* induction, accentuating the possibility that m^2A2503 plays a special role in mediating the response of the ribosome to the nascent peptide and antibiotic. Since m^2A2503 is not positioned to directly interact with the nascent peptide, it is more likely to mediate communication between sensors in the drug binding site (A2058 and A2059) and the PTC.

Unlike 14 and 15-membered macrolides, the other MLS_B antibiotics whose ribosome binding sites overlap with that of erythromycin, are incapable of inducing *ermC*. Different reasons account for this. The lincosamides and 16-member macrolides (Figure 7) are not conducive to SRC formation because they promote peptidyl-tRNA drop-off when the nascent peptide is only two to four amino acids long [49].

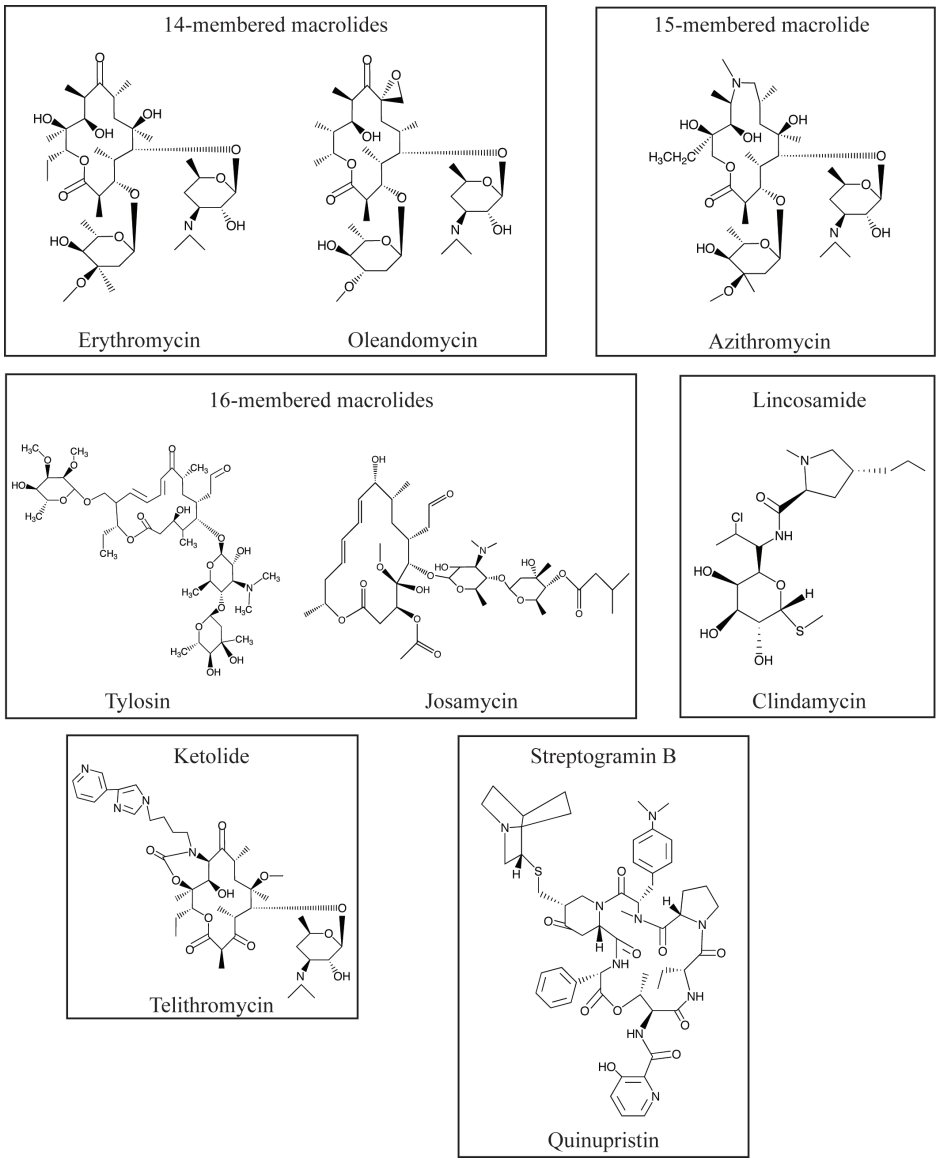

Figure 7. Structures of different antibiotics of the MLS_B group.

These drugs give the ribosome little chance to reach the ninth codon of *ermCL* and generate the $IFVI_9$ sequence required for stalling. In contrast, streptogramins B do allow for synthesis of nascent peptides comparable in length to those produced in the presence of erythromycin [49]; yet they do not induce *ermC* expression. The position of a streptogramin B molecule in the exit tunnel and molecular interactions of the drug with the ribosome and

the nascent peptide are notably different from those of macrolides [58, 60]; this difference possibly accounts for the inability of streptogramins to promote formation of a stable SRC.

E. Molecular mechanism of the ribosomal response involved in programmed translation arrest at *ermCL*, *secM* and *tnaC* ORFs

Formation of the SRC requires two specific actions from the ribosome: one, sensing the nascent peptide, and two, responding to the regulatory nascent peptide by halting translation.

1. Sensing of the nascent peptide by the ribosome

In the SRC formed at the *ermCL* ORF, the critical sequence of the stalling peptide is positioned in the upper chamber of the exit tunnel (Figure 6), which is formed by residues belonging to domains II and V of 23S rRNA [4]. Some of these nucleotides are involved in recognition of the nascent peptide. The 23S rRNA residue A2062 plays a special role in sensing the ErmCL nascent peptide and establishing the arrested state of the ribosome. Positioning of A2062 in the tunnel allows for its direct interaction with the critical IFVI residues of the ErmCL stalling peptide. Crystallographic studies have shown conformational flexibility of A2062, whose base can either lie flat against the tunnel wall or project into the tunnel lumen [61]. The immediate neighbors of A2062 (C2063 and G2061) play an important role in formation of the peptidyltransferase active site [62, 63]. Thus, A2062 is optimally positioned to sense the nature of the nascent peptide and trigger the functional response of the ribosome by allosterically altering the conformation of the PTC. Indeed, direct studies showed that mutations of A2062 completely eliminate the ribosome's ability to stall at the *ermCL* ORF [12]. Several other nearby rRNA residues, such as A2058, U2609 or the loop of

helix 35, have been implicated in sensing SecM and TnaC stalling peptides [8, 35, 64, 65]. Since most of these rRNA residues form the macrolide binding site in the ribosome, they are also inevitably involved in sensing the structural cues for the drug-dependent SRC formation at the *ermCL* ORF. The importance of two other nucleotides, m^2A2503 and C2610 for formation of the *ermCL*-SRC has already been discussed in the previous section.

Nucleotides G2583 and U2584, two highly conserved residues located in the PTC, lie in close vicinity of the 3' ends of P and A-site tRNAs and could influence their positioning [4, 66]. Mutations of these two residues affect induction mediated by TnaC-$tRNA^{Pro}$, suggesting that these nucleotides could play a role in sensing TnaC-$tRNA^{Pro}$ [67]. The role of these nucleotides in sensing ErmCL is not known.

The constricted portion of the ribosomal exit tunnel is formed by the loops of two proteins, L4 and L22 (see Figure 4C for a schematic representation) [2]. The flexible β-loop of L22 projects into the tunnel and can interact with a nascent peptide segment 8-12 amino acids away from the PTC [58, 68]. Mutations in the L22 β-loop affect erythromycin-dependent ribosome stalling at the *ermCL* ORF, as well as SRC formation at *secM* and *tnaC* [8, 12, 64, 65]. Mutations in L4 affect induction mediated by *crb*, which is a nine-codon leader ORF mediating chloramphenicol-dependent induction of *cmlA* [65]. One of the L4 mutations also affected SecM-mediated induction. This shows that both the ribosomal proteins L4 and L22 are involved in the stalling mechanism.

The identification of several rRNA nucleotides whose mutations affect nascent peptide-mediated induction and/or ribosome stalling provides some clues as to how the ribosome recognizes and responds to regulatory sequences. Cryo-EM analysis of the *E.coli* ribosome stalled at the *tnaC* ORF suggests that the nascent peptide adopts a distinct position

in the tunnel [69]. Such a conformation must be required to present the critical residues of the peptide to the sensors in the tunnel wall. The ribosome is likely to employ different ways (though some of the sensors may be common) to detect the structures of different nascent peptides and ultimately communicate a signal to the PTC to halt translation. How the ribosome catalytic center may respond to the nascent peptide is explored below.

2. Ribosomal response to the nascent peptide

When the macrolide-bound ribosome that translates the *ermCL* ORF adds Ile_9 to the growing amino acid chain and fMGIFSIFVI-$tRNA^{Ile}$ is placed in the P-site, a specific and possibly drastic change occurs in the conformation of the ribosome, which precludes continuation of translation. Although the details of the translation arrest mechanism are virtually unknown, the proximity of the tunnel sensory elements to the PTC makes the latter the most likely recipient of the stalling signal. Indeed, the ribosome stalled at *ermCL* truncated at Ile9 is unable to catalyze peptide bond formation with puromycin, which behaves as an A-site substrate of peptidyltransferase [12]. In the ribosome stalled at the *secM* ORF, majority of the peptidyl-tRNA is present as $SecM_{165}$-$tRNA^{Gly}$, which is also resistant to puromycin, showing that the stalled ribosome is defective in catalyzing peptide bond formation [28]. However, it should be noted that prolonged incubated of the translation reaction did result in the transfer of a small percentage of $SecM_{165}$ to Pro-$tRNA^{Pro}$ in the A-site [28]. In case of *tnaC*, two different scenarios have been observed depending on the sequence of TnaC. In *E.coli*, release factor-mediated hydrolysis of the peptidyl-tRNA ester bond (termination of translation) at the final proline codon is inhibited [34]. Whereas, in *P.vulgaris*, the proline 24 codon, at which stalling occurs, is followed by two lysine codons. In this case, peptide bond formation between TnaC-$tRNA^{Pro}$ and lysine is inhibited in the

SRC [70]. Thus, it appears that TnaC is capable of inhibiting both activities of the PTC from within the exit tunnel.

This inability of the PTC to carry out its functions is likely to result from conformational changes triggered in response to the presence of the stalling peptide in the exit tunnel. What these changes are remain to be explored. Alterations in the structure and activity of other functional centers of the ribosome may also contribute to SRC formation. For instance, in the Cryo-EM reconstruction of the *secM*-SRC, conformational changes were observed in various functional regions of the ribosome [27], although more recently, the conclusions of this paper were questioned by another Cryo-EM reconstruction [31]. At the same time, in the *tnaC*-SRC, such a wide range of changes in ribosome structure was not observed [69]. While many contacts were observed between the nascent peptide and rRNA residues, no specific structural changes were observed in the tunnel. Instead, two nucleotides in the PTC, A2602 and U2585, were present in conformations that would be incompatible with binding of the release factor, which is required for termination of translation. While these data are beginning to provide some insight, how the stalling signal is communicated from the tunnel to the PTC remains unclear, accentuating the need for higher resolution structures of the SRC.

F. Regulation of other macrolide resistance genes

The family of *erm* genes is diverse and *ermC* represents only one of its members [71]. Several other *erm* genes are also regulated by programmed ribosome stalling.

The *ermA* gene is found in Gram-negative (*Aggregatibacter, Bacteroides*) as well as Gram-positive (*Enterococcus, Staphylococcus, Streptococcus* etc) bacteria. The *ermA* gene

contains two upstream ORFs, *ermAL1* and *ermAL2*, which code for peptides containing 15 and 19 amino acids, respectively (Figure 8, Table I) [72, 73].

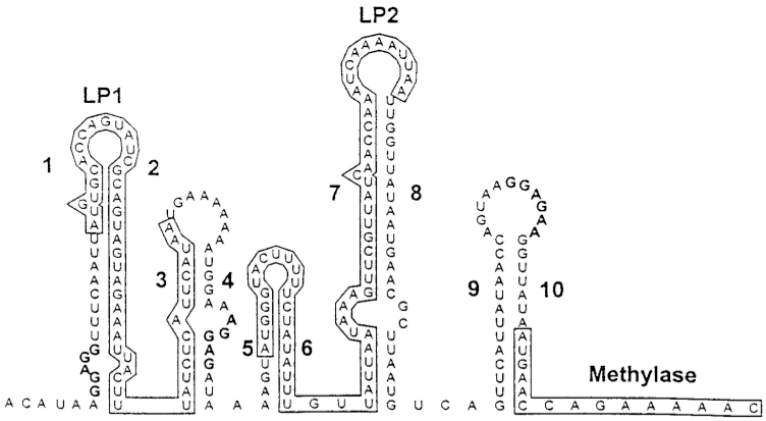

Figure 8. Predicted secondary structure of the *ermA* leader region. The RBS of *ermAL2* and *ermA* are normally sequestered in secondary structure. A cascade of ribosome stalling events, occurring at *ermAL1*, followed by *ermAL2*, is required for translation of ermA [74, 75].

TABLE I

SEQUENCES OF LEADER PEPTIDES OCCURRING UPSTREAM OF MACROLIDE RESISTANCE GENES

Leader peptide	Sequence	Genebank #
ErmAL1	MCTSIAVVEITLSHS	X03216
ErmAL2	MGTFSIFVINKVRYQPNQN	X03216
ErmBL	MLVFQMRNVDKTSTILKQTKNSDYVDKYVRLIPTSD	K00551
ErmCL	MGIFSIFVISTVHYQPNKK	V01278
ErmDL	MTHSMRLRFPTLNQ	M29832
ErmGL1	MNKYSKRDAIN	M15332
ErmGL2	MGLYSIFVIETVHYQPNEK	M15332
ErmSL	MSMGIAARPPRAALLPPPSVPRSR	M19269
ErmVL	MAANNAITNSGLGRGCAHSVRMRRGPGALTGPGSHTAR	U59450
ErmXL	MLISGTAFLRLRTNRKAFPTP	M36726
Erm38L	MSITSMAAPVAAFIRPRTA[1]	AY154657
MsrSAL	MTASMRLK	AB016613
MsrD	MYLIFM	AF274302
EreAL	MLRSRAVALKQSYAL	AF0099140

[1]Translation could initiate from the 1st or the 2nd methionine

Analysis of the *ermA* leader region led to the prediction of a secondary structure of the mRNA, invoking a translation attenuation model to explain the regulation of *ermA*. Accordingly, the ribosome binding sites of *ermAL2* and *ermA* are normally sequestered (Figure 7). Ribosome stalling at *ermAL1* is predicted to result in translation of *ermAL2*, while subsequent stalling at *ermAL2* will result in expression of *ermA* [73, 74, 76]. The sequence of the ErmAL2 peptide is almost identical to that of ErmCL (Table I), suggesting that there is a

strong possibility that ribosome stalling occurs during translation of *ermAL2*. Indeed, spontaneous deletions that remove parts of *ermAL2* result in constitutive expression of *ermA* [72, 73, 77]. On the other hand, the sequence of the peptide encoded by *ermAL1* is considerably different, making it difficult to predict the site of ribosome stalling. In one of the mutant variants of *ermA* identified in *S.aureus*, an 83 bp deletion that encompassed *ermAL2* and its translation initiation region still resulted in inducible *ermA* expression, proving that *ermAL1* is also involved in regulation of the methyltransferase [74]. The wild-type *ermA* is inducible by the 14-membered macrolide erythromycin, but not by 16-membered macrolides, lincosamides and streptogramins [73].

The *ermB* methyltransferase is extremely widespread, having been detected in *Aggregatibacter, Acinetobacter, Bacillus, Enterococcus, Clostridium, Staphylococcus,* etc [71]. *ermB* is generally inducible by all antibiotics of the MLS_B group, while variants, some of which are constitutive have also been reported [43, 78, 79]. The exact secondary structure of the *ermB* leader region is not clear, complicated by the fact that there are at least 13 complementary repeat sequences [43, 79]. One of the predicted structures is shown in Figure 9.

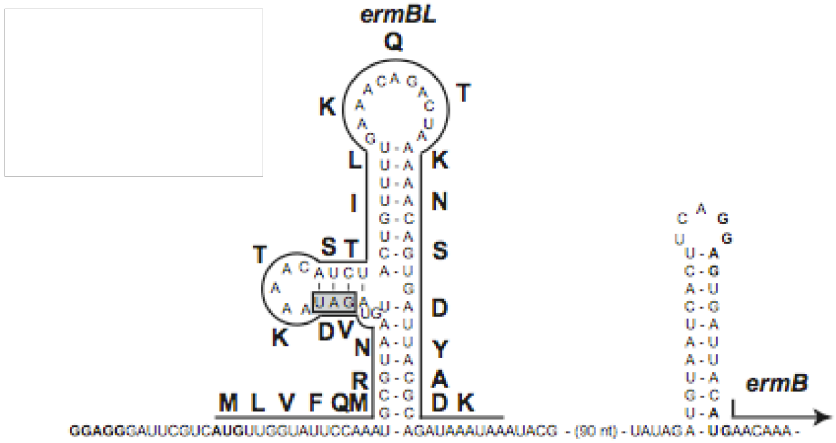

Figure 9. Predicted secondary structure of the leader region of the *ermB* operon [75].

Induction of *ermB* depends on translation of the 27-codon leader ORF *ermBL* [43] (Table I). Nonsense mutations at codon 10, but not at 11, 12 or 13 abolish *ermB* inducibility [11] suggesting that the ribosome stalls at the 10th codon of *ermBL*. In the putative nascent peptide of the *ermBL* SRC, the sequence of five C-terminal amino acid residues, MRNVD, appears to be essential for stalling since the mutations at the corresponding codons prevent *ermB* induction [11].

The *ermD* methyltransferase is found in *Salmonella* and *Bacillus*, and is inducible by erythromycin and oleandomycin [80]. The leader region contains an ORF that encodes a 14 amino acid-long peptide (Table I, Figure 10) [38].

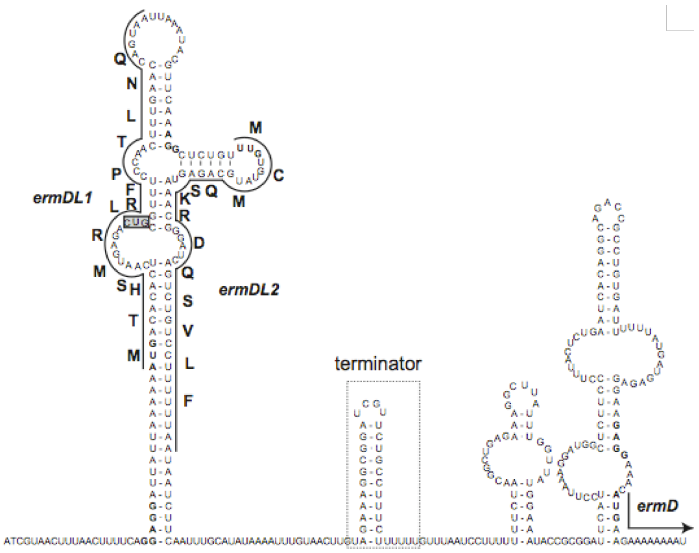

Figure 10. Predicted secondary structure of the *ermD* leader region [75, 81, 82].

Evidence for involvement of this leader ORF in *ermD* induction comes from the fact that nonsense mutations or deletions in the leader ORF result in constitutive *ermD* expression [38, 82]. Mutations at codons 4 to 7 of *ermDL* negatively affect *ermD* induction suggesting that this sequence could be important for stalling [83]. Also, the nonsense mutation at codon 7 resulted in high level, constitutive *ermD* expression, leading to the prediction that the ribosome stalls with codon 7 in the A site.

The mechanism of regulation of *ermD* is controversial, due to conflicting data. According to one group, regulation of *ermD* is believed to occur through transcriptional attenuation [82]. Evidence for this comes from the observation that synthesis of the full-length *ermD* mRNA was induced only in the presence of erythromycin. In the absence of erythromycin, only a short mRNA fragment that corresponds to a predicted transcription terminator located at nucleotide 210 was observed. In contrast, another group observed that the transcription of the full-length *ermD* mRNA was not always dependent on erythromycin

[81]. Therefore, they predicted that *ermD* is regulated by translational attenuation. Additionally, the latter group also observed that a second leader peptide is translated, even thought it carries a relatively weak Shine-Dalgarno sequence. This led to the suggestion that two leader ORFs are involved in *ermD* regulation, similar to *ermA*. The ribosome stalling site at the second leader ORF is yet to be determined.

Apart from the *erm* genes mentioned above, there are at least 30 other types of macrolide resistance *erm* methyltranferases, 18 genes that encode drug-efflux pumps (e.g. *msrA*, *mefA*, *lsa*) and 20 genes that cause resistance by drug-inactivation (e.g. *ereA*) [71, 84]. Many of these genes are thought to be drug-inducible and contain short, putative regulatory ORFs upstream (Table I). These features suggest that ribosome stalling may be the general key mechanism involved in regulation of the majority of macrolide-resistance genes, although strong experimental evidence is lacking.

G. Conclusion

Programmed ribosome stalling illustrates a fundamental ability of the ribosome to monitor the structure of the nascent peptide. Drug-dependent ribosome stalling is involved in regulation of antibiotic resistance genes, while drug-independent stalling is involved in regulation of various housekeeping genes. Analysis of putative regulatory peptides encoded in the uORFs of inducible antibiotic resistance genes shows that they are different in their sequences. It is assumed that most macrolide resistance genes originated from antibiotic producers; therefore, it is likely that the regulatory sequences have been optimized to respond to a specific inducer. In fact, mutations in the leader ORFs alter the spectrum of antibiotic inducers [44, 79, 85]. However, how the ribosome recognizes such disparate peptide sequences and potentially different antibiotic structures is not yet understood. It is clear

though that the ribosome responds appropriately to regulatory sequences by arresting translation. The nature of the signal that is communicated from the exit tunnel to the PTC in order to cause ribosome stalling, as well as the changes that occur in the PTC are unknown. In this work, our goal was to gain insight into the molecular mechanism of programmed ribosome stalling by analyzing the stalled ribosome complexes formed at various regulatory ORFs that regulate expression of macrolide resistance genes.

III. MATERIALS AND METHODS

A. Identification of ribosome stalling sites by toeprinting

1. Preparation of DNA templates

DNA templates containing leader peptide coding sequences were generated by PCR as shown below (Figure 11).

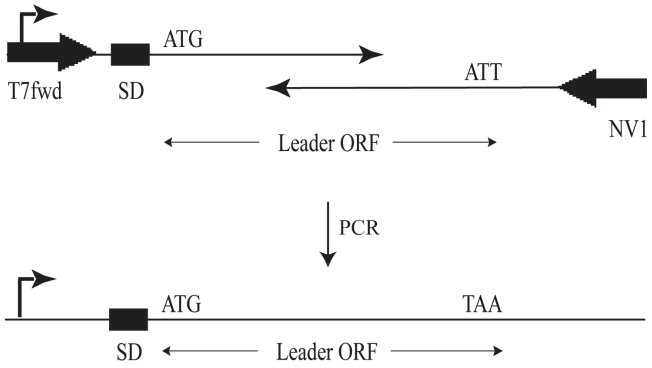

Figure 11. Generation of DNA templates containing leader ORFs by PCR. The forward primer contains T7 primer, Shine-Dalgarno (SD) region and leader ORF coding sequence. Reverse primer contains binding site for toeprinting primer (NV1). The two primers contain complementary 3' ends. The two shorter primers, T7 fwd and NV1 are indicated as block arrows.

Two DNA primers containing the leader ORF coding sequence and complementary 3' ends were synthesized (leader ORF specific primers) and obtained from Integrated DNA Technologies. The forward primer contained a T7 promoter for transcription initiation and a Shine-Dalgarno sequence for translation initiation. The reverse primer contained the binding site for the toeprinting primer. The primers (Table II) were purified by polyacrylamide gel electrophoresis; 0.75 A_{260} of primer in 1.5 µL H_2O was mixed with 1.5 µL formamide dye (95% formamide, 2 mM EDTA, 0.5% bromophenol blue, 0.5% xylene cyanol), heated at 70

°C for 2 min and loaded on a 9% denaturing polyacrylamide gel (20 cm long, 1 mm thick). The gel was run at 20W until the dye reached the bottom of the gel. The primers were visualized by UV shadowing directly on the electrophoretic plate. The band corresponding to the primer was cut from the gel and DNA was eluted into 300 µL 0.3 M NaOAc (pH 5.5) by shaking overnight in a 1.5 mL tube in an Eppendorf thermomixer, at 37 °C. The tube was centrifuged at 16000 g in a tabletop centrifuge for one minute. The supernatant was withdrawn with a pipette and primer was precipitated by adding three volumes of ethanol and incubation at -20 °C for one hour. Primer DNA was pelleted by centrifugation at 21000 g for 15 min, at 4 °C. The supernatant was aspirated; the pellet was air-dried and resuspended in 20 µL H_2O. Optical density (A_{260}) of the solution was determined using the Nanodrop spectrophotometer. Two additional shorter primers were synthesized (T7fwd and NV1) whose sequences were identical to the 5' ends of the long primers. A typical 100 µL PCR reaction contained 10 µL 10X AccuPrime PCR Buffer I (200 mM Tris-HCl (pH 8.4), 500 mM KCl, 15 mM $MgCl_2$, 2 mM dGTP, 2 mM dATP, 2 mM dTTP, 2 mM dCTP, thermostable AccuPrime™ protein and 10% glycerol), 100 pmol each of T7fwd and NV1 primers, 10 pmol each of the leader ORF specific primers and 2 U AccuPrime *Taq* DNA Polymerase High Fidelity. The PCR cycle conditions were: 94 °C (2 min), [94 °C (30 sec), 50 °C (30 sec), 68 °C (15 sec)] x 30 cycles. The PCR products were analyzed on a 2% agarose gel and purified using the Wizard SV Gel and PCR Clean-up System (Promega). PCR products were eluted in 45 µL water and their concentrations were determined using the Nanodrop Spectrophotometer. The nucleotide sequences of the PCR products were verified by capillary sequencing from the primers T7 fwd and NV1. Sequencing was done at the DNA sequencing facility (UIC).

TABLE II

PRIMERS USED FOR GENERATING LEADER ORF TEMPLATES FOR TOEPRINTING

Primer Name	Primer Sequence (5' to 3')
Universal primers for generating templates for cell-free transcription-translation	
NV1	GGTTATAATGAATTTTGCTTATTAAC
T7fwd	TAATACGACTCACTATAGGG
Oligonucleotides used for generating wild-type *ermAL1* template	
ermAfwd	TACATTAATACGACTCACTATAGGGCTTAAGTATAAGGAGGAAAAAAT ATGTGCACCAGTATCGCAGTAG
ermArev	GGTTATAATGAATTTTGCTTATTAACGATAGAATTCTATCACTTATGAAT GAGATAAAGTAATTTCTACTACTGCGATACTGGTG
Oligonucleotides used for generating synonymous mutations in *ermAL1*	
ermAL1syn-F	TAATACGACTCACTATAGGGCTTAAGTATAAGGAGGAAAAAATATGTG TACGTCAATTGCCGTGG
ermAL1syn-R	GGTTATAATGAATTTTGCTTATTAACGATAGAATTCTATCACTTATGAAT GAGATAAAGTAATTTCGACCACGGCAATTGACGTA
Oligonucleotides used for generating mutant *ermAL1* templates for alanine scanning	
ermA-A2-F (used with ermArev)	TAATACGACTCACTATAGGGCTTAAGTATAAGGAGGAAAAAATATGGC CACCAGTATCGCAGTAG
ermA-A3-F	TAATACGACTCACTATAGGGCTTAAGTATAAGGAGGAAAAAATATGTG CGCCAGTATCGCAGTAG
ermA-A3-R	GGTTATAATGAATTTTGCTTATTAACGATAGAATTCTATCACTTATGAAT GAGATAAAGTAATTTCTACTACTGCGATACTGGCG
ermA-A4-F	TAATACGACTCACTATAGGGCTTAAGTATAAGGAGGAAAAAATATGTG CACCGCAATCGCAGTAG
ermA-A4-R	GGTTATAATGAATTTTGCTTATTAACGATAGAATTCTATCACTTATGAAT GAGATAAAGTAATTTCTACTACTGCGATTGCGGTG
ermA-A5-F	TAATACGACTCACTATAGGGCTTAAGTATAAGGAGGAAAAAATATGTG CACCAGTGCAGCAGTAG
ermA-A5-R	GGTTATAATGAATTTTGCTTATTAACGATAGAATTCTATCACTTATGAAT GAGATAAAGTAATTTCTACTACTGCTGCACTGGTG
ermA-G6-F	TAATACGACTCACTATAGGGCTTAAGTATAAGGAGGAAAAAATATGTG CACCAGTATCGGAGTAG
ermA-G6-R	GGTTATAATGAATTTTGCTTATTAACGATAGAATTCTATCACTTATGAAT GAGATAAAGTAATTTCTACTACTCCGATACTGGTG
ermA-A7-F	TAATACGACTCACTATAGGGCTTAAGTATAAGGAGGAAAAAATATGTG CACCAGTATCGCAGCAG
ermA-A7-R	GGTTATAATGAATTTTGCTTATTAACGATAGAATTCTATCACTTATGAAT GAGATAAAGTAATTTCTACTGCTGCGATACTGGTG
ermA-A8-R (used with ermAfwd)	GGTTATAATGAATTTTGCTTATTAACGATAGAATTCTATCACTTATGAAT GAGATAAAGTAATTTCTGCTACTGCGATACTGGTG
ermA-A9-R (used with ermAfwd)	GGTTATAATGAATTTTGCTTATTAACGATAGAATTCTATCACTTATGAAT GAGATAAAGTAATTGCTACTACTGCGATACTGGTG
ermA-A10-R (used with ermAfwd)	GGTTATAATGAATTTTGCTTATTAACGATAGAATTCTATCACTTATGAAT GAGATAAAGTTGCTTCTACTACTGCGATACTGGTG
Oligonucleotides used for generating mutant *ermAL1* templates with codon 9 substitutions	
ermA-E10F-R	GGTTATAATGAATTTTGCTTATTAACGATAGAATTCTATCACTTATGAAT

Primer Name	Primer Sequence (5' to 3')
	GAGATAAAGTAATAAATACTACTGCGATACTGGTG
ermA-E9Q-R	GGTTATAATGAATTTTGCTTATTAACGATAGAATTCTATCACTTATGAAT GAGATAAAGTAATTTGTACTACTGCGATACTGGTG
ermA-E9K-R	GGTTATAATGAATTTTGCTTATTAACGATAGAATTCTATCACTTATGAAT GAGATAAAGTAATTTTTACTACTGCGATACTGGTG
ermA-E9P-R	GGTTATAATGAATTTTGCTTATTAACGATAGAATTCTATCACTTATGAAT GAGATAAAGTAATAGGTACTACTGCGATACTGGTG
ermA-E9D-R	GGTTATAATGAATTTTGCTTATTAACGATAGAATTCTATCACTTATGAAT GAGATAAAGTAATATCTACTACTGCGATACTGGTG
ermA-E9stop-R	GGTTATAATGAATTTTGCTTATTAACGATAGAATTCTATCACTTATGAAT GAGATAAAGTAATTTATACTACTGCGATACTGGTG
ermA-E9L-R	GGTTATAATGAATTTTGCTTATTAACGATAGAATTCTATCACTTATGAAT GAGATAAAGTAATTAATACTACTGCGATACTGGTG
ermA-E9I-R	GGTTATAATGAATTTTGCTTATTAACGATAGAATTCTATCACTTATGAAT GAGATAAAGTAATGATTACTACTGCGATACTGGTG
ermA-E9M-R	GGTTATAATGAATTTTGCTTATTAACGATAGAATTCTATCACTTATGAAT GAGATAAAGTAATCATTACTACTGCGATACTGGTG
ermA-E9V-R	GGTTATAATGAATTTTGCTTATTAACGATAGAATTCTATCACTTATGAAT GAGATAAAGTAATGACTACTACTGCGATACTGGTG
ermA-E9T-R	GGTTATAATGAATTTTGCTTATTAACGATAGAATTCTATCACTTATGAAT GAGATAAAGTAATTGTTACTACTGCGATACTGGTG
ermA-E9Y-R	GGTTATAATGAATTTTGCTTATTAACGATAGAATTCTATCACTTATGAAT GAGATAAAGTAATGTATACTACTGCGATACTGGTG
ermA-E9H-R	GGTTATAATGAATTTTGCTTATTAACGATAGAATTCTATCACTTATGAAT GAGATAAAGTAATGTGTACTACTGCGATACTGGTG
ermA-E9N-R	GGTTATAATGAATTTTGCTTATTAACGATAGAATTCTATCACTTATGAAT GAGATAAAGTAATGTTTACTACTGCGATACTGGTG
ermA-E9C-R	GGTTATAATGAATTTTGCTTATTAACGATAGAATTCTATCACTTATGAAT GAGATAAAGTAATGCATACTACTGCGATACTGGTG
ermA-E9R-R	GGTTATAATGAATTTTGCTTATTAACGATAGAATTCTATCACTTATGAAT GAGATAAAGTAATACGTACTACTGCGATACTGGTG
ermA-E9G-R	GGTTATAATGAATTTTGCTTATTAACGATAGAATTCTATCACTTATGAAT GAGATAAAGTAATACCTACTACTGCGATACTGGTG
ermA-E9W-R	GGTTATAATGAATTTTGCTTATTAACGATAGAATTCTATCACTTATGAAT GAGATAAAGTAATCCATACTACTGCGATACTGGTG
ermA-E9S-R	GGTTATAATGAATTTTGCTTATTAACGATAGAATTCTATCACTTATGAAT GAGATAAAGTAATTGATACTACTGCGATACTGGTG
ermA-E9Q2-R	GGTTATAATGAATTTTGCTTATTAACGATAGAATTCTATCACTTATGAAT GAGATAAAGTAATCTGTACTACTGCGATACTGGTG
ermA-E9S2-R	GGTTATAATGAATTTTGCTTATTAACGATAGAATTCTATCACTTATGAAT GAGATAAAGTAATACTTACTACTGCGATACTGGTG
ermA-E9L2-R	GGTTATAATGAATTTTGCTTATTAACGATAGAATTCTATCACTTATGAAT GAGATAAAGTAATGAGTACTACTGCGATACTGGTG
ermA-E9R2-R	GGTTATAATGAATTTTGCTTATTAACGATAGAATTCTATCACTTATGAAT GAGATAAAGTAATCCGTACTACTGCGATACTGGTG
Oligonucleotides used for generating *ermCL-ermAL1* hybrids	
ermC-fwd	TAATACGACTCACTATAGGGCTTAAGTATAAGGAGGAAAAAATATGGG CATTTTTAGTATTTTTGTAATC
ermC-rev	GGTTATAATGAATTTTGCTTATTAACGATAGAATTCTATCACTTAATGA ACTGTGCTGATTACAAAAATACTAAAAATGCC
ermC-S10E-R (used with ermC-fwd)	GGTTATAATGAATTTTGCTTATTAACGATAGAATTCTATCACTTAATGA ACTGTTTCGATTACAAAAATACTAAAAATGCC
ermALshort-	GGTTATAATGAATTTTGCTTATTAACGATAGAATTCTATCACTTATAAA

Primer Name	Primer Sequence (5' to 3')
rev (used with ermAfwd)[d]	GTAATTTCTACTACTGCGATACTGGTG
ermALshort-E9S-R (used with ermAfwd)	GGTTATAATGAATTTTGCTTATTAACGATAGAATTCTATCACTTATAAA GTAATTGATACTACTGCGATACTGGTG
ermCLshort-F7A-I9V-F	TAATACGACTCACTATAGGGCTTAAGTATAAGGAGGAAAAAATATGGG CATTTTTAGTATTGCAGTAGTA
ermCLshort-F7A-I9V-R	GGTTATAATGAATTTTGCTTATTAACGATAGAATTCTATCACTTAATGA ACTGTGCTTACTACTGCAATACTAAAAATGCC
ermCLshort-F7A-I9V-S10E-R (used with ermCLshort-F7A-I9V-F)	GGTTATAATGAATTTTGCTTATTAACGATAGAATTCTATCACTTAATGA ACTGTTTCTACTACTGCAATACTAAAAATGCC
ermCLshort-I9V-F	TAATACGACTCACTATAGGGCTTAAGTATAAGGAGGAAAAAATATGGG CATTTTTAGTATTTTTGTAGTA
ermCLshort-I9V-R	GGTTATAATGAATTTTGCTTATTAACGATAGAATTCTATCACTTAATGA ACTGTGCTTACTACAAAAATACTAAAAATGCC
ermCLshort-I9V-S10E-R (used with ermCLshort-I9V-F)	GGTTATAATGAATTTTGCTTATTAACGATAGAATTCTATCACTTAATGA ACTGTTTCTACTACAAAAATACTAAAAATGCC
ermCLshort-F7A-F	TAATACGACTCACTATAGGGCTTAAGTATAAGGAGGAAAAAATATGGG CATTTTTAGTATTGCTGTAATC
ermCLshort-F7A-R	GGTTATAATGAATTTTGCTTATTAACGATAGAATTCTATCACTTAATGA ACTGTGCTGATTACAGCAATACTAAAAATGCC
ermCLshort-F7A+S10E-R (used with ermCLshort-F7A-F)	GGTTATAATGAATTTTGCTTATTAACGATAGAATTCTATCACTTAATGA ACTGTTTCGATTACAGCAATACTAAAAATGCC
Oligonucleotides used for generating *ermAL2* template	
ermAL2-F	TAATACGACTCACTATAGGGCTTAAGTATAAGGAGGAAAAAATATGGG TACTTTTTCTATATTTGTTATTAATAAAGTTCG
ermAL2-R	GGTTATAATGAATTTTGCTTATTAACGATAGAATTCTATCACTTAATTTT GATTTGGTTGATAACGAACTTTATTAATAACAAA
Oligonucleotides used for generating *ermBL* template	
ermB3-F	TAATACGACTCACTATAGGGCTTAAGTATAAGGAGGAAAAAATATGTT GGTATTCCAAATGCGTAATGTAGATAAAACATCTAC
ermB3-R	GGTTATAATGAATTTTGCTTATTAACGATAGAATTCTATCACTTATTTCA AAATAGTAGATGTTTTATCTACATTACG
Oligonucleotides used for generating mutant *ermBL* templates for alanine scanning	
ermB3-A2-F (used with ermB3-R)	TAATACGACTCACTATAGGGCTTAAGTATAAGGAGGAAAAAATATGGC AGTATTCCAAATGCGTAATGTAGATAAAACATCTAC
ermB3-A3-F (used with ermB3-R)	TAATACGACTCACTATAGGGCTTAAGTATAAGGAGGAAAAAATATGTT GGCATTCCAAATGCGTAATGTAGATAAAACATCTAC
ermB3-A4-F	TAATACGACTCACTATAGGGCTTAAGTATAAGGAGGAAAAAATATGTT

Primer Name	Primer Sequence (5' to 3')
(used with ermB3-R)	GGTAGCACAAATGCGTAATGTAGATAAAACATCTAC
ermB3-A5-F (used with ermB3-R)	TAATACGACTCACTATAGGGCTTAAGTATAAGGAGGAAAAAATATGTT GGTATTCGCAATGCGTAATGTAGATAAAACATCTAC
ermB3-A6-F (used with ermB3-R)	TAATACGACTCACTATAGGGCTTAAGTATAAGGAGGAAAAAATATGTT GGTATTCCAAGCACGTAATGTAGATAAAACATCTAC
ermB3-A7-F	TAATACGACTCACTATAGGGCTTAAGTATAAGGAGGAAAAAATATGTT GGTATTCCAAATGGCAAATGTAGATAAAACATCTAC
ermB3-A7-R	GGTTATAATGAATTTTGCTTATTAACGATAGAATTCTATCACTTATTTCA AAATAGTAGATGTTTTATCTACATTTGC
ermB3-A8-F	TAATACGACTCACTATAGGGCTTAAGTATAAGGAGGAAAAAATATGTT GGTATTCCAAATGCGTGCAGTAGATAAAACATCTAC
ermB3-A8-R	GGTTATAATGAATTTTGCTTATTAACGATAGAATTCTATCACTTATTTCA AAATAGTAGATGTTTTATCTACTGCACG
ermB3-A9-F	TAATACGACTCACTATAGGGCTTAAGTATAAGGAGGAAAAAATATGTT GGTATTCCAAATGCGTAATGCAGATAAAACATCTAC
ermB3-A9-R	GGTTATAATGAATTTTGCTTATTAACGATAGAATTCTATCACTTATTTCA AAATAGTAGATGTTTTATCTGCATTACG
ermB3-A10-F	TAATACGACTCACTATAGGGCTTAAGTATAAGGAGGAAAAAATATGTT GGTATTCCAAATGCGTAATGTAGCAAAAACATCTAC
ermB3-A10-R	GGTTATAATGAATTTTGCTTATTAACGATAGAATTCTATCACTTATTTCA AAATAGTAGATGTTTTTGCTACATTACG
ermB3-A11-F	TAATACGACTCACTATAGGGCTTAAGTATAAGGAGGAAAAAATATGTT GGTATTCCAAATGCGTAATGTAGATGCAACATCTAC
ermB3-A11-R	GGTTATAATGAATTTTGCTTATTAACGATAGAATTCTATCACTTATTTCA AAATAGTAGATGTTGCATCTACATTACG
Oligonucleotides for generating *ermBL* template with Val9Gly mutation	
ermB3-G9-F	TAATACGACTCACTATAGGGCTTAAGTATAAGGAGGAAAAAATATGTT GGTATTCCAAATGCGTAATGGAGATAAAACATCTAC
ermB3-G9-R	GGTTATAATGAATTTTGCTTATTAACGATAGAATTCTATCACTTATTTCA AAATAGTAGATGTTTTATCTCCATTACG
Oligonucleotides used for generating *ermBL* templates with mutations in -2 and A-site positions	
ermB3-F8-A11-F	TAATACGACTCACTATAGGGCTTAAGTATAAGGAGGAAAAAATATGTT GGTATTCCAAATGCGTTTTGTAGATGCAACATCTAC
ermB3-F8-A11-R	GGTTATAATGAATTTTGCTTATTAACGATAGAATTCTATCACTTATTTCA AAATAGTAGATGTTGCATCTACAAAACG
ermB3-F8-K11-F	TAATACGACTCACTATAGGGCTTAAGTATAAGGAGGAAAAAATATGTT GGTATTCCAAATGCGTTTTGTAGATAAAACATCTAC
ermB3-F8-K11-R	GGTTATAATGAATTTTGCTTATTAACGATAGAATTCTATCACTTATTTCA AAATAGTAGATGTTTTATCTACAAAACG
ermB3-A8-A11-F	TAATACGACTCACTATAGGGCTTAAGTATAAGGAGGAAAAAATATGTT GGTATTCCAAATGCGTGCAGTAGATGCAACATCTAC
ermB3-A8-A11-R	GGTTATAATGAATTTTGCTTATTAACGATAGAATTCTATCACTTATTTCA AAATAGTAGATGTTGCATCTACTGCACG
Oligonucleotides used for generating *ermDL* template	
ermDfwd	TACATTAATACGACTCACTATAGGGCTTAAGTATAAGGAGGAAAAAAT ATGACACACTCAATGAGACTTCGTT
ermDrev	GGTTATAATGAATTTTGCTTATTAACGATAGAATTCTATCA**C**TTACTGGT TCAAAGTTGGGAAACGAAGTCTCATTGAGT
Oligonucleotides used for generating mutant *ermDL* templates for alanine scanning	
ermD-A2-F	TAATACGACTCACTATAGGGCTTAAGTATAAGGAGGAAAAAATATGGC ACACTCAATGAGACTTCGTTTCCCA

Primer Name	Primer Sequence (5' to 3')
ermD-A2-R	GGTTATAATGAATTTTGCTTATTAACGATAGAATTCTATCACTTACTGGT TCAAAGTTGGGAAACGAAGTCTCAT
ermD-A3-F (used with ermD-A2-R)	TAATACGACTCACTATAGGGCTTAAGTATAAGGAGGAAAAAATATGAC AGCATCAATGAGACTTCGTTTCCCA
ermD-A4-F (used with ermD-A2-R)	TAATACGACTCACTATAGGGCTTAAGTATAAGGAGGAAAAAATATGAC ACACGCAATGAGACTTCGTTTCCCA
ermD-A5-F	TAATACGACTCACTATAGGGCTTAAGTATAAGGAGGAAAAAATATGAC ACACTCAGCAAGACTTCGTTTCCCA
ermD-A5-R	GGTTATAATGAATTTTGCTTATTAACGATAGAATTCTATCACTTACTGGT TCAAAGTTGGGAAACGAAGTCTTGC
ermD-A6-F	TAATACGACTCACTATAGGGCTTAAGTATAAGGAGGAAAAAATATGAC ACACTCAATGGCACTTCGTTTCCCA
ermD-A6-R	GGTTATAATGAATTTTGCTTATTAACGATAGAATTCTATCACTTACTGGT TCAAAGTTGGGAAACGAAGTGCCAT
ermD-A7-F	TAATACGACTCACTATAGGGCTTAAGTATAAGGAGGAAAAAATATGAC ACACTCAATGAGAGCACGTTTCCCA
ermD-A7-R	GGTTATAATGAATTTTGCTTATTAACGATAGAATTCTATCACTTACTGGT TCAAAGTTGGGAAACGTGCTCTCAT
ermD-A8-F	TAATACGACTCACTATAGGGCTTAAGTATAAGGAGGAAAAAATATGAC ACACTCAATGAGACTTGCATTCCCA
ermD-A8-R	GGTTATAATGAATTTTGCTTATTAACGATAGAATTCTATCACTTACTGGT TCAAAGTTGGGAATGCAAGTCTCAT
Oligonucleotides for generating *ermDL* with deletion of codons 2-3 of *ermDL*	
ermD-del2-3-F (used with ermD-A2-R)	TAATACGACTCACTATAGGGCTTAAGTATAAGGAGGAAAAAATATGTC AATGAGACTTCGTTTCCCA
Oligonucleotides for generating wild-type sequences of other leader ORFs	
erm36L	
ermMLfwd	TACATTAATACGACTCACTATAGGGCTTAAGTATAAGGAGGAAAAAAT ATGGGTAGTCCATCAATTGCAGTGACCCGGTTCC
ermMLrev	GGTTATAATGAATTTTGCTTATTAACGATAGAATTCTATCACCTAGAAG CGGCGGAACCGGGTCACTG
msrCL	
msrC1fwd	TAATACGACTCACTATAGGGCTTAAGTATAAGGAGGAAAAAATATGAC TGCATCGATGAAATTACGTTTCGAACTTTTGAATA
msrC1rev	GGTTATAATGAATTTTGCTTATTAACGATAGAATTCTATCACTTAGTTGT TATTCAAAAGTTCGAAACGTAAT
msrSAL	
msrSA1fwd	TAATACGACTCACTATAGGGCTTAAGTATAAGGAGGAAAAAATATGAC AGCTTCTATGAGACTCAAATAA
msrSA1rev	GGTTATAATGAATTTTGCTTATTAACGATAGAATTCTATCACTTATTTGA GTCTCATAGAAGCTGTC
ereAL	
ereA2fwd	TAATACGACTCACTATAGGGCTTAAGTATAAGGAGGAAAAAATATGTT ACGCAGCAGGGCAGTC
ereA2rev	GGTTATAATGAATTTTGCTTATTAACGATAGAATTCTATCACTCACAGA GCATAACTTTGTTTTAGGGCGACTGCCCTGCTGCGT
erm34L	
erm34fwd	TAATACGACTCACTATAGGGCTTAAGTATAAGGAGGAAAAAATATGCA TTTCATAAGATTGCGTTTTCTCGTTTTG
erm34rev	GGTTATAATGAATTTTGCTTATTAACGATAGAATTCTATCACTTACTTGT TCAAAACGAGAAAACGCAATC

Primer Name	Primer Sequence (5' to 3')
msrDL	
mel1fwd	TAATACGACTCACTATAGGGCTTAAGTATAAGGAGGAAAAAATATGTA TCTTATTTTCATGTAAGTGATAGAA
mel1rev	GGTTATAATGAATTTTGCTTATTAACGATAGAATTCTATCACTTACATGA AAATAAGATACATAT
ermXL	
ermX1fwd	TAATACGACTCACTATAGGGCTTAAGTATAAGGAGGAAAAAATATGTT GATTTCAGGTACCGCTTTCTTGCGGTTGCGCAC
ermX1rev	GGTTATAATGAATTTTGCTTATTAACGATAGAATTCTATCACCTACGGG GTAGGAAACGCCTTACGGTTGGTGCGCAACCGCAAGAAAG
ermSL	
ermS1fwd	TAATACGACTCACTATAGGGCTTAAGTATAAGGAGGAAAAAATATGAG TATGGGTATCGCGGCCCGACCACCCAGGGCCGCGCTGCTC
ermS1rev	GGTTATAATGAATTTTGCTTATTAACGATAGAATTCTATCACTCATCGG GAACGCGGTACAGACGGCGGCGGGAGCAGCGCGGCCCTG
erm38L	
erm38fwd	TAATACGACTCACTATAGGGCTTAAGTATAAGGAGGAAAAAATATGTC GATCACTTCGATGGCCGCCCCGGTCGCGGCCTTCATCCGG
erm38rev	GGTTATAATGAATTTTGCTTATTAACGATAGAATTCTATCACCTAGGCG GTGCGGGGCCGGATGAAGGCCGCGAC
ereAL'	
ereA1fwd	TAATACGACTCACTATAGGGCTTAAGTATAAGGAGGAAAAAATATGAC GCCTAACAATTCATTCAAGCCGACACC
ereA1rev	GGTTATAATGAATTTTGCTTATTAACGATAGAATTCTATCACTTAAGCC GCGCCGCGAAGCGGTGTCGGCTTGAATGAAT
ermGL2	
ermG2fwd	TAATACGACTCACTATAGGGCTTAAGTATAAGGAGGAAAAAATATGAA CCATGAGTACGTTCTTTTCTCAAAAAAC
ermG2rev	TATAATGAATTTTGCTTATTAACGATAGAATTCTATCACTTATTGCATCT CTTTTCGAATATTTATGTTTTTTGAGAAAAGAACGTACTC
erm37L	
erm37fwd	TAATACGACTCACTATAGGGCTTAAGTATAAGGAGGAAAAAATATGCG GACGGCGCCAGAGCCCT
erm37rev	GGTTATAATGAATTTTGCTTATTAACGATAGAATTCTATCACTCACCAG CCCCAGGGCTCTGGCGCCGT

2. In vitro transcription-translation

The purified PCR products containing leader ORFs of interest were used as templates for *in vitro* transcription-translation using a reconstituted *E. coli* cell-free system (PURE SYSTEM) [86]. PURE SYSTEM is assembled from individually purified components including T7 RNA polymerase, *E.coli* ribosomes, all aminoacyl tRNA synthetases, translation factors and energy regeneration enzymes. The system was purchased from BioComber or New England Biolabs. Each 5 μL reaction contained 2.5 μL Solution A (all the enzymes and buffers), 1 μL Solution B (4-8 pmol ribosomes), 1 μL DNA template (0.2-1 pmol) and either 0.5 μL H_2O or 0.5 μL antibiotic (500 μM stock solution in H_2O). The reactions were incubated for 15-60 min at 37 °C in a water bath followed by toeprinting analysis.

3. Primer extension inhibition analysis ('Toeprinting')

Toeprinting analysis was carried out following the general protocol of Gold and coworkers [87]. The toeprinting DNA primer NV1 was labeled in a 10 μL reaction containing 10 pmol NV1 primer, 3 μL γ^{32}P ATP (6000 Ci/mmol), 1 μL 10X Buffer A (500 mM Tris-HCl, pH 7.6, 100 mM $MgCl_2$, 50 mM DTT, 1 mM spermidine) and 1 μL (10 U) T4 polynucleotide kinase (Fermentas). The reaction was incubated at 37 °C for 30 min and the enzyme was inactivated by heating at 90 °C for 2 min. 0.8 μL (0.8 pmol) of the labeled primer was mixed with 0.3 μL (12 U) RiboLock RNase Inhibitor (Fermentas) and added to the translation reaction that previously has run for 15-60 min. After a brief vortexing and quick spin, the reaction was incubated at 37 °C for 2 min and then on ice for 5 min. Reverse transcriptase (Seikagaku, 30 U/μL) was diluted 10X with PURE System Buffer (9 mM

magnesium acetate, 5 mM potassium phosphate, pH 7.3, 95 mM potassium glutamate, 5 mM ammonium chloride, 0.5 mM calcium chloride, 1 mM spermidine, 8 mM putrescine and 1 mM DTT). The diluted RT was mixed 1:1 with a 4 mM mixture of dNTPs. 1 µL of this mixture was added to the reaction and reverse transcription was carried out at 37 °C for 15-30 min. After completion of the reaction, 1 µL 10 N NaOH was added in order to hydrolyze RNA and incubated at 37 °C for 15 min. Alkali was then neutralized by adding 0.8 µL concentrated HCl. 200 µL resuspension buffer (0.3 M NaOAc, pH 5.5, 5 mM EDTA and 0.5 % SDS) was added to the reaction and DNA was extracted with 1 volume Tris-saturated phenol, followed by 1 volume chloroform. 3 volumes of ethanol was added and incubated in dry ice/ethanol bath for 10 min. The tubes were centrifuged for 30 min at 4 °C in a tabletop microcentrifuge at 21,000 g. Ethanol was aspirated, the pellets were washed with 200 µL 70 % ethanol and subsequently air-dried for 10 min at room temperature. The pellets were resuspended in 6 µL formamide dye, heated at 95 °C for 2 min and 2 µL was loaded on a 6 % sequencing (0.4 mm) gel along with sequencing reactions of the template DNA. (In this case, sequencing was carried out using the fmol DNA Cycle Sequencing System from Promega, using the NV1 primer and the same DNA template that was used in the translation reaction). The 40 cm gel was run at 40 W for about 1.5 hrs until the bromophenol blue tracing dye reached the bottom of the gel. Gels were transferred to the paper, dried and exposed to the phosphorimager screen.

B. Northern blot

1. *In vitro* translation and gel electrophoresis

Northern blotting was carried out to determine identity of peptidyl-tRNA accumulated in the *ermAL1*-SRC. The *ermAL1* sequence containing a T7 promoter and Shine-Dalgarno sequence upstream and binding site for the toeprinting primer (NV1) downstream was synthesized (BioBasic, Inc) and cloned between the BamHI and ApaI sites of the vector pUC57 to produce the plasmid permAL. This plasmid was used to direct the *in vitro* transcription-translation reaction carried out using the *E. coli* T7 S30 Extract System for Circular DNA (Promega). The reaction (10 μL) was set up according to manufacturer's protocol and was supplemented with 0.8 μg plasmid. When necessary, erythromycin was added to a final concentration of 50 μM. The reactions were incubated at 37 °C for 40 min and chilled on ice for 10 min. Upon completion of the reaction, 50 μL Pure System Buffer containing 1 μL (40 U) RNase inhibitor and 50 μM erythromycin was added. The samples were then filtered through a Microcon YM-100 filter (molecular weight cut-off of 100 kDa) by centrifugation at 500 g for 15 min at 4 °C in a tabletop centrifuge. 20 μL Pure System Buffer (with 50 μM erythromycin) was added to the filter and the centrifugation was repeated. The sample was then collected from the filter by inverting the top chamber into an eppendorf tube and carrying out a quick spin in the tabletop centrifuge. 200 μL of 0.3 M NaOAc, pH 4.0 was added to the sample and peptidyl-RNA was extracted with 250 μL acidic phenol followed by extraction with 250 μL chloroform. The material was precipitated from the aqueous phase with 3 volumes of ethanol upon incubation in a dry ice/ethanol bath for 15 min. The precipitate was collected by centrifugation for 30 min at 4 °C in a tabletop centrifuge at 14,000 g. The supernatant was discarded and the pellet was washed with 200 μL

70 % ethanol and air-dried for 10 min at room temperature. The pellet was resuspended in 6 μL loading acidic buffer (7 M urea in 0.1 M NaOAc, pH 5.2, 0.5 % xylene cyanol and 0.5 % bromophenol blue). 3 μL of each reaction was loaded onto a 6.5% denaturing acidic gel (6.5 % polyacrylamide), 8 M urea, 0.1 M NaOAc, pH 5.2) [88]. The gel (40 cm x 20 cm x 1 mm) was run using 0.1 M NaOAc, pH 5.2 as the running buffer, at 10 W for 23 hrs in the cold room. The gel was stained with ethidium bromide to visualize the RNA.

2. Electroblotting of the RNA

The Trans-Blot SD Semi-Dry Electrophoretic Transfer Cell (BioRad) was used to transfer the RNA from the gel to a Hybond N+ membrane (GE Healthcare). The electroblotting was carried out at a constant current (current mAmp = 3X area of the gel), according to manufacturer's instructions, using 0.1 M NaOAc, pH 5.2 as the transfer buffer. The transfer was carried out for 30 min, following which, the membrane was dried at 42 °C for 30 min. The RNA was then crosslinked to the membrane at 80,000 μJ/cm^2 (Stratalinker UV Crosslinker, Stratagene).

3. Probing the membrane with radioactive probes

The oligonucleotide probes complementary to tRNA^{Val} (UAC) or tRNA^{Glu} (UUC) (Table III) were 5'-labeled with γ^{32}P-ATP (6000 Ci/mmol), as described in the toeprinting section, except for the following modifications. The reaction volume was scaled up to 20 μL and contained 20 pmol oligo and 9.5 μL (95 μCi) of γ^{32}P-ATP.

TABLE III

OLIGONUCLEOTIDE PROBES FOR NORTHERN HYBRIDIZATION

Name	Sequence (5' to 3')
$tRNA^{Val}$ (UAC)	TGGGTGATGACGGGATCGAACCGCCGACCCCCTCCTTGTAAGGGAG GTGCTCTCCCAGCTGAGCTAATCACCC
$tRNA^{Glu}$ (UUC)	CGTCCCCTAGGGGATTCGAACCCCTGTTACCGCCGTGAAAGGGCGG TGTCCTGGGCCTCTAGACGAAGGGGAC

Hybridization was carried out in the Hybridization Incubator (Lab-line). The membranes were pre-hybridized in 10 mL of hybridization solution (5X Denhardt solution, 6X SSC, 0.1% SDS) for 30 min at room temperature, in 50 mL tubes, with constant rotation. The labeled oligonucleotide probes were added to 15 mL of hybridization solution and hybridization was carried out overnight at 60 °C for 12 hrs, in a plastic pouch. The membranes were then washed with 6X SSC, 0.1% SDS (3 times, 10 min each at 35 °C); 6X SSC (10 min, 35 °C); 2X SSC (15 min, 30 °C) and 0.2 X SSC (15 min, 30 °C). The membranes were air-dried, wrapped in plastic and exposed to a phosphor imager screen. Screens were scanned using a Storm PhosphorImager (Molecular Dynamics).

C. Analysis of translation products of wild-type and mutant *ermAL1*

To enable visualization of ErmAL1 leader peptide by gel electrophoresis, the length of *ermAL1* ORF in permAL plasmid was extended to 72 codons by introducing a frameshift mutation. Specifically, two nucleotides were deleted in codon 12 of *ermAL1* by PCR (QuikChange II XL Site-Directed Mutagenesis kit, Stratagene), using the primers ermAL-shift1 and ermAL-shift2 (Table IV).

TABLE IV

OLIGONUCLEOTIDES USED FOR SITE-DIRECTED MUTAGENESIS OF CLONED *ermAL1*

Name	Sequence (5' to 3')
ermAL-shift1	TCGCAGTAGTAGAAATTACTATCTCATTCATAAGTGATAG
ermAL-shift2	CTATCACTTATGAATGAGATAGTAATTTCTACTACTGCGA
permAL.FS-E9F-F	GCACCAGTATCGCAGTAGTATTCATTACTATCTCATTCATAAG

The mutagenizing PCR reaction contained in a volume of 50 µL: 5 µL 10X reaction buffer, 1 µL permAL (5 ng), 125 ng of each primer, 1 µL dNTP mix and 1 µL *PfuUltra* high-fidelity DNA polymerase (2.5 U/µL). The PCR conditions were as follows: 95 °C (30 sec), [95 °C (30 sec), 55 °C (1 min), 68 °C (3 min)] X 18 cycles. The reaction was treated with 1 µL (10 U) DpnI for 1 hr at 37 °C and subsequently purified using the Wizard SV Gel and PCR Clean-up System (Promega). The sample was eluted with 40 µL H_2O and concentrated to 10 µL using a SpeedVac. 5 µL of the sample was used to transform 45 µL XL-10 Gold ultracompetent cells (Stratagene) and plated on LB agar plates containing 100 µg/mL ampicillin. Plasmids were isolated from 6 transformants and sequenced from the M13 forward primer (Table IV). The plasmid with the extended *ermAL1* sequence was named permAL-FS. Subsequently, an additional mutation was introduced in codon 9 of ermAL1-FS by changing the GAA (Glu) codon to TTC (Phe) using primer permAL.FS-E9F-F (Table IV) and the QuikChange Multi Site-Directed mutagenesis kit (Stratagene). The PCR reaction contained in a volume of 25 µL, 2.5 µL 10X reaction buffer, 5 ng permAL-FS, 100 ng primer, 1 µL dNTP mix and 1 µL (2.5 U) QuikChange Multi enzyme blend. The PCR conditions were as follows: 95 °C (1 min), [95 °C (1 min), 55 °C (1 min), 65 °C (5 min 42

sec)] X 30 cycles. The PCR reaction was treated with DpnI enzyme, purified and concentrated as described above. An aliquot was used to transform XL-10 Gold Ultracompetent cells. Plasmids isolated from transformants were sequenced, the correct plasmid was identified and named permAL-FS-E9F.

Plasmids permAL-FS and permAL-FS-E9F were expressed using the *E.coli* T7 S30 Extract System for Circular DNA (Promega). The reactions were carried out according to manufacturer's instructions and contained 0.5 μg plasmid DNA, 0.75 μCi ^{35}S-Met (1175 Ci/mmol), 50 μM erythromycin (when necessary) and was carried out in a total volume of 6.4 μL. The reaction was incubated at 37 °C for 15 min and then precipitated with 25 μL acetone. The pellets were resuspended in 5 μL Tricine Sample Buffer (BioRad). 2 μL of the reaction containing erythromycin and 0.5 μL of the reaction carried out in the absence of erythromycin were analyzed in a 16% polyacrylamide gel using the Tricine-SDS buffer system [89]. After the run, the gel was fixed for 10 min in a solution containing 40% methanol and 10% acetic acid and stained for 5 min with Serva Blue G (25 mg Serva Blue G in 10% acetic acid). The gel was destained for 5 min in 10% acetic acid and washed for 5 min in each: water, 10% ethanol, 20% ethanol, 30% ethanol, 40% ethanol, 10% glycerol+40% ethanol prior to drying and exposure. The gel was exposed to a phosphorimager screen.

D. Isolation of *ermAL*$_8$-SRC and testing acceptor activity of the aminoacyl-tRNA analogs in peptidyl-transfer reaction

1. Isolation of *ermAL*$_8$-SRC

RNA with the sequence AUAAGGAGGAAAAAAUAUGUGCACCAGUAUCGCAGUAGUA encoding *ermAL1* truncated at the eighth codon was synthesized by Thermo Fisher. This mRNA was used to direct translation in the *E.coli* S30 Extract System for Linear Templates (Promega). A 50 µL reaction contained 8 µM transcript, 50 µM erythromycin, 0.4 µCi/µL [^{35}S]-methionine and 2.4 U/µL RiboLock RNase Inhibitor (Fermentas) and was carried out for 30 min at 37 °C. 100 µL of gradient buffer (20 mM Tris-HCl, pH 7.5, 15 mM $MgCl_2$, 10 mM NH_4Cl and 2 mM β-mercaptoethanol) containing 50 µM erythromycin was added to the sample prior to loading onto 11 mL of 5 % - 30 % sucrose gradient prepared in the same buffer supplemented with 50 µM erythromycin. Gradients were centrifuged in a SW41 rotor at 39,000 rpm for 3 hr at 4 °C. The gradients were fractionated using ISCO UA-6 UV flow monitor equipped with a Gilson collector. 0.3 mL fractions were collected. 5 µL aliquots from each fraction were mixed with 150 µL Ultima Gold Scintillation Cocktail and the amount of radioactivity was determined using the Scintillation Counter (Beckman). The fractions containing the 70S peak were pooled and an equal volume of gradient buffer supplemented with 50 µM erythromycin was added. The sample was then concentrated using Vivaspin 100 microtube filters (Sartorius). The filters were pre-washed with 500 µL of gradient buffer. Sample was then added to the tubes and concentrated to 20 µL by centrifugation in a tabletop centrifuge at 4 °C. The retentate containing the concentrated stalled ribosome complex (*ermAL*$_8$-SRC) was collected by centrifugation and the

concentration of the ribosomes was determined by reading optical density at 260 nm. Samples were stored at -20 °C.

2. Peptidyl-transfer reaction

The A-site substrates for the *in vitro* reaction (CCA-N-Ala or CCA-N-Lys) were synthesized by Dr. Qing Dai (University of Chicago) (Figure 12).

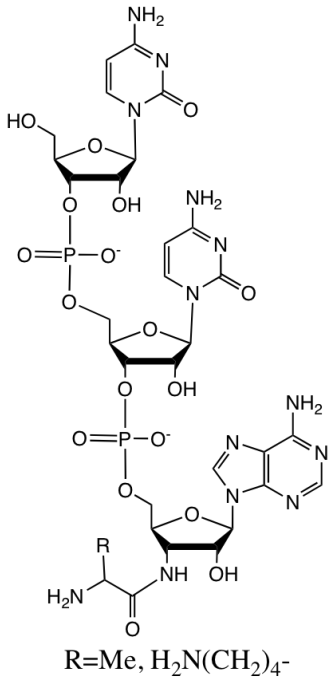

Figure 12. Structure of CCA-N-aminoacyl analogs. The R group indicates Alanine (Me) or Lysine ($H_2N(CH2)_4^-$).

0.6 μM of the *ermAL*$_8$-SRC was combined with 1 mM CCA-N-Ala or CCA-N-Lys in Pure System Buffer containing 50 μM erythromycin, in a total volume of 22 μL. Reactions were incubated at 37 °C and 5 μL aliquots were removed at 1, 2.5, 5, 15 and 30 min. Reactions were stopped by precipitation with 30 μL cold acetone. The samples were centrifuged at 14,000 rpm for 30 min at 4 °C and supernatant was discarded. Pellets were

resuspended in 5 µL of Tricine Sample Buffer (BioRad) and analyzed on a 16.5 % Bis-Tris gel, as described in http://openwetware.org/Sauer:bis-Tris_SDS_PAGE (based on US patent 6,162,338).

E. Introducing mutations in 23S rRNA, analyzing cell phenotypes and isolation of ribosomes

1. Mutagenesis of 23S rRNA

Mutations were introduced in 23S rRNA gene of the *rrnB* operon in plasmid pLK35 [90] using the QuikChange Lightning Multi Site-Directed Mutagenesis Kit (Stratagene). For each site of mutation, three different primers, each introducing one of the three possible mutations were combined in a mutagenesis experiment. Primers used are listed in Table V. In this work, mutations were introduced at U790, U1782, A2439 and C2452. Mutations in the 750 region, U2609 and U2586 were generated by Dr. Nora Vazquez-Laslop and Ms. Dorota Klepacki in this lab. Strains containing mutations in G2583, U2584 and A2587 were obtained from Dr. Suzuki (University of Tokyo, Japan) (see below).

TABLE V

PRIMERS USED FOR MUTAGENESIS OF rRNA

Name	Sequence (5' to 3')
23S-U790A-F	GGGTGAAAGGCCAAACAAACCGGGAGATAG
23S-U790G-F	GGGTGAAAGGCCAAGCAAACCGGGAGATAG
23S-U790C-F	GGGTGAAAGGCCAACCAAACCGGGAGATAG
U1782A-F	GGCTGCAACTGTTTATAAAAAACACAGCACTGTG
U1782G-F	GGCTGCAACTGTTTATGAAAAACACAGCACTGTG
U1782C-F	GGCTGCAACTGTTTATCAAAAACACAGCACTGTG
A2439U-F	CAACGGATAAAAGGTTCTCCGGGGATAACAG
A2439G-F	CAACGGATAAAAGGTGCTCCGGGGATAACAG
A2439C-F	CAACGGATAAAAGGTCCTCCGGGGATAACAG
C2452A-F	GTACTCCGGGGATAAAAGGCTGATACCGCC
C2452G-F	GTACTCCGGGGATAAGAGGCTGATACCGCC
C2452U-F	GTACTCCGGGGATAATAGGCTGATACCGCC

As per the manufacturer's recommendations, a typical PCR reaction contained in a volume of 25 µL, 2.5 µL 10X reaction buffer, 0.7 µL Quik solution, 100 ng pLK35 plasmid, 10 pmol of each of the three mutagenizing primers, 1 µL dNTP mix and 1 µL QuikChange Multi enzyme blend. The PCR cycle conditions were as follows: 95 °C (2 min), [95 °C (20 sec), 55 °C (30 sec), 65 °C (5 min)] X 30 cycles, followed by incubation at 65 °C for 5 min. The PCR reaction was treated with DpnI enzyme (as above) and 2 µL of the reaction mixture was directly used to transform XL-10 Gold Ultracompetent cells (Stratagene). Transformants were selected on LB agar plates containing 100 µg/mL ampicillin. Plasmids were isolated from 4-6 transformants and the sites of mutation were sequenced.

1 µL (~5 ng) of the mutant plasmids were then used to transform electrocompetent SQK15 cells (generated by Krishna Kannan in this lab). SQK15 is derived from SQ171

which lacks chromosomal rRNA operons, the only source of rRNA being plasmid prrnC-*sacB*, which confers resistance to kanamycin [91]. The deltaMZ15 mutation was introduced into SQ171 to make it capable of α-complementation for *lacZ* expression. Transformants were isolated on LB agar plates containing 100 µg/mL ampicillin. Elimination of the prrnC-*sacB* plasmid was carried out as described in [92], with some modifications. Specifically, for each mutant, 2 Amp^R colonies were inoculated in 1 mL LB/Amp (50 µg/mL) at 37 °C and grown until the cultures became cloudy. 10 µL of the cultures were used to inoculate 2 mL LB/Amp 50 and grown overnight. 20 µL of the overnight cultures were used to inoculate 5 mL cultures which were incubated at 37 °C until cloudy. Dilutions of the cultures (10^{-2} to 10^{-5}) were plated on LB agar plates lacking NaCl and supplemented with Amp (50 µg/mL) and sucrose (5%). Plates were incubated overnight at 37 °C, colonies were replica streaked onto LB agar/Amp 50 and LB agar/Kan 25 plates and incubated at 37 °C. Plasmids were isolated from several Amp^R/Kan^S clones and sequenced to verify the presence of the mutation.

TABLE VI

PRIMERS USED FOR SEQUENCING OF rRNA

Name	Sequence (5' to 3')	Site of mutation sequenced
L893	GTCGGGATGAC	U790
L1972	CATTCGTGCAGGTCGGAAC	U1782
L2563	TCGCGTACCACTTTA	C2452
L2470	ACTCTTGGGCGGTATCAGCCT	A2439

2. Analysis of 23S rRNA from cells carrying mutant pLK35 plasmid

Loss of wild-type rRNA from the SQK15 cells carrying mutant pLK35 plasmids and expression of a homogeneous population of mutant ribosomes was confirmed by primer extension analysis on total RNA as described below.

RNA isolation: A single colony of SQK15 cells was inoculated overnight in 3 mL LB broth containing 50 μg/mL ampicillin. The overnight cultures were diluted 100X in7 mL LB broth with 50 μg/mL ampicillin and grown until A_{600} = 1. Total RNA was isolated from the culture using the Qiagen RNeasy mini kit, following manufacturer's instructions. RNA was eluted in 50 μL of water and quantitated using the Nanodrop spectrophotometer.

Primer design: For each site of mutation, a reverse primer was designed to anneal close to the site, as shown below, to distinguish between wild-type and mutant rRNA (Figure 13). In the example shown, the wild-type 23S rRNA contains a 'U' at position 790, which was mutated to 'G'. Subsequent to RNA isolation, the primer is annealed and extended by reverse transcriptase. Extension of the primer (20 nt) in the presence of dATP, dGTP, dTTP and ddCTP results in products of different lengths, depending on the template rRNA – 21 nt (mutant rRNA) or 26 nt (wild-type rRNA). Thus, the products of the primer extension reaction can be separated on a gel (see below for details) to confirm the presence of the mutation and loss of wild-type rRNA. The primers designed for verification of mutations are listed in Table VII.

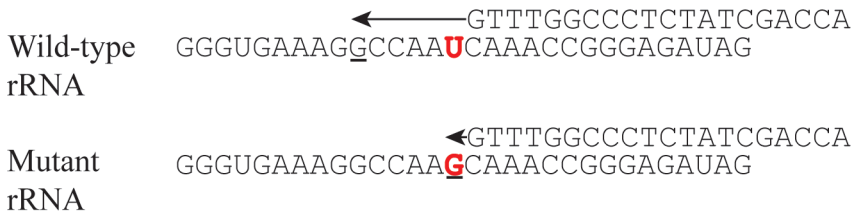

Figure 13. Principle of primer extension analysis. See text for details. Primer is shown above rRNA sequence. Arrow indicates primer extension. The original nucleotide in the wild-type rRNA and the mutation are indicated in red. Primer extension terminates at the underlined nucleotide for each rRNA sequence.

TABLE VII

PRIMERS USED FOR VERIFICATION OF rRNA MUTATIONS BY PRIMER EXTENSION

Name	Sequence (5' to 3')	Site of mutation verified
23S-L791	ACCAGCTATCTCCCGGTTTG	U790
L1783	TGCACAGTGCTGTGTTTTT	U1782
L2441	CAGCCTGTTATCCCCGGA	A2439
L2587	AACTGTCTCACGACGTTCT	G2583, U2584
L2588	GAACTGTCTCACGACGTTC	U2584, A2587
L2585	ACTGTCTCACGACGTTCT	U2586
L2608	CGCCCACGGCAGATAGGG	U2609

Primer labeling: 30 pmol primer was labeled by combining with 30 µCi γ^{32}P-ATP (6000 Ci/mmol), 1 µL 10x polynucleotide kinase buffer and 1 µL (10 U) polynucleotide kinase (Fermentas) in 10 µL reaction volume. The reaction was incubated at 37 °C for 30 min and then at 90 °C for 2 min.

Primer annealing: 1 µg of total cellular rRNA, 0.5 µL (1.5 pmol) labeled primer and 1 µL 4.5X hybridization buffer (225 mM Hepes-KOH, pH 7, 450 mM KCl) were combined in a total volume of 4.5 µL. The reaction was incubated for 1 min at 90 °C and cooled over 10 min to 47 °C.

Extension reaction: 4 µL of a mix containing 0.65 µL 10X RT reaction buffer (1.3 M Tris-HCl, pH 8.5, 100 mM $MgCl_2$, 100 mM DTT), 1.5 µL dNTP/ddXTP mix (1 mM dATP, 1 mM dGTP, 1 mM dTTP and 200 µM ddCTP for ddC termination), 1.75 µL H_2O, and 0.1 µL (3 U) reverse transcriptase (Seikagaku America) were added to 4.5 µL of the annealed rRNA/primer solution and incubated at 42 °C for 20 min. The reaction was stopped by the addition of 120 µL stop buffer (84 mM NaOAc, pH 5.5, 70% ethanol, 0.8 mM EDTA) and incubated for 5 min on ice. The tubes were then centrifuged for 10 min at 21,000 g, at 4 °C. The supernatant was removed and the pellets were dried in a vacuum dessicator for 2 min. The pellet was resuspended in 5 µL formamide dye and 2.5 µL was loaded on a 20 cm x 20 cm x 0.4 mm 12% polyacrylamide gel. The gel was run at 20W until the bromophenol dye reached the bottom. One plate was removed, the gel was transferred to a used X-ray film, wrapped in plastic wrap and exposed for 30 min to a phosphorimager screen and scanned.

3. Determination of MIC of erythromycin

SQK15 strains containing wild-type or mutant pLK35 plasmids were inoculated from frozen glycerol stocks in 3 mL LB broth containing 50 µg/mL ampicillin. Some of the rRNA mutations were present in the strain NT102, which was a kind gift from Dr. Suzuki (University of Tokyo, Japan) [93]. NT102 is derived from the *E.coli* strain TA542 which is similar to SQK15 in that all chromosomal rRNA operons were deleted, leaving a single plasmid-borne rRNA operon as the source of ribosomes [91]. NT102 strains expressing wild-type or mutant rRNA were inoculated similarly to SQK15, except, they contained 25 µg/mL kanamycin instead of ampicillin. Wild-type strains were included as controls. The cultures were incubated at 37 °C for several hours and then diluted 1:100 and incubated at 37 °C until optical density reached A_{600} = 0.3-0.6. MIC testing was done in a 96-

well plate. 75 µL of LB broth containing 50 µg/mL ampicillin or 25 µg/mL kanamycin was added to all the wells except A12, to which 144.9 µL of the respective broth was added. 5.12 µL of a 60 mg/mL stock solution of erythromycin was added to well A12, to a final concentration of 2048 µg/mL. After mixing, 75 µL of the broth from A12 was transferred to A11. Subsequent two-fold serial dilutions were repeated until well A2, from which 75 µL of the final broth was discarded. To well A1, 75 µL of LB broth containing 50 µg/mL ampicillin or 25 µg/mL kanamycin was added (no erythromycin control). To each well, 75 µL of exponential bacterial culture, diluted to A_{600} = 0.004 was added, to get a final A_{600} = 0.002. The final concentration of erythromycin ranged from 1024 µg/mL (well A12) to 1 µg/mL (well A1). The plates were incubated at 37 °C overnight and scored for cell growth by visual inspection.

4. <u>Isolation of ribosomes</u>

Ribosomes were prepared from SQK15 or NT102 cells expressing wild-type or mutant rRNA by the method of Ohashi et al (2007) [94]. Cells were grown in 1 L of LB broth (with 50 µg/mL ampicillin in case of SQK15 mutants or 25 µg/mL kanamycin in case of NT-102 mutants) at 37 °C, until A_{600} = 0.6. The cells were pelleted in a JLA 10.5 rotor, at 5000 rpm for 12 min at 4 °C. The cell pellets were resuspended in 10 mL of cold suspension buffer (10 mM Hepes-KOH, pH 7.6, 50 mM KCl, 10 mM $Mg(OAc)_2$ and 7 mM ß-mercaptoethanol) and lysed by passing cell suspension through French press at 7,000-10,000 psi. The lysate was centrifuged at 20,000 g in a JA 25.5 rotor for 30 min at 4 °C and filtered through a 0.45 micron filter. The clarified lysate was then loaded onto a 5 mL HiTrap Butyl FF column (GE Healthcare) equilibrated with Buffer A (20 mM Hepes-KOH, pH 7.6, 10 mM $Mg(OAc)_2$, 1.5 M $(NH_4)_2SO_4$, 7 mM ß-mercaptoethanol). The column was washed

with buffer Buffer A, containing 1.2 M $(NH_4)_2SO_4$. Ribosomes were then eluted with Buffer A containing 0.75 M $(NH_4)_2SO_4$. The eluate was overlayed onto an equal volume of cushion buffer (20 mM Hepes-KOH, pH 7.6, 10 mM $Mg(OAc)_2$, 30 mM NH_4Cl, 30% sucrose and 7 mM ß-mercaptoethanol) in a 32.4 mL Beckman Optiseal polyallomer tube and ribosomes were pelleted by ultracentrifugation at 36,000 rpm for 16 hr in a Beckman Ti70 rotor. The pellet containing the ribosomes was resuspended in ~100 µL cold ribosome buffer (20 mM Hepes-KOH, pH 7.6, 30 mM KCl, 6 mM $Mg(OAc)_2$, and 7 mM ß-mercaptoethanol). Ribosomes were distributed into aliquots, snap frozen and stored at -80 °C.

IV. RESULTS

A. Identification and classification of putative regulatory peptides encoded upstream of MLS_B resistance genes

The goal of this project was to understand the molecular mechanism of drug and nascent peptide-dependent ribosome stalling. Most of macrolide resistance genes are known to be inducible. For a limited number of genes, induction was shown to be controlled by drug-dependent ribosome stalling during translation of short upstream ORFs. However, a systematic analysis of the leader ORFs of macrolide resistance genes has not been done so far. Therefore, in order to identify the variety of peptides that could possibly direct drug-dependent ribosome stalling we started by analyzing the upstream sequences of currently known MLS_B resistance genes, searching for putative leader ORFs.

The web-based resource for MLS_B resistance genes, maintained by Dr. M. Roberts (University of Washington) currently contains a list of 35 rRNA methyltransferases (*erm*), 18 efflux genes (e.g. *mef* and *msr*) and 20 drug-inactivating enzymes (e.g. erythromycin esterase *ereA* and macrolide phosphorylase *mphA*). For some of these genes, especially the rRNA methyltransferases, putative leader ORFs have been mentioned in literature [85, 95, 96]. For the others, we obtained the sequences of the upstream regions from GenBank and analyzed the upstream regions for the presence of short ORFs. The analysis was carried out using a software program developed by Sai Lakshmi Subramanian in this lab. The software looks for ORFs in a specified sequence segment and looks for the presence of a putative ribosome binding site Shine-Dalgarno (SD) region [97, 98]. The analysis showed that short ORFs can be found in the leader regions of 30% of the macrolide resistance genes in the database. A list of the identified leader peptide sequences is shown in Table VIII.

TABLE VIII

LEADER PEPTIDES OF MLS_B RESISTANCE GENES

Name[1]	Leader peptide sequence	Genbank Accession No.[2]
IFVI peptides		
ErmAL2	MGMFS**IFVI**ERFHYQPNQK	AF002716
ErmAL2	MGTFS**IFVI**NKVRYQPNQN	X03216
ErmCL	MGIFS**IFVI**STVHYQPNKK	V01278
ErmGL2	MGLYS**IFVI**ETVHYQPNEK	M15332
ErmTL	MGIFS**IFVI**NTVHYQPNKK	AY894138
ErmTL	MGIFS**IFVI**NTVHYQPNKK	M64090
ErmYL	MGNCS**LFVI**NTVHYQPNEK	AB014481
Erm33L	MGIFS**IFVI**NTVHYQPNKK	AJ313523
IAVV peptides		
ErmAL1	MCTC**IAVV**DITLSHL	AF002716
ErmAL1	MCTS**IAVV**EITLSHS	X03216
Erm36L	MGSPS**IAVT**RFRRF	AF462611
RLR peptides		
EreAL	**MLR**SRAVALKQSYAL	AF099140
Erm34L	MHFI**RLR**FLVLNK	AY234334
ErmDL	MTHSM**RLR**FPTLNQ	M29832
MefAL	MTASM**RLR**	AF274302
MsrAL	MTASM**RLK**	AB013298
MsrAL	MTASM**RLK**	AB016613
MsrCL	MTASM**KLR**FELLNNN	AY004350
ErmXL	MLISGTAFL**RLR**TNR	U21300
ErmXL	MLISGTAFL**RLR**TNRKAFPTP	M36726
ErmQL	MIMNGGIASI**RLR**R	L22689
ErmWL	MGFSFTGSAFI**RLR**TA	D14532
ErmFL	MKTPTGLSGSISQ**RVR**TLVK	M17808
Miscellaneous peptides		
MefBL	MYLIFM	FJ196385
MsrDL	MYLIFM	AF274302
ErmGL1	MRIDDYCS	L42817
MphCL	MYQIKNGN	AF167161
EreAL	MSLVIGEAKV	AF512546
Erm37L	MRTAPEPWGW	BX842578
MphBL	MAKEALEVQGS	D85892
ErmGL1	MNKYSKRDAIN	M15332
ErmEL	MRVSVRVAACARC	M11200
ErmFL	MMLCCRLSFFLLSR	M62487
MphAL	MNKTKGCLIANFATVPD	D16251
Erm38L	MSITSMAAPVAAFIRPRTA	AY154657
EreAL	MQLTVKSFVRFACYASYRN	AF512546
ErmGL2	MNHEYVLFSKNINIRKEMQ	L42817
EreBL	MRIXRKTAYARPCALAEEGRX	A15097
EreBL	MRINRKTAYARPCALAEEGRG	AB207867
Erm41L	MMVLRRVRPTVATPVGLVSAH	EU177504
ErmSL	MSMGIAARPPRAALLPPPSVPRSR	M19269
ErmTL	MRNVDKTSTVLKQTKNSDYADK	AJ488494
ErmBL	MLVFQMRNVDKTSTVLKQTKNSDLRR	AF299292
ErmBL	MLVFQMCNVDKTSTVLKQTKNSDYADK	U86375
ErmBL	MLVFQMRNVDKTSTVLKQTKNSDYADK	M11180

Name[1]	Leader peptide sequence	Genbank Accession No.[2]
ErmBL	MLVFQIRNVDKTSTGLKQTKNSDYADK	AF080450
ErmBL	MLVFQMRYQMRYVDKTSTVLKQTKKSDYADK	M19270
ErmBL	MLVFQMRNVDKTSTILKQTKNSDYVDKYVRLIPTSD	K00551
ErmFL	MLSAFIFSSFSLIYRAKLLNLPLYNYKRISL	M62487
ErmNL	MARTLFAGRTELWAPAIEPPVKAATHTAVRRD	X97721
ErmVL	MAANNAITNSGLGRGCAHSVRMRRGPGALTGPGSHTAR	U59450

[1]'L' indicates leader

[2]References for the leader peptide sequences can be found within the Genbank records

Many of these leader ORFs have a well-defined SD sequence upstream, strongly indicating that they are translated. However, even the absence of a SD sequence does not necessarily rule out a role for the leader ORFs in regulation, since bacterial genomes contain a significant proportion of leaderless genes as well as genes with weak or poorly recognizable SD sequence [99]. We analyzed the sequences of the predicted leader ORFs and determined that the encoded peptides can be grouped into several sequence classes (Table VIII).

The most familiar class is that of the 'IFVI' peptides, of which the prototype is ErmCL. As discussed in the Literature Review section, ribosome stalling occurs at the Ile_9 codon of *ermCL*, in the presence of erythromycin [12]. All the peptides of the 'IFVI' group are 19 amino acids long. Notably, in all peptides, the conserved '$IFVI_9$' domain, which is critical for ribosome stalling at *ermCL*, is located at the same distance from the N-terminus of the sequence, as in ErmCL.

In the second group, i.e., the 'IAVV' group of peptides, the encoded peptides are 14 or 15 amino acids long. The site of ribosome stalling at any of these ORFs was yet to be determined; although, as mentioned earlier, there was strong genetic evidence that translation of *ermAL1* is involved in regulation of *ermA* [74].

The third, 'RLR' group contains a much more diverse set of peptides, with lengths ranging from 8 to 21 amino acids. Unexpectedly, among peptides of this group, the 'RLR' motif or its slight variations are present at a varying distance from the N-terminus. *In vivo* genetic evidence predicted that ribosome stalling occurs when the Leu7 codon of this motif in the *ermDL* ORF enters the A-site [83]. However, no biochemical confirmation of this prediction has been ever carried out.

The fourth, fairly large group represents peptides that we classified as 'miscellaneous'. These peptides do not show homology to any of the other peptides enocded in the leader regions of macrolide resistance genes. The only leader ORF in this group which has been studied to some extent is *ermBL* (Genbank accession number K00551). Genetic analysis suggests that ribosome stalling should occur at codon 10 [11]. However, the interpretation of these studies could be complicated by using a reporter system which could be affected by the inducing antibiotic in a variety of ways.

The near ubiquitous presence of likely translatable ORFs in the leader regions of many macrolide resistance genes indicates that they possibly play a role in regulation of expression of resistance. Furthermore, several available examples and sequence convergence of some ORFs argue that programmed ribosome stalling could be a common theme in the mechanism of induction.

The large variety of the identified ORFs precluded us from analyzing ribosome stalling at all of the sequences. Instead, we chose representatives of the major sequence classes of putative stalling peptides and investigated whether they direct drug-dependent programmed translation arrest. In the following sections, we describe analysis of some of these leader ORFs which involved mapping of ribosome stalling sites and characterization of the stalled ribosome complexes.

B. Identification of ribosome stalling sites at leader ORFs of macrolide resistance genes

Based on the classification of putative regulatory peptides presented in Table VIII, we determined the ability of a few representative ORFs from each group to direct formation of a stalled ribosome complex (SRC), *in vitro*. For this purpose, we used the method of primer

extension inhibition analysis commonly known as toeprinting [8, 28, 87]. In a typical experiment, a specific mRNA is translated in a cell-free translation system. In the presence of an inducing antibiotic, SRC is formed (Figure 14).

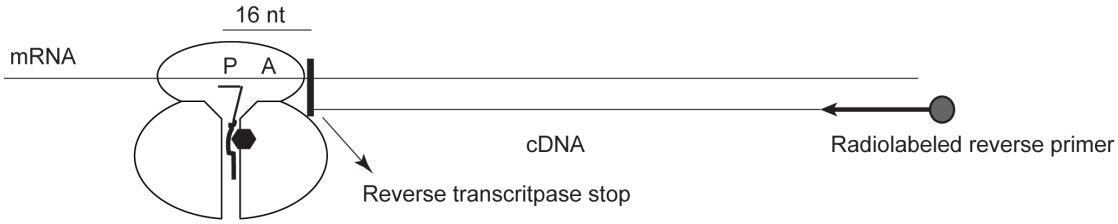

Figure 14. Principle of toeprinting assay. A stalled ribosome carrying peptidyl-tRNA and bound erythromycin (hexagon) inhibits progression of reverse transcriptase. P and A-sites of the SRC are indicated. The distance between the reverse transcriptase stop and the P-site codon is approximately 16-17 nt. Radiolabeled cDNA products are visualized on a sequencing gel to identify the ribosome stalling site.

Subsequently, a radiolabeled DNA primer is annealed downstream of the putative stalling site and is extended by reverse transcriptase. An SRC inhibits the progression of reverse transcriptase when the enzyme encounters the leading edge of the ribosome (Figure 14). The 3' end of the resulting cDNA is located approximately 16-17 nucleotides from the 1st nucleotide of the P-site codon. Therefore, upon separation of the resulting radiolabeled cDNA fragments in a denaturing gel along with sequencing reactions, the codon at which ribosome stalling occurs can be accurately determined. This method has been used previously for identification of ribosome stalling site at *secM* and *ermCL* regulatory ORFs [12, 28].

DNA templates carrying 16 different leader ORFs were generated by PCR as described in Materials and Methods (Figure 11). These templates were used to direct coupled transcription-translation reactions, in the presence or absence of erythromycin (50 μM), using

an *E.coli* cell-free system assembled from purified components (PURE SYSTEM) [86]. Subsequently, primer extension analysis was carried out using a radiolabeled primer to detect SRC formation and locate the position of the stalled ribosome. Altogether, we looked for indications of programmed ribosome stalling at 16 leader ORFs. Of these, strong toeprint signals indicative of stable SRC formation were obtained for 11 sequences (Figures 15-17). Three more leader ORFs gave weak, but clear toeprint signals, indicating weak or transient ribosome stalling. For the remaining two leader ORFs, we did not obtain any toeprint signal, indicating a lack of ribosome stalling under our experimental conditions. The results of the toeprinting analysis are summarized in Table IX.

In the 'IFVI' group of peptides, the sequence of ErmAL2 is highly homologous to ErmCL and not surprisingly, ribosome stalling at *ermAL2* was observed at the Ile9 codon (Figure 15A), identical to *ermCL*.

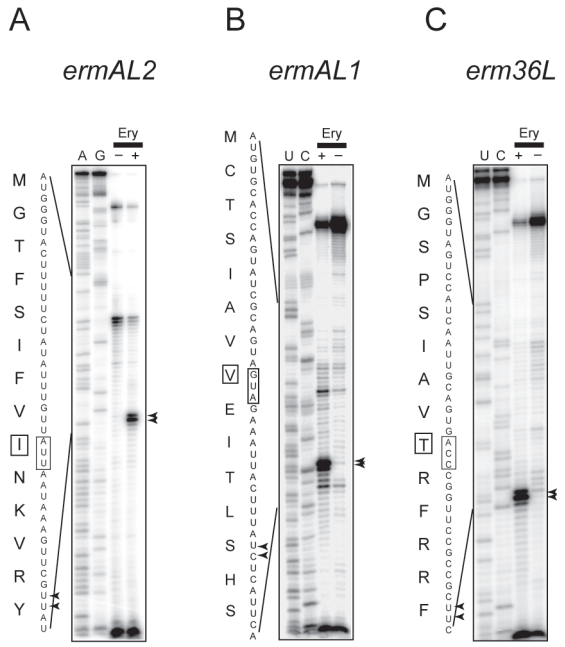

Figure 15. Primer extension inhibition analysis [87] of leader ORFs encoding peptides of the 'IFVI' and 'IAVV' groups. The ORFs indicated above each gel were translated *in vitro* in the absence (-) or presence (+) of erythromycin (Ery). A primer was annealed to the 3' end of the mRNA and extended with reverse transcriptase [12, 28]. The same primer was used to generate sequencing lanes (U, C). The sequence of the leader ORF gene and the encoded peptide sequence are shown to the left of the gel. Reverse transcriptase stops (toeprints) are indicated by arrowheads. The codon located in the P-site of the stalled ribosome is boxed.

In the peptides of the 'IAVV' class, ribosome stalling was observed at the 4th codon of this motif, which encodes valine in *ermAL1* (IAVV) or threonine in *erm36L* (IAVT), at homologous positions (Figure 15B and C). Since ribosome stalling occurs within the conserved motif, it was tempting to think that the 'IAVV/T' sequence plays an important role in ribosome stalling.

In the 'RLR' group, ribosome stalling occurred at the conserved leucine codon of this motif in all the tested ORFs irrespective of the location of the motif relative to the peptide's

N-terminus (*ermDL*, *msrCL*, *msrSAL*, *erm34L* and *ermXL*) (Figure 16A-C, E and F), except for *ereAL* (Figure 16D).

In *ermDL*, it was incorrectly predicted that leucine7 is present in the A-site of the SRC based on induction of a reporter gene fused to *ermD* [83]. The *ereAL* ORF caused drug-dependent ribosome stalling at the third arginine codon of the 'MLR' motif. This indicates that in the *ereAL*-SRC, the peptidyl-tRNA carries a peptide of only 3 amino acids (if the A-site amino acid is not incorporated in the peptide chain) or 4 amino acids (if the A-site amino acid is incorporated). In either case, the length of the peptide is unexpectedly short for a stable SRC, since it has been reported that tRNAs carrying such short peptides are prone to rapid dissociation from the ribosome [100].

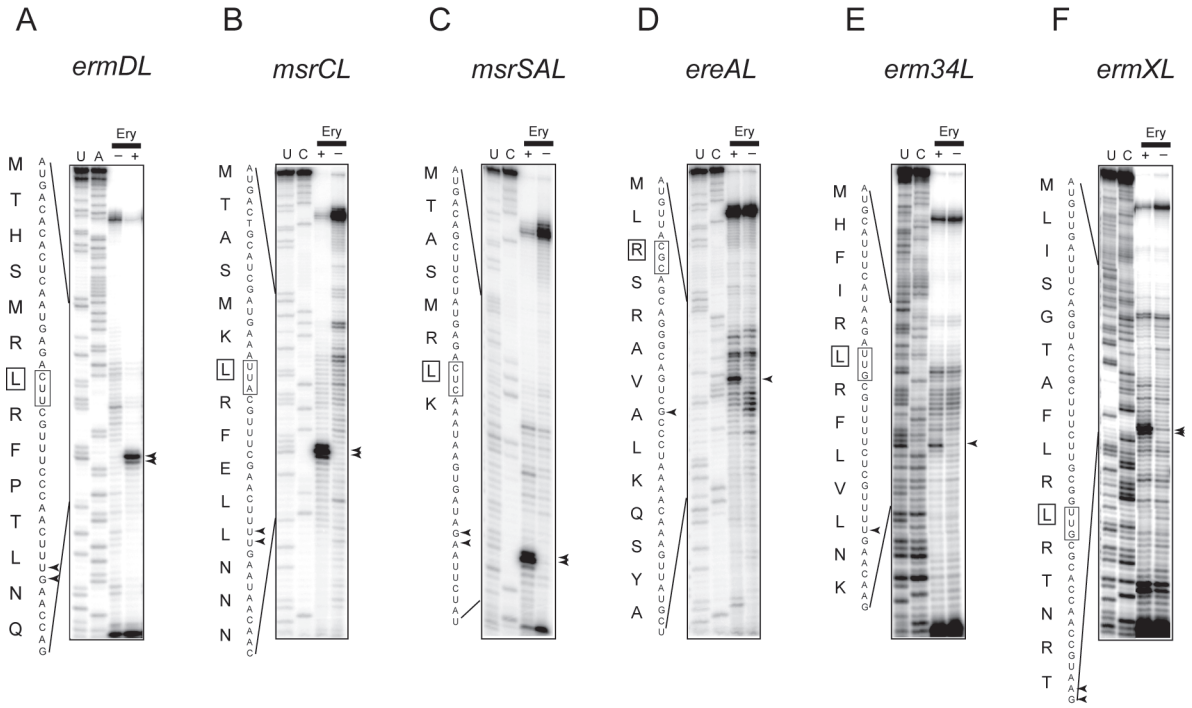

Figure 16. Primer extension inhibition analysis of leader ORFs encoding peptides of the 'RLR' class.

Strong erythromycin-dependent toeprints were detected at *ermBL* and *msrDL* ORFs, which belong to the Miscellaneous group (Figure 17A and B). In agreement with genetic data, translation of *ermBL* resulted in formation of a SRC, with the P-site located at the Asp10 codon [11]. Translation of peptide encoded in the *msrDL* ORF (MYLIFM) in the presence of erythromycin resulted in a strong toeprint at the last sense codon, Met6. Thus, alongside with EreAL, MsrDL peptide represents another very short stalling peptide.

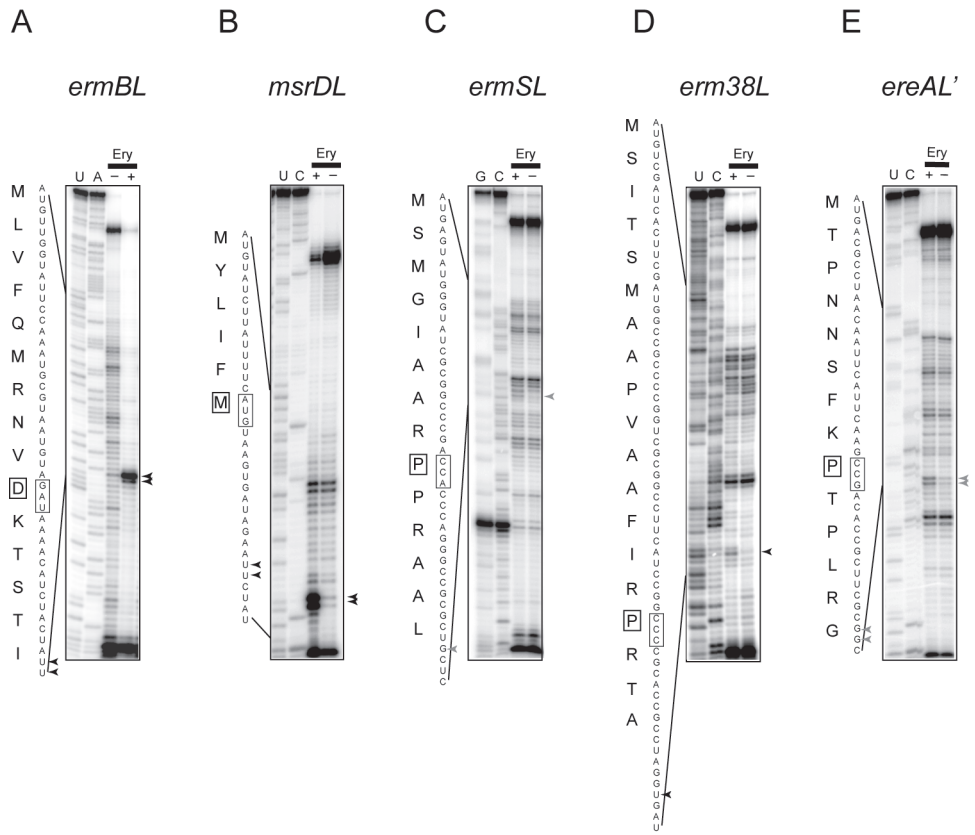

Figure 17. Primer extension inhibition analysis of leader ORFs encoding peptides of the 'miscellaneous' class.

Translation of *ermSL*, *erm38L* and *ereAL'* resulted in weak but distinct toeprints at proline codons (Figure 17C-E). Interestingly, proline is preceded by a positively charged amino acid, either arginine or lysine, in all these three leaders. Thus, ErmSL, Erm38L and EreAL' can be grouped as stalling peptides characterized by the 'R/KP' motif. Therefore in Table IX we grouped them into a new class of R/KP peptides.

Translation of *ermGL2* and *erm37L* did not result in any toeprint, indicating that erythromycin does not induce strong stalling at these ORFs (Figure 18A and B).

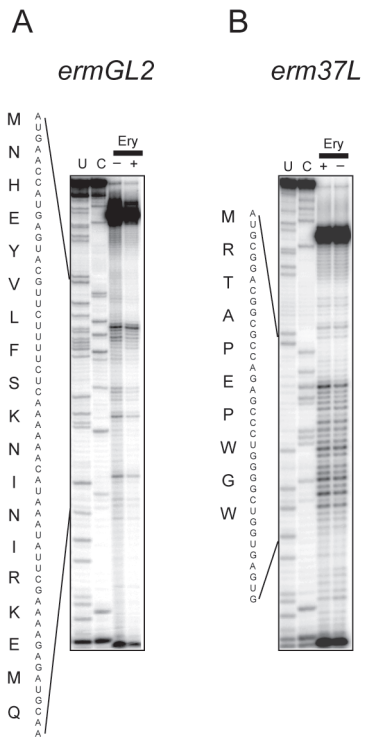

Figure 18. Primer extension inhibition analysis of leader ORFs encoding some of the 'miscellaneous class' peptides.

The *ermGL2* sequence analyzed here is the second of two leader ORFs which occur upstream of *ermG* in *Bacteroides thetaiotaomicron* (GenBank accession number L42817). In this strain, it is predicted that the resistance gene is expressed constitutively, although conclusive proof is lacking [101]. On the other hand, another *ermG* gene, present in *B. sphaericus* (GenBank accession number M15332) is inducible by erythromycin [102]. However, the leader regions of these two *ermG* genes show very weak homology. In case of the latter inducible *ermG*, the second leader ORF is in fact very similar to *ermCL*. Therefore, it is possible that the leader region of *ermG* from *B. thetaiotamicron* represents a constitutive version of the original inducible gene, which has undergone significant changes through

mutations. This would explain why erythromycin-induced stalling was not observed at this leader ORF in our experiments.

The *erm37* methyltransferase is encoded by *M.tuberculosis* and is known to be expressed inducibly, in response to erythromycin and other macrolide antibiotics [103]. However, induction of *erm37* was shown to occur through activation of the transcriptional regulator, *whiB7*, that controls multidrug resistance [104]. Due to the presence of a short ORF upstream of inducible *erm37*, we wanted to determine if this gene could be regulated by programmed ribosome stalling and thus could contribute to the induction mechanism. In view of our finding that the drug does not induce ribosome stalling at *erm37L*, this possibility seems unlikely. Furthermore, no other putative regulatory ORFs were detected in the upstream region of *erm37*.

TABLE IX

SUMMARY OF PRIMER EXTENSION ANALYSIS OF VARIOUS LEADER ORFs

Leader peptide	Leader peptide sequence with ribosome stalling site[1]	Strength of toeprint
IFVI peptides		
ErmCL[1]	MGIFS**IFVI**STVHYQPNKK	Strong
ErmAL2	MGTFS**IFVI**NKVRYQPNQN	Strong
IAVV peptides		
ErmAL1	MCTS**IAVV**EITLSHS	Strong
Erm36L	MGSPS**IAVT**RFRRF	Strong
RLR peptides		
EreAL	**MLR**SRAVALKQSYAL	Strong
Erm34L	MHFI**RLR**FLVLNK	Strong
ErmDL	MTHSM**RLR**FPTLNQ	Strong
MsrSAL	MTASM**RLK**	Strong
MsrCL	MTASM**KLR**FELLNNN	Strong
ErmXL	MLISGTAFL**RLR**TNRKAFPTP	Strong
R/KP peptides		
Erm38L	MSITSMAAPVAAFIR**P**RTA	Weak
EreAL′	MTPNNSFK**P**TPLRGAA	Weak
ErmSL	MSMGIAAR**P**PRAALLPPPSVPRSR	Weak
Miscellaneous peptides		
MsrDL	MYLIF**M**	Strong
ErmBL	MLVFQMRNV**D**KTSTILKQTKNSDYVDKYVRLIPTSD	Strong
ErmGL2	MNHEYVLFSKNINIRKEMQ	None
Erm37L	MRTAPEPWGW	None

[1]Codons corresponding to the amino acids indicated in red were determined to be located in the P-site of the SRC, by toeprint analysis. The conserved motif in each group of leader peptides is indicated in bold.

C. Characterization of ribosome stalling at the *ermAL1* ORF

In this section we investigated in more detail the nascent peptide sequence requirements for formation of the stalled ribosome complex at the *ermAL1* ORF.

1. Role of the *ermAL1* nascent peptide sequence in ribosome stalling

We suspected that the structure of ErmAL1 peptide or its gene is critical for ribosome stalling. Therefore, we first tested if changes in mRNA structure that do not

affect the peptide sequence would affect stalling. A total of 9 synonymous mutations were introduced simultaneously at *ermAL1* codons 2-7 (Figure 19). Erythromycin-dependent stalling of the ribosome at the mutant mRNA was as prominent as with wild-type mRNA, arguing that the structure of mRNA has little influence on SRC formation.

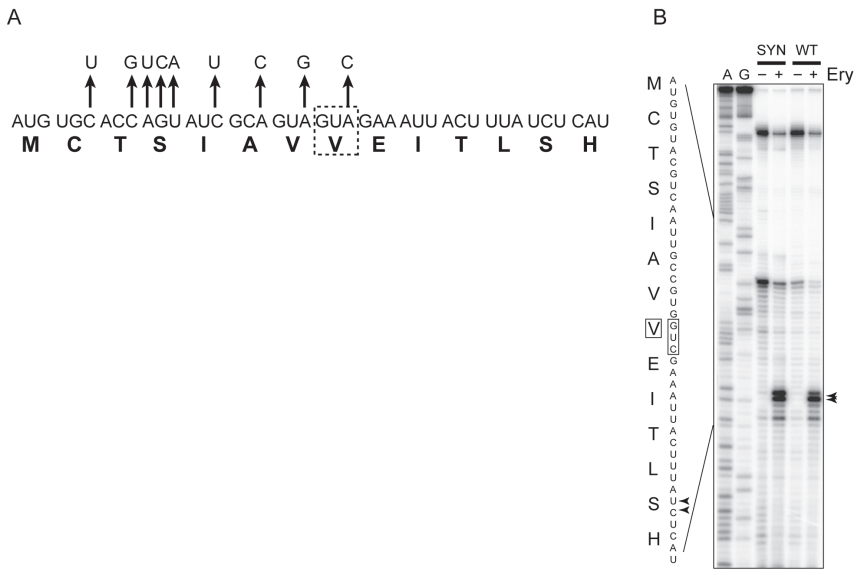

Figure 19. Effect of synonymous codon mutations on ribosome stalling at *ermAL1*. (A) Sequence of the *ermAL1* ORF and the encoded peptide. Arrows indicate the synonymous mutations that were introduced simultaneously at nine positions in *ermAL1*. (B) Primer extension inhibition analysis of erythromycin-dependent ribosome stalling at mutant *ermAL1* carrying synonymous mutations (SYN) or wild-type *ermAL1* (WT) [105].

We then determined whether altering the amino acid residues of ErmAL1 would influence ribosome stalling. Amino acid residues 2-8 of ErmAL1 were mutated one at a time to alanine (position 6, which is alanine in the wild-type ErmAL1 sequence was mutated to glycine). While changing codons 2-4 had no effect on SRC formation, mutations of codons

Ile5, Ala6, Val7, or Val8 abolished ribosome stalling (Figure 20). Thus we could conclude that C-terminal four-aa-sequence of the *ermAL1* nascent peptide directs programmed translation arrest in the presence of erythromycin.

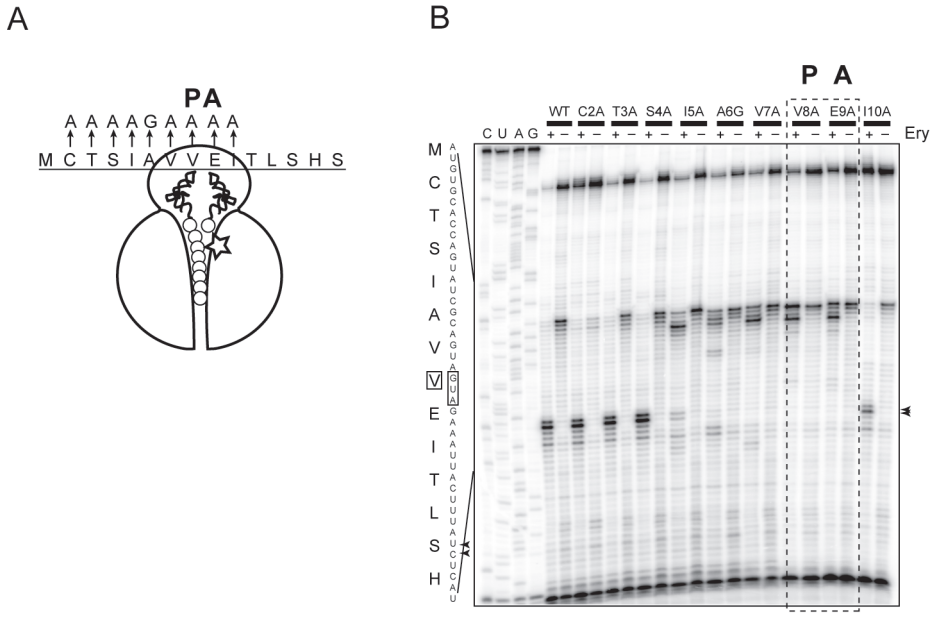

Figure 20. Effect of mutations of codons 2-10 of *ermAL1* on ribosome stalling. The amino acid changes associated with the codon mutations are indicated in the cartoon (A) and above the corresponding lanes of the gel (B). The primer extension bands representing SRC at the *ermAL1* eighth codon are shown by arrowheads. Lanes representing mutations at P- site and A-site codons are boxed. In the cartoon, the star represents erythromycin bound in the tunnel [105].

2. Stalled ribosome is unable to catalyze peptide bond formation

Translation arrest at the 8th codon of *ermAL1*, as determined above, is compatible with two scenarios (Figure 21).

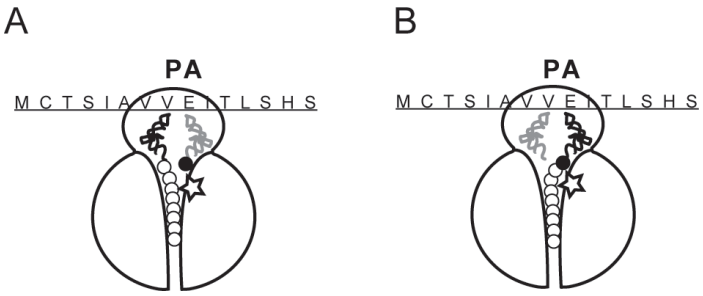

Figure 21. Two scenarios of ErmAL1-peptidyl-tRNA in the SRC. P-site of the SRC is located at valine in both scenarios. (A) 8 amino acid-long peptide terminating in valine is linked to valyl-tRNA in the P-site. (B) 9 amino acid-long peptide terminating in glutamic acid (filled circle) is linked to glutamyl-tRNA in the A site. Erythromycin molecule bound in the exit tunnel is represented by a star [105].

The ribosome may stall because peptide bond formation is impaired; in this case an octapeptide encoded in the first eight codons of *ermAL1* would be esterified to the P-site $tRNA^{Val}$ (Figure 21A). Alternatively, if translation is arrested after the next peptide bond is formed, then a 9–amino acid peptide would be esterified to the A-site $tRNA^{Glu}$, leaving a deacylated $tRNA^{Val}$ in the P-site (Figure 21B). To distinguish between these possibilities, the nature of peptidyl-tRNA in the SRC was analyzed by Northern blotting. The products of the *in vitro* translation reaction of the *ermAL1* ORF carried out in the absence or presence of antibiotic were separated in denaturing acidic polyacrylamide gel, transferred to a nylon membrane and probed with radioactive probes specific for either $tRNA_1^{Val}$ or $tRNA^{Glu}$. Results are shown in Figure 22.

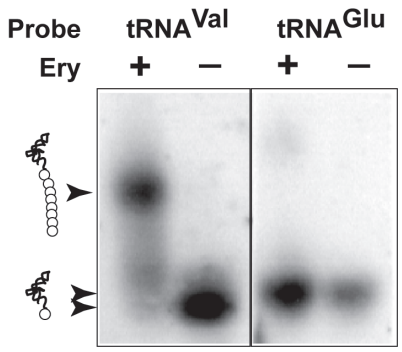

Figure 22. Identification of peptidyl-tRNA in the *ermAL1*-SRC. The gel represents Northern blot analysis of tRNA associated with the stalled ribosome. Positions of aminoacyl-tRNAs and peptidyl-tRNA are indicated [105].

In the presence of erythromycin, $tRNA_1^{Val}$ decoding the *ermAL1* 8th codon GUA migrated more slowly in the gel, indicating its association with the nascent peptide (Figure 22). In contrast, the mobility of $tRNA^{Glu}$ corresponding to the *ermAL1* 9th codon remained unchanged upon translation of *ermAL1* in the presence of erythromycin. This result shows that the ribosome arrested at the 8th codon of *ermAL1* is unable to catalyze transfer of the 8–amino acid nascent peptide to the glutamyl moiety of Glu-$tRNA^{Glu}$ decoding the A-site codon (Figure 21A). Thus we concluded that translation arrest results from impairment in the activity of the PTC, which prevents catalysis of peptide bond formation.

3. The nature of the A-site amino acid is critical for stalling

Previous studies of ribosome stalling at the *ermCL* regulatory ORF indicated that mutations of the codon located in the SRC A-site had little effect on stalling [12, 45]. In striking contrast to those results, replacement of the Glu_9 codon of *ermAL1* with an Ala (GCA) codon dramatically reduced the efficiency of SRC formation (Figure 20). This indicates that the identity of the A-site codon and thus the nature of the aminoacyl-tRNA in the A-site are critical for drug and nascent peptide–dependent translation arrest at *ermAL1*.

We further verified this important conclusion by replacing the wild-type Glu_9 codon with codons specifying each of the other 18 conventional amino acids. Only a subset of the tested codons was found to be conducive to SRC formation (Figure 23).

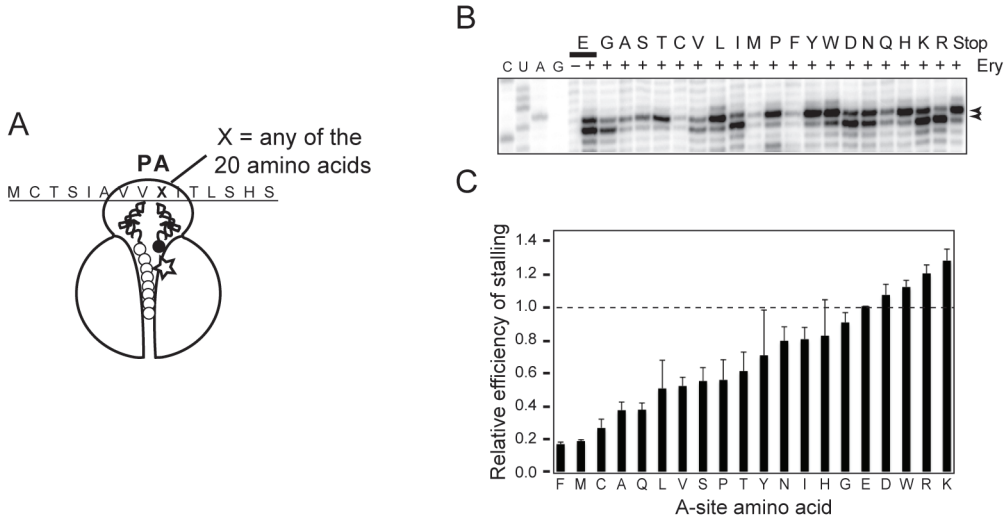

Figure 23. Effects of mutations in the 9th codon of *ermAL1* on ribosome stalling. (A) The A-site codon of the *ermAL1* ORF was mutated to represent each of the other 19 amino acids. (B) Result of toeprint analysis of *ermAL1* mutants. The control (no erythromycin) lane is shown only for the wild-type *ermAL1* sequence. (C) The bar diagram represents the results of quantitation of the intensity of the "stalled ribosome" bands (an average of three independent experiments) [105].

Stalling was especially prominent with codons corresponding to charged amino acids (Glu, Asp, Lys, Arg, His). Codons specifying certain uncharged amino acids (Trp, Ile, Tyr) also strongly promoted translation arrest. In contrast, we found that in addition to the Ala codon, SRC formation was significantly inhibited or even completely abolished when Phe, Met, or Cys codons replaced the Glu_9 codon of *ermAL1*. This unexpected observation that SRC formation at the *ermAL1* ORF depends on the nature of the aminoacyl-tRNA specified by the A-site codon unveiled the importance of the ribosomal A-site in the mechanism of

drug and nascent peptide–controlled translation arrest.

Mutations at the A-site codon result in binding of aminoacyl-tRNAs that differ from the wild-type Glu-tRNA^{Glu} both in the structure of the tRNA body and the nature of the acceptor amino acid substrate placed in the PTC. To discern which of these two features is central to the ribosome stalling response, we compared effects of pairs of tRNA isoacceptors differing in the structure of tRNA but delivering the same amino acid. The 9th codon of *ermAL1* was replaced with pairs of synonymous codons decoded by glutamine, serine, leucine, and arginine tRNA isoacceptors (Figure 24).

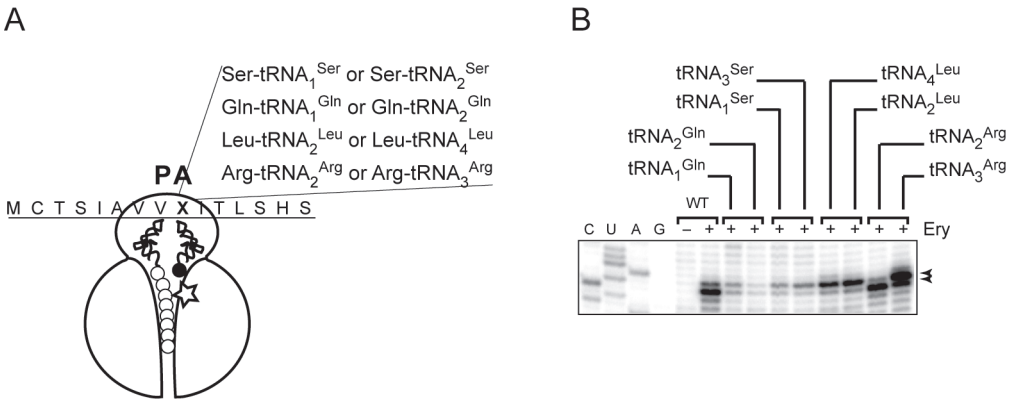

Figure 24. Effects of A-site codons decoded by different tRNA isoacceptors on ribosome stalling. Note that a single nucleotide shift in the position of the band observed with tRNA^{Arg} isoacceptors apparently reflects change in the ribosome geometry in response to binding of different tRNAs which affects the precise site where reverse transcriptase stops. This effect was also seen when binding of different tRNAs was directed to the A-site (see gel in Figure 23) [105].

Primer extension inhibition analysis showed that with each pair of synonymous codons, both isoacceptor aminoacyl-tRNAs were either equally conducive to SRC formation (pairs of tRNA^{Leu} or tRNA^{Arg}) or were similarly inefficient in promoting stalling (tRNA^{Gln} or

$tRNA^{Ser}$ pairs). This observation led us to conclude that the structure of tRNA itself had little influence upon translation arrest, which left the amino acid residue delivered to the PTC A-site as the primary determinant for discrimination.

4. In the stalled ribosome complex, certain amino acids serve as poor acceptors of the ErmAL1 nascent peptide

The Northern blot analysis (Figure 22) showed that the ribosome stalled at the 8^{th} codon of *ermAL1* is unable to transfer peptide from peptidyl-$tRNA^{Val}$ to Glu-$tRNA^{Glu}$ positioned in the ribosomal A-site. The A-site codon mutations revealed that only a subset of aminoacyl-tRNAs is conducive to stalling (Figure 23). We therefore hypothesized that in the stalled ribosome, some ("stalling") amino acids serve as particularly poor acceptors in the peptidyl transfer reaction, whereas other ("non-stalling") amino acids are still able to function as fairly efficient acceptor substrates in the reaction of peptide bond formation. To directly test this hypothesis, we analyzed transfer of the ErmAL1 N-terminal octapeptide to model A-site substrates CCA-N-Lys or CCA-N-Ala in which the aminoacyl-tRNA 3' end analog CCA is linked via a stable amide bond to a stalling (Lys) or nonstalling (Ala) amino acid (Figure 25).

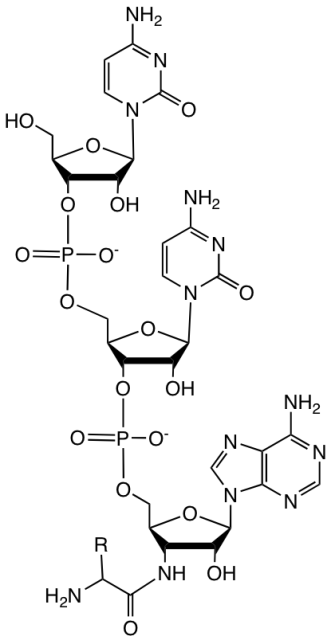

R=Me, $H_2N(CH_2)_4$-

Figure 25. Structure of CCA-N-aminoacyl analogs. The R group indicates Alanine (Me) or Lysine ($H_2N(CH2)_4$).

Importantly, because binding of these substrates is codon-independent, this experiment directly focuses on the role of the A-site amino acid in the formation of the stalled translation complex. The *ermAL1* mRNA, truncated after the 8th codon, was translated *in vitro* in the presence of (^{35}S)-methionine and erythromycin. The SRC carrying radiolabeled peptidyl-tRNA was isolated by sucrose gradient centrifugation and allowed to react with an excess (1 mM) of CCA-N-Lys or CCA-N-Ala (Figure 26A).

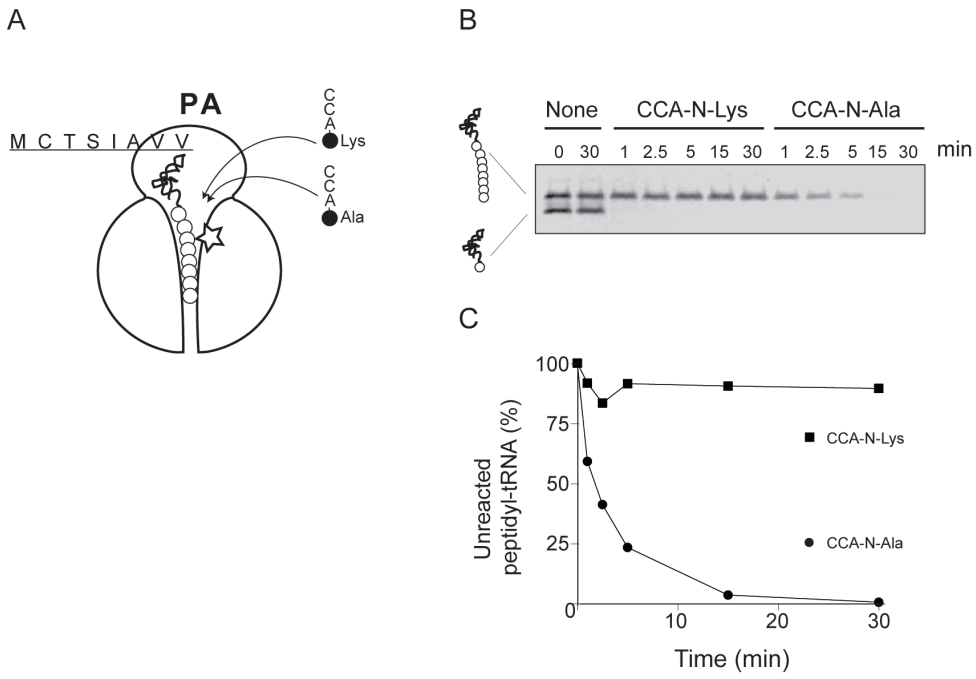

Figure 26. Differential acceptor activity of stalling and non-stalling amino acids in the peptidyltransferase reaction of the SRC. (A) The ribosome stalled at the end of the truncated *ermAL1* mRNA was allowed to react for a specified time at 37°C with 1 mM CCA-N-Ala or CCA-N-Lys and the remaining unreacted peptidyl-tRNA was resolved by gel electrophoresis. (B) The first two lanes in the gel show samples incubated for 0 or 30 min in the absence of aminoacyl-tRNA analogs. (C) The graph represents the results of quantitation of the amount of radioactivity in the peptidyl-tRNA bands [105].

We monitored progression of the reaction by quantifying the amount of unreacted peptidyl-tRNA resolved on a Tricine-SDS polyacrylamide gel (the reaction products CCA-N-nonapeptides were too small to for a distinct band in the gel suitable for direct quantitation). The ErmAL1 nascent peptide in the SRC showed a strikingly different reactivity to the tested aminoacyl-tRNA analogs. The peptide was virtually unreactive with the substrate that contained the stalling amino acid (CCA-N-Lys) as could be judged from the essentially unchanged intensity of the peptidyl-tRNA band even after 30 min of incubation at 37°C. In contrast, the amount of SRC-associated peptidyl-tRNA rapidly decreased on incubation with CCA-N-Ala (Figure 26B), indicating that the ribosome could fairly efficiently catalyze

transfer of the ErmAL1 nascent peptide to a non-stalling amino acid. While the tested aminoacyl-tRNA analogs showed a remarkably different reactivity with the peptidyl-tRNA in the SRC, both of them could be readily used as acceptors in the uninhibited reaction of peptide bond formation. When 70S initiation complex carrying fMet-tRNA in the P-site was reacted with these substrates in the absence of antibiotic, transfer of formyl-methionine to either CCA-N-Ala or CCA-N-Lys occurred very quickly: the band of fMet-tRNA completely disappeared after only 30 sec of incubation—the shortest time point we could reliably test in our experimental setup (Figure 27).

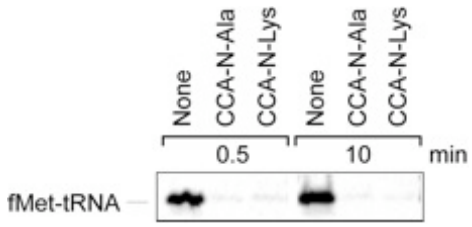

Figure 27. Reactivity of aminoacyl-tRNA analogs with fMet-tRNA^{fMet}. Ribosomes stalled on *ermAL1* mRNA truncated at the 8th codon and containing fMet-tRNA^{fMet} bound in the P-site were reacted with CCA-N-Ala or CCA-N-Lys. Remaining unreacted fMet-tRNAfMet was resolved by gel electrophoresis [105].

Thus, the results of the experiments with the model A-site substrates strongly supported our assertion that the presence of ErmAL1 nascent peptide and erythromycin in the NPET alters properties of the PTC A-site in such a way that peptide bond formation in SRC becomes particularly slow with certain amino acids. Codons of such amino acids, including the wild type Glu9 codon of *ermAL1* promote formation of a stable SRC.

We independently verified this conclusion by analyzing how the nature of the 9th amino acid in the ErmAL1 peptide (the A-site amino acid in the SRC) affects the frequency at which the ribosome can bypass the *ermAL1* stalling site. Since the wild-type ErmAL1 peptide cannot be reliably resolved in a gel because of its small size, we introduced a frameshift mutation in codon 12 of *ermAL1* which extended the ORF to 72 codons. In the presence of erythromycin, only a small fraction of the translating ribosomes could continue translation beyond the stalling site in the wild-type *ermAL1*: minute amounts of the full-length polypeptide were synthesized and a large amount of peptidyl-tRNA (likely corresponding to peptidyl-tRNA^{Val} in the SRC) accumulated (Figure 25).

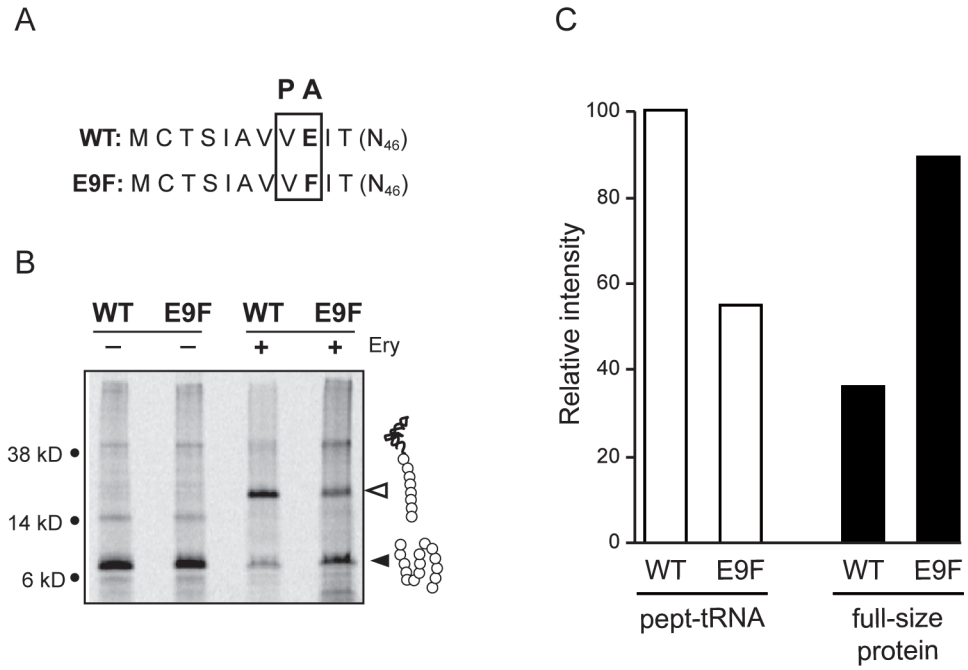

Figure 28. Translation of an extended *ermAL1* ORF encoding a stalling or non-stalling amino acid in the 9th codon. (A) The *ermAL1* ORF, extended to 72 codons and carrying Glu (wild-type, stalling) or Phe (mutant, non-stalling) in the 9th position was translated in the presence or absence of erythromycin. The codons located in the P and A-sites of the SRC are boxed. The position of gel bands representing a 72–amino acid full-size translation product and peptidyl-tRNA esterified by an 8–amino acid nascent peptide are marked by filled and contoured arrowheads, respectively. Four-fold less material was loaded onto the no-erythromycin lanes compared with the erythromycin lanes. (B) The bar diagram represents the results of quantitation of the amount of radioactivity in the gel bands in the samples containing erythromycin [105].

When the *ermAL1* 9th (Glu) codon was replaced with a codon of the "non-stalling" amino acid Phe, more than twice the amount of full-length polypeptide was produced with a concomitant decrease in accumulated peptidyl-tRNA. This observation was compatible with the notion that nascent peptide in the SRC could be transferred more efficiently to a non-stalling amino acid as compared with the wild-type (stalling) amino acid.

Altogether, these results illuminated an unexpected selectivity of the PTC A-site in the stalled ribosome, imposed by the presence of an antibiotic and a specific nascent peptide

in the NPET. The versatile A-site, which efficiently operates with all types of natural aminoacyl-tRNAs in the "normal" ribosome, becomes highly selective to the nature of the acceptor substrate in the SRC. As a result, the PTC is unable to catalyze peptide bond formation with a range of natural amino acids.

5. The properties of the PTC A-site depend on the nascent peptide sequence

The attributes of SRCs formed at the *ermCL* and *ermAL1* regulatory ORFs are substantially different. While the nature of the A-site amino acid dramatically affects the efficiency of stalling at the *ermAL1* ORF (Figures 20-26), ribosome stalling at the *ermCL* ORF is much less sensitive to the identity of the codon in the A-site of the stalled ribosome [12, 45]. The ribosome that has polymerized the MGIFSIFVI sequence of the ErmCL peptide stalls irrespective of whether the A-site codon is Ser (wild type) or is mutated to Glu (Figure 29).

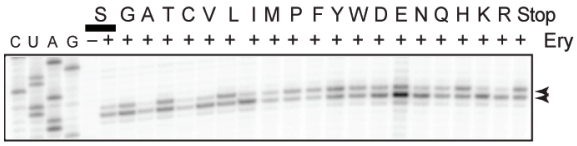

Figure 29. Effects of mutations in the 10th codon of *ermCL*1 on ribosome stalling. The control (no erythromycin) lane is shown only for the wild-type sequence [105].

In contrast, the ribosome that has polymerized the eight N-terminal amino acids of the ErmAL1 peptide (MCTSIAVV) stalls when the 9th (A-site) codon is Glu (wild type) but would not stall if the 9th codon is mutated to Ser (Figure 23). Because in both cases ribosome stalling is controlled by the same drug (erythromycin) but different nascent peptides, it is

most reasonable to think that the PTC A-site properties depend on the structure of the nascent peptide in the NPET. We then asked, which of the critical amino acid residues of the stalling peptide in the tunnel define the properties of the A-site in the PTC?

Although the ErmCL (MGIFSIFVI) and ErmAL1 (MCTSIAVV) stalling nascent peptides are substantially different, the four C-terminal amino acids (IFVI in ErmCL and IAVV in ErmAL1) in both cases are critical for stalling (Figure 20 and [12]). When we transplanted the C-terminal sequence of the ErmAL1 stalling peptide to the ErmCL peptide rendering the hybrid sequence MGIFSIAVV, the stalled complex that formed at the 9^{th} codon of the hybrid ORF acquired A-site selectivity characteristic of the ribosome stalled at *ermAL1*: SRC formed with Glu in the A-site but not with Ser (Figure 30).

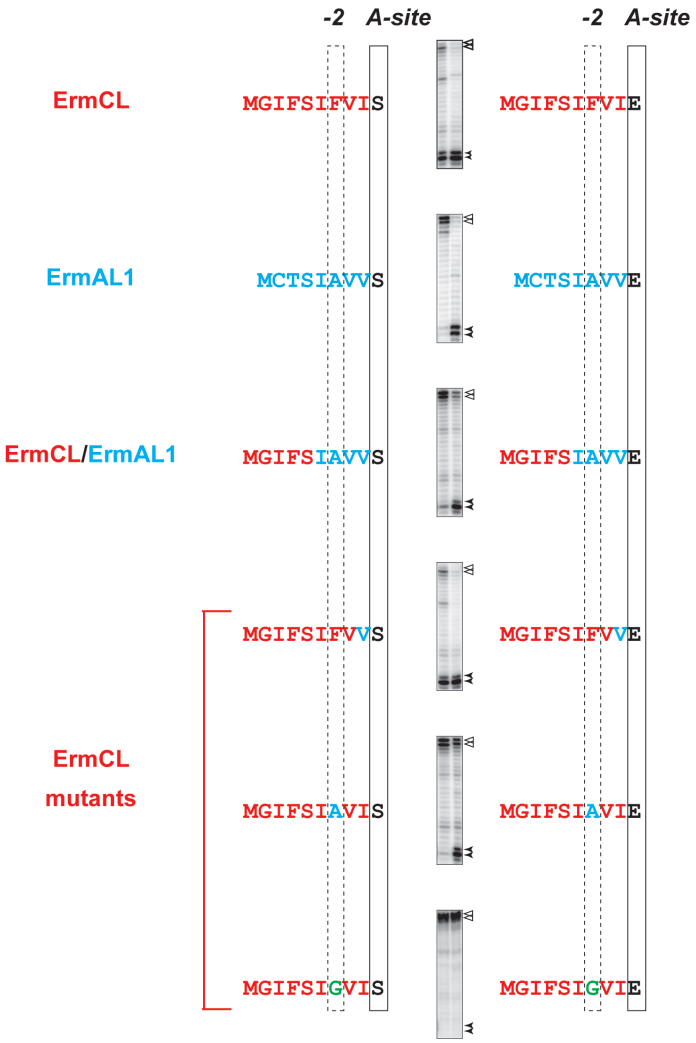

Figure 30. Effect of nascent peptide sequence on properties of the PTC A-site. The gels show the primer extension inhibition signal (bold arrowheads) representing SRC formation at different ORFs (erythromycin was present in all the samples). Bands corresponding to translation initiation sites at the *erm* ORFs are shown for reference and are indicated by thin arrows. The amino acid sequences corresponding to the ErmCL peptide are red, and those representing the ErmAL1 peptide are blue. The Gly mutation at position 7 of ErmCL is shown in green, and the A-site amino acid is black. Amino acids located in the A-site of the PTC in the stalled ribosome are boxed with solid lines. The amino acid position -2 relative to the nascent peptide C-terminus is boxed with a dashed line [105].

Hence, determinants of the A-site properties reside within the four C-terminal amino acids of the stalling peptide. ErmCL wild type (MGIFSIFVI), insensitive to the A-site codon, and the hybrid peptide (MGIFSIAVV), which shows a clear A-site codon selectivity, differ at only two residues: the 9th amino acid (Ile/Val) that in the SRC esterifies the P-site tRNA and

the 7th amino acid (Phe/Ala), at position -2 relative to the nascent peptide C-terminus. Mutation of Ile_9 to Val in ErmCL had little effect on A-site selectivity. However, when Phe_7 of ErmCL was mutated to Ala, the SRC became sensitive to the nature of the A-site codon. If the same residue (Phe_7) was mutated to Gly, stalling was abolished altogether, irrespective of whether the 9th codon was Ser or Glu. Thus, within the context of the ErmCL nascent peptide, the identity of a single amino acid located in the NPET two residues away from the PTC defines the catalytic properties of the PTC active site.

In summary, analysis of the SRC formed at the *ermAL1* ORF indicated that the sequence of the 4 C-terminal amino acids of the nascent peptide is critical for stalling ('$IAVV_8$'). Translation arrest occurs at codon 8 because the ribosome is unable to catalyze formation of the next peptide bond. The combined presence of the nascent peptide and antibiotic in the ribosomal exit tunnel influence the properties of the A-site of the PTC, due to which certain amino acids are restricted from serving as acceptors of the nascent peptide. The nascent peptide residue that is present in the -2 position relative to the P-site plays the key role in affecting the PTC A-site.

D. Characterization of ribosome stalling at *ermBL* and *ermDL* ORFs

Having identified specific features of the drug and nascent peptide-directed stalling at the *ermAL1* regulatory ORF, we wanted to expand this analysis to several other stalling peptides. Comparing SRC formation controlled by peptides with substantially different sequences could illuminate the general and idiosyncratic principles of nascent peptide-dependent translation arrest. In the subsequent experiments, we included a peptide from the RLR class (ErmDL) and one from the miscellaneous class (ErmBL). Both of these peptides (ErmDL – MTHSMRLRFPTLNQ, ErmBL -

MLVFQMRNVDKTSTILKQTKNSDYVDKYVRLIPTSD) differ significantly from the ErmAL1 and ErmCL peptides studied previously.

1. Nascent peptide sequence requirements for ribosome stalling at the *ermBL* ORF

The wild-type *ermBL* ORF directs erythromycin-dependent ribosome stalling at codon 10 (Figure 17A). To determine the role of the ErmBL nascent peptide sequence in stalling, alanine mutations were introduced in codons 2-11 of *ermBL*. The effect of the mutations on ribosome stalling was monitored by toeprinting. Alanine scanning mutagenesis showed that positions 7 (Arg), 9 (Val) and 10 (Asp, P-site codon) contain the key residues because SRC formation was completely abolished by the mutations (Figure 31).

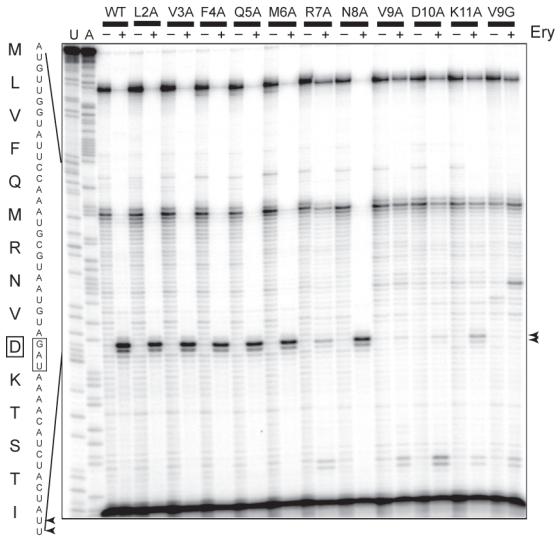

Figure 31. Alanine scanning mutagenesis of *ermBL* and *ermDL* ORFs. (A) Effect of alanine mutations in codons 2-11 and mutation of codon 9 to glycine on ribosome stalling at *ermBL* ORF. (B). Effect of alanine mutations in codons 2-8 of *ermDL* ORF.

Moreover, similar to the phenomenon found with *ermAL1*, SRC formation during translation of *ermBL* was abolished when the A-site codon (Lys) was mutated to Ala. Previous genetic evidence suggested that Val-9-Gly mutation at codon 9 of *ermBL* interferes with ErmBL-controlled induction of the reporter gene [11]. Consistent with these data, this mutation completely abolished SRC formation at codon 10 (Figure 31, last two lanes on the right). Thus, similar to the ErmAL1 peptide, it is the C-terminal sequence of ErmBL nascent peptide as well as the nature of the A-site codon which are critical for SRC formation.

2. ErmBL affects properties of the A-site of the peptidyltransferase center

Translation of *ermBL* in the presence of erythromycin results in ribosome stalling at Asp10, with the nascent peptide sequence being $MLVFQMRNVD_{10}$ (Figure 31). The *ermBL* codon located in the A-site of the SRC encodes Lys11. Mutation of this A-site codon to alanine abolishes ribosome stalling at *ermBL*. This situation is similar to ribosome stalling at *ermAL1*, where mutation of the A-site codon (Glu) to alanine prevents stalling (Figure 20). On the other hand, formation of SRC at the *ermCL* ORF is much less sensitive to the identity of the A-site codon (Figure 29). Previously, we have shown that properties of the PTC A-site is determined by the nascent peptide sequence (see section C, part 5). Specifically, identity of the amino acid located in the position -2 of ErmAL1 and ErmCL nascent peptides (where P-site amino acid is designated '0') defines the properties of the A-site. In the ErmAL1 nascent peptide, this key -2 amino acid is alanine, while that of ErmCL is phenylalanine (Figure 30). Based on this, we asked if the A-site sensitivity of SRC formed at the *ermBL* ORF could also be dictated by the amino acid in the position -2 of the nascent peptide. Thus, we mutated the *ermBL* codons specifying amino acid residues in position -2 of

the peptide in the stalled complex, as well as the A-site codon, in order to emulate the *ermAL1* and *ermCL* systems (Figure 32).

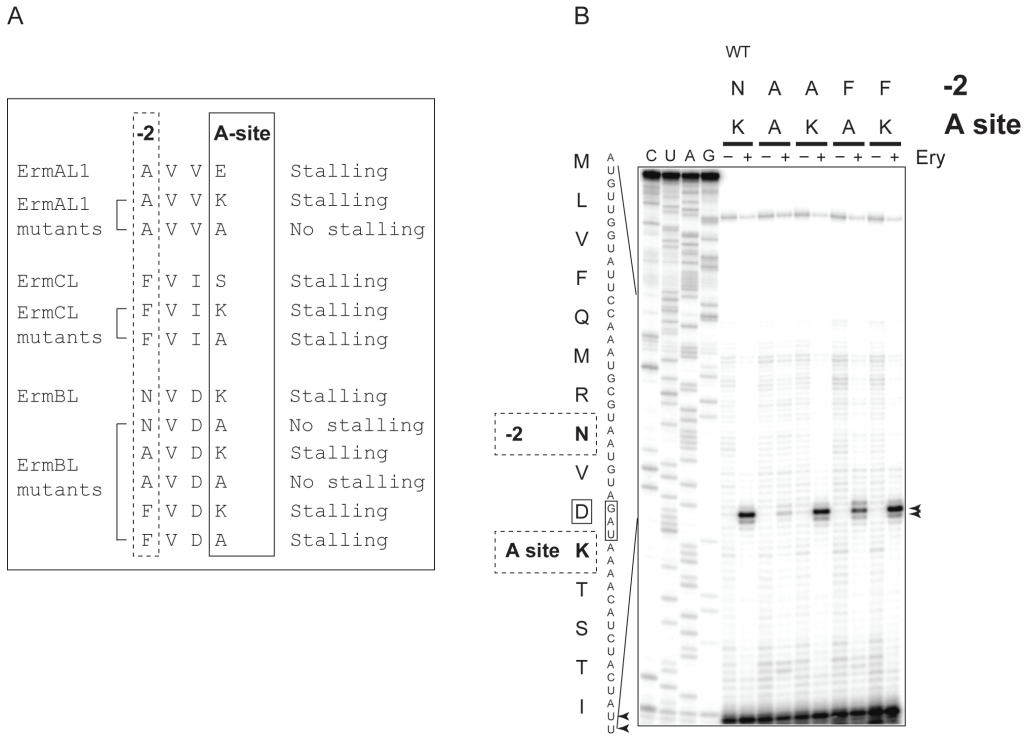

Figure 32. Nascent peptide sequence influences properties of the PTC A-site. (A) Effect of mutations in the -2 position and A-site codons of *ermAL1*, *ermCL* and *ermBL* ORFs on ribosome stalling. Data for *ermAL1* and *ermCL* are derived from Figures 21, 26 and 27. Data for *ermBL* is derived from Figures 28A and 29B. (B) Effect of mutations in the -2 position and A-site codons of *ermBL* ORFs on ribosome stalling. Amino acid changes occurring as a result of mutations in the -2 and A-site codons are indicated above the gel; 'WT' indicates wild-type sequence.

When the wild-type Asn_8 codon in *ermBL* was replaced with Ala, *ermBL*-SRC was formed when lysine but not alanine codon was present in the A-site of the SRC (Figure 32B). This shows that alanine in the -2 position of the ErmBL nascent peptide makes the A-site selective, similar to ErmAL1. On the other hand, when Asn_8 codon of *ermBL* was replaced

with the Phe codon, the SRC formed irrespective of the amino acid encoded in the A-site (alanine or lysine). This scenario resembles that of ErmCL, where the A-site becomes restrictive to all amino acids. Altogether, these results demonstrate that control of the properties of the PTC A-site by the amino acid residue in position -2 of the nascent peptide in the SRC is a universal feature which applies to stalling peptides with substantially different sequences.

3. Nascent peptide sequence requirements for ribosome stalling at *ermDL* ORF

Erythromycin-dependent SRC forms at the 7th codon of wild-type *ermDL* ORF (Figure 16A). To assess the role of the nascent peptide sequence, alanine scanning of *ermDL* codons 2-8 was carried out. This showed that mutations at positions 2 (Thr), 5 (Met) and 7 (P-site codon encoding Leu) abolished ribosome stalling (Figure 33). Mutation of the A-site Arg codon to Ala did not prevent SRC formation. This interesting result indicates that, unlike ErmCL, ErmAL1 or ErmBL, the key stalling amino acids of ErmDL do not form a domain clustered in the C-terminus, but are instead scattered throughout the length of the peptide. Also, unlike the other three peptides, ribosome stalling does not depend on the identity of the A-site codon.

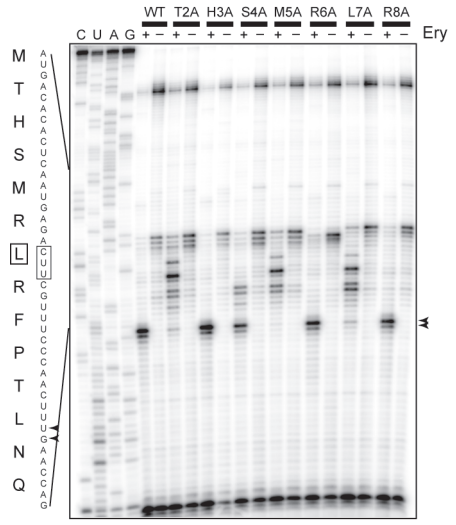

Figure 33. Alanine scanning mutagenesis of *ermDL*.

E. Ribosome stalling at *ermBL* and *ermDL* ORFs has significantly different requirements for the structure of inducing antibiotic compared to *ermAL1* and *ermCL*

Previous studies have shown that the structure of the drug plays a critical role in SRC formation at the *ermCL* ORF [12, 44]. In order to elucidate the drug structure requirement for SRC formation at diverse ORFs, we expanded this analysis to the *ermAL1*, *ermBL* and *ermDL* ORFs and tested the effects of different antibiotics of the MLS_B group on formation of the SRC (Figure 34).

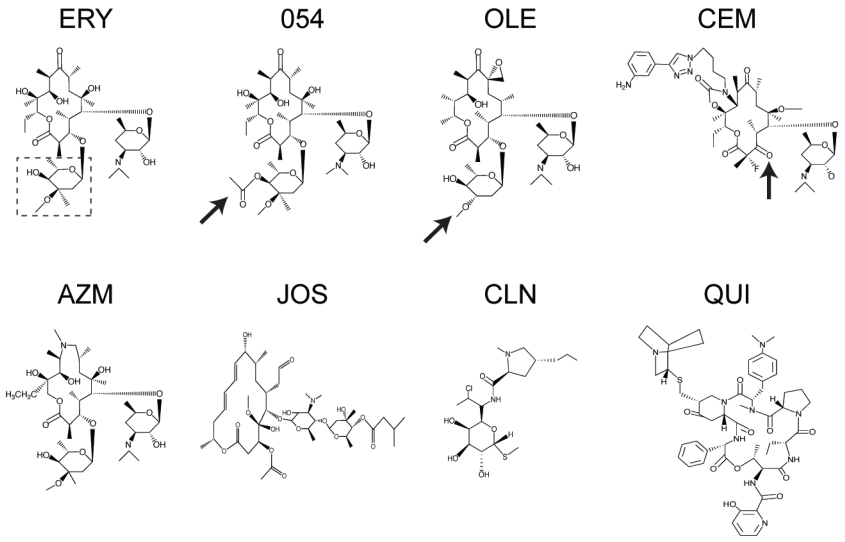

Figure 34. Structures of MLS_B antibiotics used in toeprint analysis. The order of antibiotics is as follows: Erythromycin, ITR-054, Oleandomycin, CEM-101, Azithromycin, Josamycin, Clindamycin and Quinupristin. C3-cladinose sugar of ERY is boxed with a dashed line and arrows indicate key modifications or loss of the cladinose in other macrolide and ketolide antibiotics.

In this analysis we included two 14-membered macrolides (ITR-054 and oleandomycin), the ketolide CEM-101, the 15-membered macrolide azithromycin, the 16-membered macrolide josamycin, the lincosamide clindamycin and the streptogramin B antibiotic, quinupristin. Macrolides basically contain a lactone ring that is 14-membered in case of the three antibiotics, erythromycin, ITR-054 and oleandomycin. In erythromycin, a cladinose sugar is attached to the C3 position and a desosamine sugar is attached to the C5 position of the lactone ring. ITR-054 is almost identical, except for acetylation of the C3-cladinose. In oleandomycin, the C3-cladinose is substituted by the oleandrose sugar, where there is loss of a methyl group and inversion of stereochemistry at the C3 position of the sugar compared to cladinose. There are also other subtle differences in the lactone rings of erythromycin and oleandomcyin, which are not expected to affect ribosome stalling. Azithromycin is a 15-membered macrolide which is similar to erythromycin in terms of the

sugars attached at the C3 and C5 positions. Josamycin is a 16-membered macrolide, which carries a disaccharide at the C5 position of the lactone ring unlike the single sugar in the other macrolides mentioned above. Lincosamides are chemically completely different from macrolides, with a structure consisting of amino acid and sugar moieties. Streptogramins B contain a macrocyclic lactone ring, that is much larger than that of the macrolides mentioned above. Ketolides are derivatives of macrolides, where the C3-cladinose sugar has been replaced with a keto function. In the ketolide CEM-101, an additional alky-aryl side chain is attached at C11, C12 carbon atoms of the lactone ring. There is also a fluorine atom at the C2 position of the lactone ring.

All of the above antibiotics bind to the entrance of the polypeptide exit tunnel, adjacent to the peptidyltransferase center [58, 61] and inhibit translation by causing drop-off of peptidyl-tRNA [49]. However, structural differences between the different groups cause the nascent peptide to grow to different lengths before dissociation of peptidyl-tRNA occurs. The 14-membered macrolides cause drop-off of peptidyl-tRNA containing 6-8 amino acids [49]. Since the disaccharide of josamycin reaches the PTC, it causes drop-off of peptidyl-tRNA containing as few as 2-3 amino acids. The lincosamide, clindamycin has a very similar effect because its binding site partially overlaps with the A and P-sites of the 50S ribosomal subunit. Streptogramins B (quinupristin) are similar to erythromycin in their effect on inhibiting translation. Ketolides allow polymerization of nine or ten amino acids before causing drop-off of peptidyl-tRNA [49, 106].

Previous studies have established that the C3-cladinose in macrolides is extremely important for ribosome stalling at *ermCL* [12]. Even small modifications in the structure of the C3-cladinose have strong negative effects upon *ermCL*-SRC formation (Vazquez-Laslop

et al., in press). Thus, acetylation of the cladinose sugar at position C17 (in ITR-054, Figure 34) or altering stereochemistry of the C3 sugar as in oleandrose of oleandomycin significantly reduces stalled complex formation at *ermCL*.

The effect of antibiotics on ribosome stalling at the *ermAL1* ORF was generally similar to that observed with *ermCL* (Figure 35A).

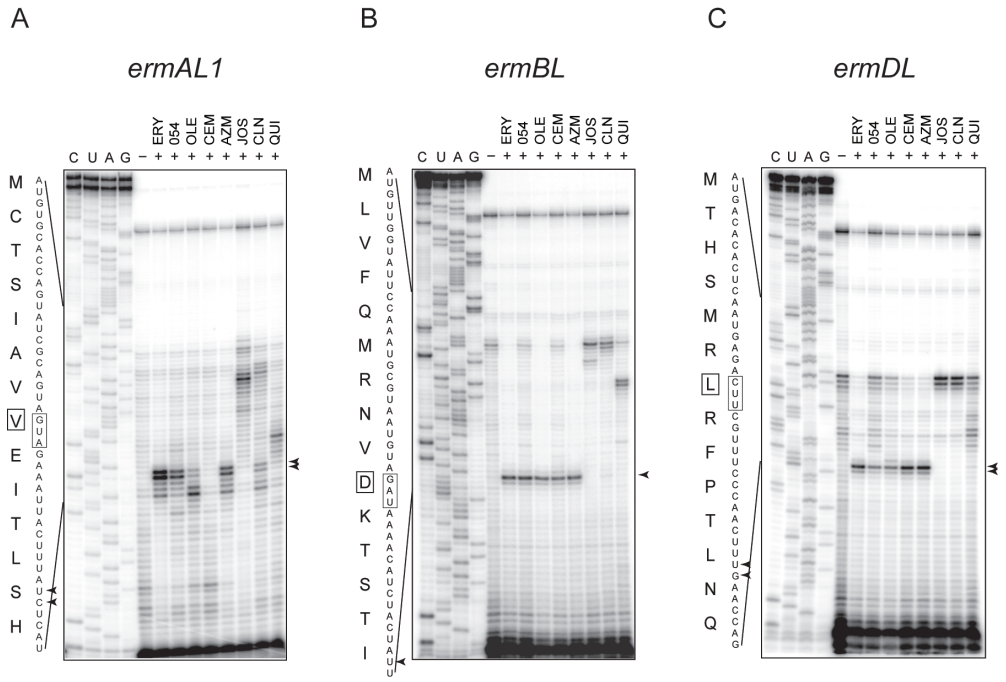

Figure 35. Effect of MLS_B antibiotics on ribosome stalling at *ermAL1*, *ermBL* and *ermDL* ORFs.

Antibiotics that contain C3-cladinose (ERY and AZM) readily induce stalling. Replacement of cladinose with oleandrose (in oleandomycin) prevented stalling and acetylation of cladinose (in ITR-054) reduced efficiency of stalling (although to a lesser extent than that at *ermCL*). Ketolide CEM-101 that lacks C3 cladinose, lincosamide

clindamycin (CLD) and streptogramin B compound quinupristin (QUI) were unable to induce efficient stalling, although a weak toeprint band could be observed in the sample containing clindamycin. The 16-member ring macrolide josamycin (JOS) that inhibits formation of the first and second peptide bond also abolished SRC formation at *ermAL1*.

The effect of the drugs upon SRC formation at *ermBL* and *ermDL* ORFs was notably different. Here, modifications of the C3 sugar residue or even its complete absence (as in CEM-101) did not prevent the drug from serving as an efficient cofactor of stalling (Figure 35B and C). JOS, that affects formation of the first and second peptide bond precluded induction possibly because the ribosome was not able to synthesize nascent peptide. QUI was also unable to induce. Clindamycin could not stimulate SRC formation at *ermDL* but a weak band was observed in the *ermBL* sample possible indicative of a transient stalling.

These experiments revealed an important difference between programmed translation arrest at *ermCL*/*ermAL1* ORFs vs *ermBL*/*ermDL*. While ribosome stalling at *ermCL*/*ermAL1* ORFs shows strong dependence on the presence and exact structure of the C3 cladinose sugar, SRC formation at *ermBL*/*ermDL* does not appear to depend on this feature of the antibiotic. This result clearly distinguishes *ermBL*/*ermDL* SRC from *ermCL*/*ermAL1* SRC.

F. Identification of ribosomal RNA sensors of the nascent peptide

One of the most pertinent questions concerning the mechanism of programmed ribosome stalling is how the ribosome senses the special nature of a stalling nascent peptide. Identification of rRNA residues that are critical for formation of the SRC is one way to answer this question. Previous studies have shown that mutations at conserved A2062 and m^2A2503 abolish SRC formation at *ermCL* [59]. Testing these mutations with *ermAL1* ORF showed that they also prevent ribosome stalling directed by ErmAL1 nascent peptide.

Surprisingly, however, the same mutations had no effect upon stalling at *ermBL* or *ermDL*, suggesting that the ErmBL and ErmDL nascent peptides rely on a different set of rRNA sensors to transmit the arrest signal to the PTC. To pinpoint the sensors that could be involved in sensing ErmBL or ErmDL nascent peptides, or additionally involved in sensing ErmAL1, we subjected an extended spectrum of 23S rRNA residues to mutagenesis (Figure 36).

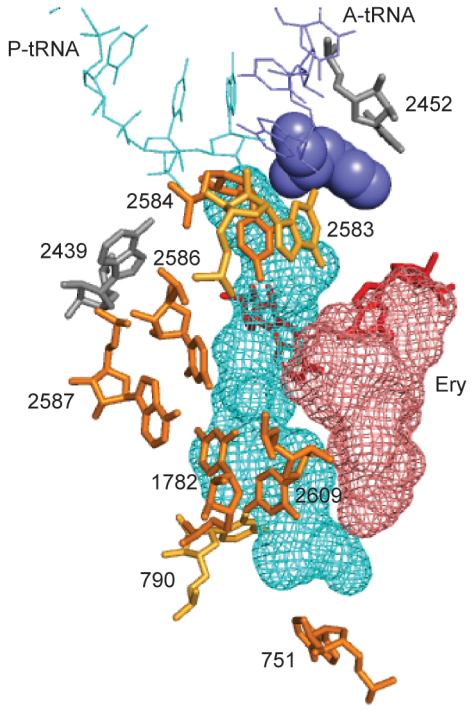

Figure 36. 23S rRNA nucleotides in the exit tunnel chosen for mutagenesis. Model of the ErmAL1$_8$ nascent peptide and erythromycin bound in the nascent peptide exit tunnel of the 50S ribosomal subunit. Peptidyl-tRNA in the P-site is shown in cyan, with the peptide moiety in mesh format. A-site tRNA is shown in purple, with the aminoacyl moiety in spheres. Erythromycin (Ery) is shown as a salmon mesh. 23S rRNA nucleotides mutated in this study are shown in orange. m^2A2503 and A2062, which are located are shown in red (behind the nascent peptide and erythromycin). A2439 and C2452, at which mutations were not viable, are shown in grey.

We focused our attention on nucleotides that are located in the PTC (G2583, U2584 and C2452) or in the wall of the exit tunnel (A2439, U2586, A2587, U1782, U2609, U790

and A751+) (Figure 36). Mutations of G2583 and U2584 were shown to affect induction mediated by the TnaC nascent peptide, suggesting that these nucleotides could play a role in sensing the stalled TnaC-tRNA^{Pro} [67]. C2452, together with A2451 forms a part of the PTC A-site cavity where side chain of the aminoacyl moiety of the A-site bound aa-tRNA is located [107]. A2439, U2586 and A2587 are located in the PTC-proximal part of the tunnel, opposite to the macrolide-binding site. Since the binding of the antibiotic narrows the tunnel lumen, it is likely that the nascent peptide is pushed towards the other wall, making contact with one or both of these residues. In the cryo-EM analysis of the *E.coli* ribosome stalled at an extended *tnaC* ORF, densities for U2586 and U1782, which is located below U2586, were closely linked to that of the nascent peptide, suggesting direct interaction [69]. U1782 is positioned adjacent to U2609, whose mutation to C or A significantly affected induction mediated by TnaC [64]. Located further below, are residues from domain II of 23S rRNA, which include the 750 region and U790. Insertion of an adenine in the 750 region had a strong negative effect on SecM-dependent induction and accumulation of TnaC-tRNA^{Pro} [8, 64]. U790 is also a promising candidate, located in the tunnel wall, opposite to the macrolide-binding site.

Our goal was to test the effect of one mutation at each position of interest. Mutations at A752, U790, U1782 and U2609 were introduced in the plasmid pLK35, which carries the *rrnB* rRNA operon. These mutant ribosomes were expressed in the *E.coli* strain SQK15 that lacks the chromosomal rRNA operons, leaving plasmid as the only source of rRNA [91]. Mutations at A2439 and C2452 were found to be lethal and could not be expressed as a pure population in the SQK15 cells. These mutants were excluded from further analysis. *E.coli* strain NT102, carrying mutations in G2583, U2584, U2586 or A2587 and lacking wild-type

rRNA operons, were a kind gift from Dr. Suzuki (University of Tokyo, Japan) [93]. The NT102 strain, similar to SQK15, expresses a pure population of mutant ribosomes. SQK15 and NT102 strains carrying the various rRNA mutations were tested for their sensitivity to erythromycin. Erythromycin MIC ranged from 64 to 128 μg/mL for all of the strains (Table X), showing that none of the rRNA mutations notably affected binding of erythromycin to the ribosome.

TABLE X

MIC OF ERYTHROMYCIN FOR *E.coli* STRAINS

E.coli strain	MIC (μg/mL)
SQK15 wt	128
SQK15-U790G	128
SQK15-U1782C	128
NT102-G2583A	128
NT102-U2584C	128
NT102-U2586C	128
NT102-A2587U	128
SQK15-U2609C	64
SQK15-A751+	64

Mutant ribosomes were isolated and tested in a cell-free system for their ability to translate the *dhfr* template and were determined to be active in translation (Figure 37).

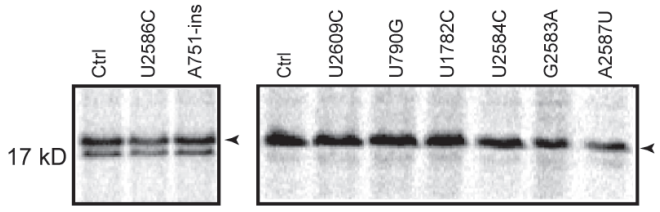

Figure 37. Translation activity of purified ribosomes. Ribosomes carrying the mutations indicated above the gel were purified and tested for their ability to translate the *E.coli dhfr* gene *in vitro*, using the delta-ribosome PURE SYSTEM. 'Ctrl' indicates wild-type ribosomes. Reaction products were resolved in SDS gel.

This demonstrated that the mutations did not affect translation capacity of the ribosomes in any significant manner. We then determined the effect of the rRNA mutations on ribosome stalling at *ermAL1*, *ermBL* or *ermDL* ORFs, by toeprint analysis. This analysis showed that the U1782C mutation completely prevented SRC formation during translation of *ermAL1* (Figure 38A). The same mutation prevented stalling at *ermCL* (these experiments were carried out by D. Klepacki and N. Vazquez-Laslop). Thus, U1782 expands the spectrum of rRNA residues directly participating in the ribosomal response to the ErmAL1 and ErmCL stalling peptides. Additionally, U2586C, A2587U and U2609C mutations somewhat reduced the amount of the SRC formed at *ermAL1*.

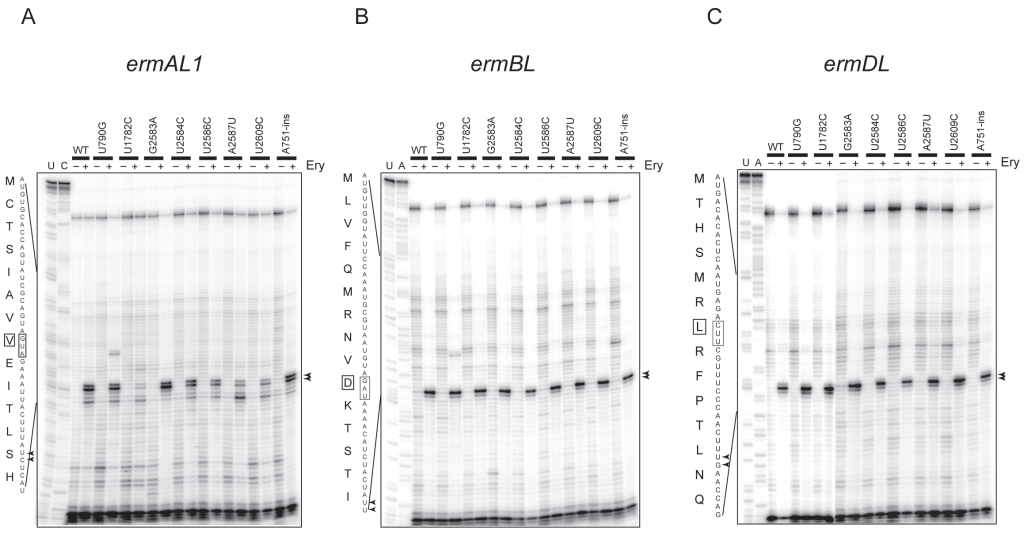

Figure 38. Effect of 23S rRNA mutations on ribosome stalling. The effect of mutations in 23S rRNA nucleotides (indicated above the gel) on formation of SRC at (A) *ermBL*, (B) *ermDL* and (C) *ermAL1* ORFs was determined by toeprint analysis.

Surprisingly, none of the tested rRNA mutations had any effect on programmed translation arrest at either *ermBL* or *ermDL* ORFs, as shown by the unchanged appearance of the strong toeprint at Asp-10 of *ermBL* or Leu-7 of *ermDL* (Figure 38B and C).

Thus, none of the putative tunnel sensors tested so far had any noticeable effect upon programmed translation arrest at *ermBL* or *ermDL* ORFs. This observation, as well as a notable difference in antibiotic requirement of ribosome stalling at these two ORFs clearly indicate that mechanisms that underlie programmed translation arrest at *ermCL* and *ermAL1* ORFs are principally different from those of SRC formation at *ermBL* and *ermDL* ORFs.

V. DISCUSSION

The ribosome has the amazing ability to communicate with the nascent peptide and functionally respond to this interaction. An extreme demonstration of this ability is the halting of translation in response to synthesizing certain nascent peptides. This general strategy is central to regulation of expression of genes involved in a wide variety of cellular functions ranging from secretion to metabolism to, in the case of the main topic of this work, antibiotic resistance. Despite the importance of the subject, how the ribosome carries out this critical task remains poorly understood.

It had been known for 30 years that drug and nascent peptide-dependent ribosome stalling is involved in regulation of expression of the clinically important family of *erm* genes encoding resistance to macrolide, lincosamide and streptogramin B (MLS_B) antibiotics. However, the study of antibiotic-mediated inducible resistance, mainly from the clinical and genetic standpoints, had been focused on just a few of the members of the *erm* family, mainly *ermC*, *ermB* and *ermD*. Furthermore, only recently, efforts to understand nascent peptide-ribosome interactions at the molecular level were initiated in this research group [7, 12, 108, 109]. Previous work in the laboratory was focused on characterizing the formation of the stalled complex between the ribosome with bound erythromycin and the ErmCL leader peptide, responsible for regulating expression of the gene *ermC*. However, even a brief expedition into the ample clinical literature on resistance genes of the MLS_B group of antibiotics, revealed that many of these genes are potentially inducible; some of the reports also mention putative upstream regulatory genes. Therefore, drug-mediated ribosome stalling could be potentially involved in activating a large variety of MLS_B resistance genes. Furthermore, a quick inspection of some of the putative leader ORFs showed that the

Leader ORFs encoded a big variety of amino acid sequences, opening up the exciting possibility of enriching our understanding of how the ribosome, in response to the presence of an antibiotic, senses and responds to different nascent peptides.

Thus, our first step was to carefully analyze upstream regions of most of the known MLS_B resistance genes for the identification of putative regulatory ORFs [75]. Our analysis revealed that potentially translatable ORFs could be found in approximately 30% of the MLS_B resistance genes [75] (see Table VIII in the Results section for a list of leader peptides). While most of these genes are preceded by a single leader ORF, two of the *erm* genes, *ermA* and *ermG* contain two leader ORFs. It is not clear why these genes evolved to have two regulatory sequences although it has been speculated that the presence of the two ORFs increases the dynamic response range of the resistance inducibility [73]. In general, it appears that drug-dependent inducibility is a general property of many MLS_B resistance genes. Constitutive gene expression often observed in clinical isolates results from point mutations, deletions or insertions, which disrupts the operation of the induction mechanism often resulting in an 'induced' conformation of the mRNA, irrespective of the antibiotic presence [95, 110]. Such mutations occur when bacteria with inducible resistance genes are exposed to non-inducing antibiotics, such as exposure of *S. aureus* containing *ermC* to lincosamides and streptogramins B [110].

Comparison of the peptide sequences encoded by the various leader ORFs allowed us to group encoded putative stalling peptides into four sequence classes characterized by conservation of the sequence motifs IFVI, IAVV, RLR and R/KP. The remaining peptides which did not show any discernable sequence convergence were grouped in the 'Miscellaneous' category [7]. The prototype of the 'IFVI' group of peptides is ErmCL;

detailed analysis of the SRC formed during translation of *ermCL* has shown that ribosome stalling occurs at the Ile9 codon, which is the C-terminal codon of the 'IFVI' motif [12]. We showed that translation of another leader ORF of the same group, *ermAL2*, also causes ribosome stalling at Ile9 (Figure 15C). The peptides of the 'IFVI' group show remarkably high similarity. The 'IFVI$_9$' domain, which is critical for stalling at *ermCL* [12] is present at the same conserved distance from the N-terminus in all peptides of this group (Table VIII). This corroborates the earlier finding that adding or removing codons prior to Ile9 in the *ermCL* ORF negatively affects the efficiency of stalling [12].

The 'IAVV/T' peptides also show very high sequence similarity (Table VIII). We determined by toeprint analysis that drug-dependent ribosome stalling occurs at the last codon of this motif (valine in *ermAL1* and threonine in *erm36L*) (Figures 15B and 15C, respectively). The motif 'IAVV', which is present at the C-terminus of the nascent peptide in the SRC, is absolutely essential for ribosome stalling (Figure 20). Thus, ErmCL and ErmAL1 are very similar in that the key amino acids are located in the C-terminus of the nascent peptide, in the vicinity of the peptidyltransferase center and are hydrophobic in nature. Although the stalling domains of these peptides (IFVI and IAVV) show obvious resemblance, we think it is reasonable to group these peptides into distinct classes because the identity of the A-site codon is crucial for ribosome stalling in case of peptides of the IAVV class (ErmAL1, Figure 20), but not the peptides of the IFVI class (*e.g.* ErmCL), [12] (discussed below in further detail).

The peptides of third sequence class are characterized by the presence of the 'RLR' motif. However, there is significant sequence variation among peptides of this group and the distance of 'RLR' from the N-terminus is not conserved (Table VIII). Therefore, prior to this

study, it was unclear whether this motif bears any functional significance. Nevertheless, experimental studies showed that erythromycin-induced ribosome stalling invariably occurs at the conserved leucine codon within the motif (Figure 16 and Table IX) irrespective of its position relative to the peptide's N-terminus. This finding reveals the RLR motif is one of the important determinants of stalled complex formation, which was unknown until now. However, more detailed investigation of the sequence requirement of SRC formation at one of the ORFs encoding an RLR peptide, ErmDL, showed that unlike ErmCL and ErmAL1, the critical amino acids are not confined to the 'RLR' motif ($MTXXMXL_7$) (Figure 33). These additional amino acid residues found to be important for the ribosome stalling at the ErmDL peptide are not conserved in the other peptides of the RLR class (Table VIII). Therefore, the structural context of the peptide stalling domain in this case appears to be more complex than a simple sequence conservation described for the peptides of IFVI and IAVV class. Elucidating this context could be a subject of the future study and will require mutational analysis of several stalling peptides from this group.

The similarity of the peptides of the R/KP class (*ermSL*, *erm38L* and *ereAL'*) was not initially recognized on the basis of their sequence analysis because the conserved motif was too short and its distance from the putative N-terminal methionine does not appear to be conserved. However, toeprinting analysis showed antibiotic-dependent stalling at the Pro codon of the R/KP motif in three different peptides (Figure 17C-D) which prompted us to group these in a separate class (Table IX). The intensity of the toeprinting signal obtained with the peptides of this class was notably weaker compared to most of the other tested peptides. One possible explanation is that erythromycin is not the optimal stalling cofactor for these peptides. For example, the *ermSL* ORF regulates *ermS*, which is found in the tylosin

producer, *S. fradiae*. Yet, in the laboratory conditions, *ermS* was reported to be induced by erythromycin but not tylosin [96]. However, induction of *ermS* does occur in response to high concentration of tylosin when A748 and A2058 in 23S rRNA are already methylated due to the action of TlrB and TlrD methyltransferases which are also present in *S. fradiae* [111]. Thus it is possible that only the ribosome monomethylated at A748 and A2058 is capable of tylosin-induced stalling at the *ermS* regulatory ORF. In the other examples of genes regulated by R/KP peptides, one can envision that with the 'proper' antibiotic, stalling would become stronger than that seen with erythromycin as an inducer. Identifying the antibiotic-producing species that contains genes controlled by the R/KP peptides or testing a large array of MLS_B antibiotics may help to identify a true cofactor of SRC formation that cooperates with the peptides of this group to stall the ribosome.

The RP sequence of the peptide encoded in the *erm38L* ORF is located at a considerable distance (15 aa) from the putative N-terminal methionine (Table IX). This ORF also contains another methionine codon at the 6^{th} position that, if used as an initiator codon, would place the RP stalling sequence at a more conventional distance (10 aa) from the peptide's N-terminus. None of the two Met codons is preceded by a strong Shine-Dalgarno sequence, therefore, it was possible that not the first, but the second Met codon is used for initiation of translation of the regulatory peptide. However, in our *erm38L* construct used for *in vitro* translation and toeprinting analysis, when we deleted the first five codons thus forcing translation to initiate at the downstream AUG codon, translation of this mutant ORF in the presence of erythromycin resulted in complete loss of the toeprint signal, showing that the original 'extended' N-terminal sequence of the Erm38L peptide is important for ribosome stalling (Figure 39).

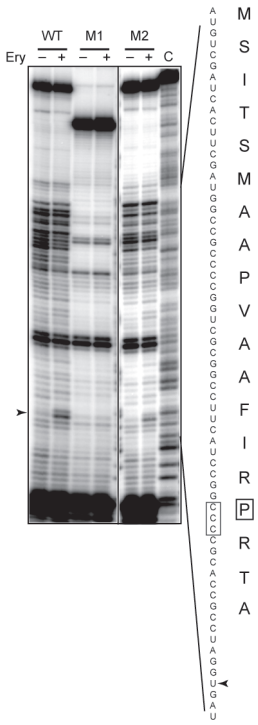

Figure 39. Effect of mutations in *erm38L* on ribosome stalling. 'WT' indicates wild-type *erm38L*. 'M1' indicates the mutant where the first five codons of the ORF were deleted. 'M2' indicates the mutant where the 2nd methionine (codon 6) was mutated to alanine. Sequence of wild-type *erm38L* is indicated to the right.

In agreement, with this conclusion, mutation of the 2nd methionine to alanine resulted in the same toeprint signal as the wild-type sequence. In the original host *M.smegmatis*, *erm38* was shown to methylate a very small proportion of rRNA molecules when induced with erythromycin [112]. Given its poor activity, it is likely that transient ribosome stalling at the leader ORF is sufficient to maintain A2058 methylation within the desired level in the cell. Also, induction with some other MLS_B antibiotic may increase the degree of stalling and A2058 dimethylation. Similar to *erm38L*, transient stalling at *ereAL'* ORF may be sufficient to control induction of the *ereA'* expression with the proper inducing antibiotic. Alternatively, the *ereAL'* sequence analyzed here could also represent a mutant version of the original inducible leader ORF, since the described *ereA'* was reported to be expressed

constitutively [113]. An interesting observation that emerged from toeprint analysis of the leader peptides of the R/KP class, ErmSL, Erm38L and EreAL' is that the SRC was formed when peptidyl-tRNA^{Pro} was present in the ribosomal P site which is preceded by a positively charged amino acid, arginine or lysine. Proline codons are known to be 'problematic' and peptidyl-tRNA^{Pro} serves as a poor donor in the peptidyl transfer reaction even in the absence of erythromycin [114]. Thus, presence of the macrolide antibiotic in conjunction with the 'right' nascent peptide may accentuate the difficulty that the ribosome experiences in 'dealing' with proline in the PTC.

Among the peptides from the miscellaneous class, translation of the *ermBL* ORF resulted in a strong toeprint (at Asp10, Figure 17A). This result provided biochemical underpinning for the conclusions obtained previously by Min et al [11] by genetic means and the use of a reporter system. Our mutational studies of the ribosome stalling at the *ermBL* ORF showed that SRC formation depends on the identity of the four amino acids located in the C-terminus of the nascent peptide (MXXXXXRNVD), as well as the nature of the codon placed in the A-site of the SRC (Figures 31 and 32). Although the importance of the C-terminal domain for stalling and the importance of the A-site codon for SRC formation at the *ermBL* ORF resembles our observations obtained with the peptides of the IAVV group, in most of the other features (spectrum of inducing antibiotics, the lack of the known ribosome sensors) the ErmBL peptide is clearly distinct. The other two tested peptides of the miscellaneous group (*ermGL2* and *erm37L*) did not direct stalling *in vitro* in the presence of erythromycin. These peptides can represent a mutated 'non-stalling' version of the putative original stalling peptide or they might be induced by an antibiotic other than erythromycin. In

case of the *M.tuberculosis erm37*, the methyltranferase is known to be induced by a transcriptional regulator which controls multi-drug resistance [104].

Altogether, our analysis of a collection of regulatory peptides that control expression of many MLS_B resistance genes has presented strong evidence that programmed drug-dependent ribosome stalling can occur at a wide variety of leader ORFs and that thus nascent peptides with different amino acid sequence can cooperate with a macrolide molecule in inducing the translation arrest state of the ribosome. This information can be used as a starting point for detailed investigation of translation arrest requirement at different regulatory ORFs and in the long run may provide invaluable information about common and specific features that govern drug and nascent peptide –controlled ribosomal response.

Once we classified putative stalling peptides, we investigated the role of the antibiotic cofactors in SRC formation. Previous analysis of the structural features of the antibiotic that are required for ribosome stalling at *ermCL* had established that the cladinose sugar in the C3 position of the lactone ring of macrolides is indispensable for ribosome stalling at *ermCL* [12, 57]. This correlates with the observation that ketolides are considered poor inducers of *erm* [109, 115]. Our analysis of the effect of modification of the cladinose sugar on ribosome stalling at other leader ORFs shows that ErmAL1 is highly similar to ErmCL – both require the C3-cladinose and minimal modifications are tolerated (Figure 30D). Unexpectedly, we found that ketolides, that fail to stall the ribosome at *ermCL* or *ermAL1* ORFs, are perfectly conducive to ribosome stalling at *ermBL* and *ermDL* ORFs, showing that the mode of interaction of the ErmBL and ErmDL nascent peptides with the antibiotic, and likely the ribosome, involves different atomic contacts. The finding that ‘different peptides’ can cooperate with ‘different antibiotics’ in order to stall the ribosome open interesting

biotechnological perspectives hypothetically allowing one to tune the peptide sequence to arrest translation in response to specific small molecules, even those without antibiotic properties.

16-membered macrolides, lincosamides and streptogramin B antibiotics do not cause ribosome stalling at any of the leader ORFs tested. 16-membered macrolides and lincosamides inhibit peptide bond formation and cause peptidyl-tRNA drop-off when the peptide is only 1-3 amino acids long [49]. Thus in the presence of these antibiotics, it would be impossible for the ribosome to reach the stalling codon in case of *ermCL* (Ile9), *ermAL1*, *ermBL* (Asp10) or *ermDL* (Leu7). It remains to be determined if any of these antibiotics can support ribosome stalling at *ereAL*, where we showed that ribosome stalling occurs unexpectedly close to the N-terminus, at the third codon of the ORF (Figure 17D). Streptogramin B antibiotics are structurally different from macrolides but interact with the same region of the NPET. Nevertheless, streptogramins, whose main macrocycle projects into the tunnel lumen, much more significantly obstruct the tunnel compared to macrolides, whose macrolactone ring lays flat against the tunnel wall [58] [60]. This position of the drug probably prevents the nascent peptide to advance far enough along the tunnel and therefore probably makes streptogramins B unsuitable as cofactor for SRC formation. Interestingly, 16-membered macrolides, lincosamides and streptogramin B antibiotics have been reported to induce expression of *ermB* [43]. Our results suggest that the mechanism of induction by these antibiotics does not rely on programmed translation arrest.

In the absence of the detailed structural information, the general operation of the molecular mechanisms of drug and nascent peptide-controlled programmed translation arrest remains poorly understood. However, our finding of the importance of the PTC A-site in

stalled complex formation provides a deeper understanding of the ribosome stalling mechanism. Comparison of SRCs that form at regulatory ORFs *ermAL1*, *ermCL* and *ermBL* showed that the amino acid residue at position -2 relative to the C-terminus of the nascent peptide controls the property of the PTC A-site. Our findings lead to a simple model (Figure 40).

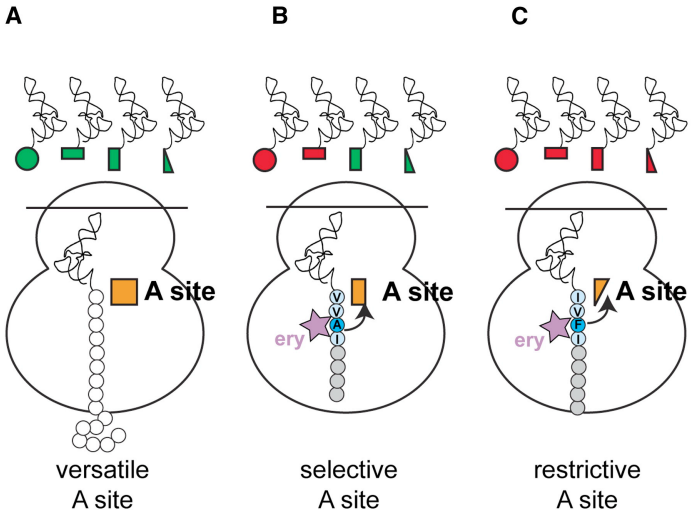

Figure 40. Nascent peptide controls properties of the PTC A-site. (A) During normal translation, the PTC A-site (orange) is in the versatile state. (B) In the presence of an inducing antibiotic (ery) and nascent peptide (e.g. ErmAL1), the A-site becomes selective. Peptide bond formation with certain amino acids (red) becomes very slow; the corresponding A-site codons are conducive to SRC formation. (C) Certain peptides (e.g. ErmCL) can render the peptide restrictive, the SRC is formed irrespective of the A-site codon [105].

Depending on the structure of the peptide in the NPET, the A-site can be in different states. During normal translation, the PTC A-site is in the versatile state where it can properly accommodate any of the natural amino acids delivered by aminoacyl-tRNA. Peptide bond formation with any of the incoming amino acids is efficient. In the presence of an inducing antibiotic and specific nascent peptides, the A-site becomes selective. Here, peptide bond formation with certain amino acids (red) becomes very slow; the corresponding A-site codons are conducive to SRC formation. Because of this, SRC forms during translation of the

ermAL1 ORF when only certain amino acids, including the wild-type Glu, are placed in the PTC A-site (Figure 23). Peptide sequences such as ErmCL can impair the A-site even further, rendering it highly restrictive so that almost no amino acids can be comfortably accommodated; essentially no natural amino acids can be efficiently used as peptide acceptor and the SRC is formed irrespective of the A-site codon (Figure 29).

These properties of the A-site are controlled by the nascent peptide and critically depend on the identity of the amino acid at positon -2 relative to the peptide's C-terminus. Thus, in the ErmCL mutant, where the -2 residue of the nascent peptide is mutated from Phe to Gly, the A-site of the ribosome translating the *ermCL* ORF is switched from restrictive state to versatile, i.e., stalling does not occur irrespective of the nature of the A-site amino acid (Figure 30). And if the same nascent peptide residue is mutated Ala, the A-site in the SRC becomes selective, as in ErmAL1-controlled stalling. Similarly, in the ErmBL-SRC, with asparagine in the -2 position, ribosome stalling occurs when lysine, but not alanine, is encoded in the A-site codon (Figure 31, compare WT and K11A lanes) revealing the selective state of the PTC A-site. But stalling at ErmBL becomes A-site codon independent (and thus, A-site becomes restrictive) if Asn is mutated to Phe.

According to this model, the operational state of the PTC A-site can be directly influenced by the nascent peptide in the NPET and the properties of the A-site can be progressively altered depending on the nascent peptide sequence. One can envision several different scenarios that could lead to alterations of A-site properties in response to the placement of specific nascent peptide and inducing antibiotic in the NPET.

One possibility is that in the antibiotic-bound ribosome with the restricted space in the tunnel, specific nascent peptides can adopt the 'stalling' conformation. This could alter

critical contacts between the 3'-terminus of peptidyl-tRNA and the PTC which in turn could affect the A-site making it less amenable to accommodation of aa-tRNA [116]. One such signal relay pathway that occurs via the peptide has been proposed for TnaC as well [69]. Another possibility is that the peptide and the drug engage specific sensors in the tunnel which can relay the stalling signal to the PTC, allosterically altering the active conformation of the PTC A-site.

Our model of the A-site involvement in the mechanism of stalling is not limited to drug-dependent translation arrest but can also account for key results of previous studies of drug-independent nascent peptide–controlled ribosome stalling. SRC formation at the natural or genetically modified *secM* regulatory ORF requires the presence of a proline codon in the A-site of the stalled ribosome [28, 117]. Similarly, ribosome stalling at the sequences selected from a randomized peptide library requires the presence of a proline codon in the SRC A-site [118]. In these cases, the nascent peptides are likely to infringe on the A-site just enough to prevent use of the most structurally constrained amino acid, proline. In another extensively studied example of nascent peptide–dependent translation arrest, the ribosome stalls at the end of the *tnaC* regulatory cistron when either a stop codon or codons specifying Trp, Arg, Lys, or Ile are present in the A-site; however, stalling is diminished with certain other A-site codons [9, 70]. In this case, the A-site appears to be more restrictive because it excludes a broader range of amino acids. Noteworthy is that the A-site codons that promote stalling at *tnaC* match the best-stalling codons we identified with *ermAL1*, suggesting that they are generally the easiest to discriminate against.

Except for proline, which is known to be a fairly inefficient nascent peptide acceptor because of alkylation of the α-amino group [29], the exact trend that distinguishes amino

acids conducive to SRC formation at *ermAL1* is unclear. The nature of the amino acid is known to influence aminoacyl-tRNA binding to the ribosome, indicating that each amino acid interacts with the PTC in a unique way [119]. However, little structural information is currently available about the specifics of placement of different amino acids in the A-site. Only binding of Phe-tRNA or puromycin derivatives in the PTC A-site has been examined so far by high-resolution crystallographic analysis [4, 120]. In the analyzed complexes, the aromatic side chains of phenylalanine or puromycin are drawn into the hydrophobic crevice formed by the 23S rRNA residues A2451 and C2452 [4, 121]. However, precise molecular contacts of the amino acid side chains may vary depending on their chemical nature, even though the placement of the α-amino group that participates in the nucleophilic attack that drives the reaction of peptide bond formation should remain invariant. Thus, it is conceivable that even small alterations in the orientation of 23S nucleotides that constitute the PTC A-site may have a dramatic effect on the accurate placement of side chains of specific amino acids and thus, their activity as peptidyl acceptors. Alternatively, the nascent peptide in the exit tunnel may alter 23S rRNA residues which constitute the accommodation corridor, affecting entry of the incoming aa-tRNA into the PTC. Computational simulations of the tRNA accommodation process show that to achieve the fully accommodated state in the A-site, the aa-tRNA has to overcome multiple entropic as well as steric barriers [122]. The 3'-aminocyl end of tRNA particularly samples various orientations prior to final accommodation. It is possible that the exact profile of the PTC entry pathway differs for various aminoacyl-tRNAs depending on the nature of the incoming amino acid. If the entry corridor is altered in response to the placement of the stalling nascent peptide in the exit tunnel, certain aa-tRNAs could still be successful in navigating the accommodation pathway, while others would fail.

In case of ErmCL, the accommodation pathway would be completely restrictive for any aminoacyl-tRNA.

How is the signal generated in response to the presence of a stalling nascent peptide in the exit tunnel and, more specifically, about the nature of the amino acid residue at position -2 communicated to the PTC A-site? From the ribosome side, the identity of the 23S rRNA residues A2062, A2503 and U1782 located in the NPET were found to be critical for programmed translation arrest at *ermCL* and *ermAL1* [12, 59]. From the side of an inducing macrolide antibiotic bound in the NPET, the presence of C3-cladinose is essential for stalling [12]. If we are to assume that the 9–amino acid ErmCL nascent peptide can thread through the opening of the tunnel constricted by the bound antibiotic, then Phe_7 (occupying position -2 of the nascent peptide) would be located only a short distance (2-4 Å) from both the cladinose sugar of the inducing antibiotic and A2062 of the 23S rRNA (Figure 41).

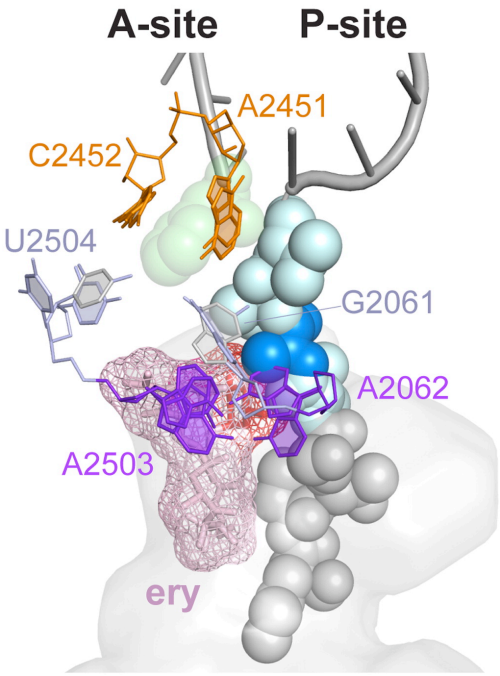

Figure 41. Signal relay pathway in the SRC. The 8-amino acid ErmAL1 nascent peptide was modeled in the structure of the *T.thermophilus* 70S ribosome (PDB accession 2WDL, [121]). C-terminal amino acids critical for stalling are in cyan. The amino acid residue in the -2 position which controls properties of the A-site is in blue. A2451 and C2452 form the A-site crevice. Erythromycin is in violet sticks and mesh, with the cladinose highlighted in red. Mutations of A2062 and A2503 abolish stalling. Neighboring residues 2061 and 2504 may participate in communicating the stalling signal to the A-site crevice [105].

Thus, the presence of the cladinose-containing antibiotic ensures interaction of the nascent peptide (probably specifically the amino acid at position -2) with the highly flexible base of A2062, which serves as the peptide sensor. Reorientation of A2062 can alter the pose of A2503. Displacement of A2062 and A2503 can allosterically, via their immediate neighbors G2061 and U2504, affect the opening of the A2451/C2452 A-site crevice. This signal relay pathway is supported by rigid theory analysis of the statics of the tunnel [123] and cryo-EM structural studies of drug-independent SRC complex formed at the *tnaC* regulatory ORF [69]. Noteworthy, the extent of the A-site impairment in the SRC formed at the *ermCL* ORF conspicuously correlates with the size of the amino acid in position -2 of the

nascent peptide: the bulkiest Phe renders the A-site restrictive, the intermediate-sized Ala renders the A-site selective, and the smallest Gly leaves the A-site versatile. In terms of our model, a larger residue at position -2 of the nascent peptide would cause a stronger displacement of the tunnel sensors resulting in a more pronounced A-site distortion. We do realize, however, that the size of amino acid in position -2 of the peptide is likely not the only characteristic that defines its role in stalling. Hydrophobicity, charge, and other chemical properties of this amino acid residue, and more importantly, the sequence context of the nascent peptide may influence its interactions with the NPET sensors. Investigation of these effects could be the subject of the future studies.

The A-site impairment is likely only one component of the stalling mechanism, even though it is critical. The identity of the P-site amino acid also has a direct effect on SRC formation [9, 12, 28, 118]. It is generally possible that the selectivity of the A-site in SRC revealed by our data is induced via improper placement of peptidyl-tRNA in the ribosomal P-site, which can be affected by specific interactions of the nascent peptide with the tunnel walls and the presence of additional ligands in the tunnel or PTC. In fact, this could be the key mechanism involved in ribosome stalling at *ermBL* and *ermDL* ORFs, since none of the 23S rRNA residues in the exit tunnel appear to be involved in the ribosomal response to the ErmBL and ErmDL nascent peptides (Figure 38B and C).

Different stalling peptides may affect the A-site properties via different relay pathways [59, 69]. Nevertheless, the importance of the nature of the A-site codon for ribosome stalling at a variety of regulatory ORFs (*ermAL1*, *ermCL*, *ermBL*, *secM* and *tnaC*) shows that nascent peptide-induced selectivity of the PTC A-site is a common theme in the mechanism of programmed translation arrest.

The main subject of our study was investigation of the molecular mechanisms of drug and nascent peptide dependent translation arrest that operates during induction of certain antibiotic resistance genes. Although understanding of these mechanisms has a clear medical relevance, we feel that our study illuminated more fundamental principles of regulation of translation by the nascent peptide. All of the currently known examples of nascent-peptide dependent regulation of protein synthesis involve ribosome stalling. Such stalling could be viewed as an extreme case of a variety of milder responses (pausing, acceleration or deceleration of the elongation rate, etc) that have evaded detection because of their transient nature. However, such modes of regulation may have a profound influence on the efficiency of protein synthesis through affecting protein folding, targeting and posttranslational modification. We believe that these mechanisms could operate using the same principles that we uncovered in our study of drug-dependent stalling. For example, the sequence of the proteins could have been evolutionarily optimized to modulate the properties of the PTC A-site to properly adjust the uneven rate of the ribosome progression along mRNA to facilitate protein biogenesis. The large collection of the stalling peptides that our study produced offers an important tool to unravel the details of such mechanisms in future studies.

VI. CONCLUSIONS

In this work, the molecular mechanism of drug and nascent peptide-dependent ribosome stalling was investigated. An extensive analysis of the genetic database was carried out to identify putative regulatory ORFs upstream of genes that confer resistance to macrolide, lincosamide and streptogramin B antibiotics. About 30% of the MLS_B resistance genes were determined to contain leader ORFs. Comparison of the sequences of the peptides encoded in these leader ORFs revealed that many of the peptides contain conserved motifs. Based on these motifs, the leader peptides were grouped as 'IFVI', 'IAVV', 'RLR', 'R/KP' or 'miscellaneous' peptides. While the 'IFVI' and 'IAVV' motifs are present at almost the same distance from the N-terminus of the peptides within each group, the distance between the N-terminus and the 'RLR' or 'R/KP' motifs is not conserved.

A total of 16 leader ORFs were tested for their ability to allow formation of a stalled ribosome complex (SRC). Among these, erythromycin-dependent SRCs were detected at 14 leader ORFs. The *ermAL2* ORF ('IFVI' group) caused strong ribosome stalling at the last Ile codon of this motif, similar to the previously characterized prototype, *ermCL*. In the 'IAVV' group, *ermAL1* and *erm36L*, showed formation of SRC at the last codon of this motif (which is threonine in *erm36L*). From the 'RLR' group, stable SRC formation was detected at the conserved leucine codon of *ermDL*, *msrCL*, *msrSAL*, *ereAL*, *erm34L* and *ermXL*. In the 'miscellaneous' category, strong ribosome stalling occurred during translation of *ermBL* and *msrDL*. The remaining ORFs from this group, *ermSL*, *erm38L* and *ereAL'* gave weak toeprint signals, indicating transient ribosome stalling, while *ermGL2* and *erm37L* showed no toeprints at all, indicating lack of ribosome stalling. Overall, ribosome stalling occurred at the

conserved sequence motifs present in each group of peptides, indicating the importance of the nascent peptide sequence for translation arrest.

Mutagenesis of *ermAL1*, *ermBL* and *ermDL* ORFs indicated that specific residues in each peptide are crucial for translation arrest. For ErmAL1, the conserved 'IAVV' sequence, which is present at the C-terminus of the nascent peptide in the SRC is critical. For ErmBL also, the C-terminal amino acids of the nascent peptide, 'RNVD' are extremely important. In addition, ribosome stalling at both of these leader ORFs is dependent on the identity of the codon located in the A-site of the SRC, which is glutamate in *ermAL1* and lysine in *ermBL*. On the other hand, *ermCL* and *ermDL*-SRC formations occur independent of the A-site codon.

Further mutational analysis of the above leader ORFs revealed that the nascent peptide has a strong influence on the A-site of the PTC. The A-site is affected differently, depending on the residue located at the third position (designated -2) from the last amino acid (designated 0) of the nascent peptide in the SRC. Glycine in the -2 position allows the A-site to be in its normal versatile state, allowing peptide bond formation with any incoming amino acid. Alanine in the -2 position causes the A-site to become selective; therefore certain amino acids can be incorporated to allow continuation of translation, while others can not be accommodated, resulting in halting of translation. When phenylalanine is encoded in the -2 position, the A-site becomes almost completely restrictive to all amino acids, allowing SRC formation. These rules are common to ErmAL1, ErmCL and ErmBL nascent peptides, showing universality of the influence of the nascent peptide on the ribosomal catalytic center.

Investigation of the role of the antibiotic in supporting formation of the SRC revealed that ErmAL1 is similar to ErmCL in that the C3-cladinose sugar attachment of the lactone

ring of macrolide antibiotics is absolutely essential. On the other hand, the cladinose sugar is not required for ribosome stalling mediated by ErmBL and ErmDL nascent peptides. Therefore, ketolide antibiotics, where the cladinose sugar of macrolides is replaced by a keto function, cause ribosome stalling at *ermBL* and *ermDL* but not *ermAL1* and *ermCL* ORFs. While 14 and 15-membered macrolides do support ribosome stalling all of the above ORFs, 16-membered macrolides, lincosamides and streptogramins B are incapable of causing ribosome stalling. This indicated that the principles of interaction between the nascent peptide and the antibiotic could be different for different stalling peptides. Such interactions could be evolutionarily conserved, depending on the antibiotic producer from which the resistance gene operon originated.

Mutational analysis of 23S rRNA residues located in the vicinity of the nascent peptide again showed important differences between the ErmAL1/ErmCL peptides and the ErmBL/ErmDL peptides. Ribosome stalling mediated by ErmAL1 and ErmCL were affected by mutations in the residue U1782, in addition to A2062 and A2053, which have been shown previously. On the other hand, ErmBL and ErmDL-mediated ribosome stalling was not affected by any of the rRNA mutations that disrupt drug-dependent stalling (ErmCL or ErmAL1) or drug-independent stalling (SecM or TnaC). Thus, while ErmAL1/ErmCL, SecM and TnaC-type of peptides may be recognized by the ribosome using sensors in the wall of the tunnel, information regarding the ErmBL/ErmDL nascent peptide sequence could be propagated through the peptide itself, from the tunnel to the PTC. Ribosome stalling at *secM* and *tnaC* ORFs also has an effect on the A-site of the PTC. Therefore, the influence of a large variety of nascent peptides on the selectivity of the ribosomal A-site nevertheless reveals a possibly ubiquitous principle of the mechanism of programmed ribosome stalling.

CITED LITERATURE

1. Yonath, A., K.R. Leonard, and H.G. Wittmann, *A tunnel in the large ribosomal subunit revealed by three-dimensional image reconstruction.* Science, 1987. 236(4803): p. 813-6.
2. Ban, N., et al., *The complete atomic structure of the large ribosomal subunit at 2.4 A resolution.* Science, 2000. 289(5481): p. 905-20.
3. Voss, N.R., et al., *The geometry of the ribosomal polypeptide exit tunnel.* J Mol Biol, 2006. 360(4): p. 893-906.
4. Nissen, P., et al., *The structural basis of ribosome activity in peptide bond synthesis.* Science, 2000. 289(5481): p. 920-30.
5. Pfister, P., et al., *The Structural Basis of Macrolide-Ribosome Binding Assessed Using Mutagenesis of 23 S rRNA Positions 2058 and 2059.* Journal of Molecular Biology, 2004. 342(5): p. 1569-1581.
6. Woolhead, C.A., P.J. McCormick, and A.E. Johnson, *Nascent membrane and secretory proteins differ in FRET-detected folding far inside the ribosome and in their exposure to ribosomal proteins.* Cell, 2004. 116(5): p. 725-36.
7. Ramu, H., A. Mankin, and N. Vazquez-Laslop, *Programmed drug-dependent ribosome stalling.* Mol Microbiol, 2009. 71(4): p. 811-24.
8. Nakatogawa, H. and K. Ito, *The ribosomal exit tunnel functions as a discriminating gate.* Cell, 2002. 108(5): p. 629-36.
9. Gong, F. and C. Yanofsky, *Instruction of translating ribosome by nascent peptide.* Science, 2002. 297(5588): p. 1864-7.
10. Weisblum, B., *Insights into erythromycin action from studies of its activity as inducer of resistance.* Antimicrob Agents Chemother, 1995. 39(4): p. 797-805.
11. Min, Y.H., et al., *Translational Attenuation and mRNA Stabilization as Induction Mechanisms of erm(B) by Erythromycin.* Antimicrob Agents Chemother, 2008.
12. Vazquez-Laslop, N., C. Thum, and A.S. Mankin, *Molecular mechanism of drug-dependent ribosome stalling.* Mol Cell, 2008. 30(2): p. 190-202.
13. Lovett, P.S. and E.J. Rogers, *Ribosome regulation by the nascent peptide.* Microbiol Rev, 1996. 60(2): p. 366-85.
14. Palva, A., et al., *Nucleotide sequence of the tetracycline resistance gene of pBC16 from Bacillus cereus.* Nucleic Acids Res, 1990. 18(6): p. 1635.
15. Su, Y.A., P. He, and D.B. Clewell, *Characterization of the tet(M) determinant of Tn916: evidence for regulation by transcription attenuation.* Antimicrob Agents Chemother, 1992. 36(4): p. 769-78.
16. Yanagitani, K., et al., *Translational pausing ensures membrane targeting and cytoplasmic splicing of XBP1u mRNA.* Science, 2011. 331(6017): p. 586-9.
17. Delbecq, P., et al., *Functional analysis of the leader peptide of the yeast gene CPA1 and heterologous regulation by other fungal peptides.* Curr Genet, 2000. 38(3): p. 105-12.
18. Fang, P., Z. Wang, and M.S. Sachs, *Evolutionarily conserved features of the arginine attenuator peptide provide the necessary requirements for its function in translational regulation.* J Biol Chem, 2000. 275(35): p. 26710-9.
19. Law, G.L., et al., *Polyamine regulation of ribosome pausing at the upstream open reading frame of S-adenosylmethionine decarboxylase.* J Biol Chem, 2001. 276(41): p. 38036-43.
20. Raney, A., et al., *Regulated translation termination at the upstream open reading frame in s-adenosylmethionine decarboxylase mRNA.* J Biol Chem, 2002. 277(8): p. 5988-94.
21. Tenson, T. and M. Ehrenberg, *Regulatory nascent peptides in the ribosomal tunnel.* Cell, 2002. 108(5): p. 591-4.
22. Nakatogawa, H., A. Murakami, and K. Ito, *Control of SecA and SecM translation by protein secretion.* Curr Opin Microbiol, 2004. 7(2): p. 145-50.
23. Butkus, M.E., L.B. Prundeanu, and D.B. Oliver, *Translocon "pulling" of nascent SecM controls the duration of its translational pause and secretion-responsive secA regulation.* J Bacteriol, 2003. 185(22): p. 6719-22.
24. Nakatogawa, H. and K. Ito, *Intraribosomal regulation of expression and fate of proteins.* Chembiochem, 2004. 5(1): p. 48-51.
25. Nakatogawa, H. and K. Ito, *Secretion monitor, SecM, undergoes self-translation arrest in the cytosol.* Mol Cell, 2001. 7(1): p. 185-92.

26. Garza-Sanchez, F., B.D. Janssen, and C.S. Hayes, *Prolyl-tRNAPro in the A-site of SecM-arrested Ribosomes Inhibits the Recruitment of Transfer-messenger RNA.* J. Biol. Chem., 2006. 281(45): p. 34258-34268.
27. Mitra, K., et al., *Elongation arrest by SecM via a cascade of ribosomal RNA rearrangements.* Mol Cell, 2006. 22(4): p. 533-43.
28. Muto, H., H. Nakatogawa, and K. Ito, *Genetically encoded but nonpolypeptide prolyl-tRNA functions in the A site for SecM-mediated ribosomal stall.* Mol Cell, 2006. 22(4): p. 545-52.
29. Pavlov, M.Y., et al., *Slow peptide bond formation by proline and other N-alkylamino acids in translation.* Proc Natl Acad Sci U S A, 2009. 106(1): p. 50-4.
30. Woolhead, C.A., A.E. Johnson, and H.D. Bernstein, *Translation arrest requires two-way communication between a nascent polypeptide and the ribosome.* Mol Cell, 2006. 22(5): p. 587-98.
31. Bhushan, S., et al., *SecM-stalled ribosomes adopt an altered geometry at the peptidyl transferase center.* PLoS Biol, 2011. 9(1): p. e1000581.
32. Cruz-Vera, L.R. and C. Yanofsky, *Conserved Residues Asp16 and Pro24 of TnaC-tRNAPro Participate in Tryptophan Induction of tna Operon Expression.* J Bacteriol, 2008.
33. Konan, K.V. and C. Yanofsky, *Regulation of the Escherichia coli tna operon: nascent leader peptide control at the tnaC stop codon.* J Bacteriol, 1997. 179(5): p. 1774-9.
34. Gong, F., et al., *The mechanism of tryptophan induction of tryptophanase operon expression: tryptophan inhibits release factor-mediated cleavage of TnaC-peptidyl-tRNA(Pro).* Proc Natl Acad Sci U S A, 2001. 98(16): p. 8997-9001.
35. Cruz-Vera, L.R., et al., *Ribosomal features essential for tna operon induction: tryptophan binding at the peptidyl transferase center.* J Bacteriol, 2007. 189(8): p. 3140-6.
36. Gong, F. and C. Yanofsky, *Analysis of tryptophanase operon expression in vitro: accumulation of TnaC-peptidyl-tRNA in a release factor 2-depleted S-30 extract prevents Rho factor action, simulating induction.* J Biol Chem, 2002. 277(19): p. 17095-100.
37. Weisblum, B., *Erythromycin resistance by ribosome modification.* Antimicrob Agents Chemother, 1995. 39(3): p. 577-85.
38. Gryczan, T., et al., *DNA sequence and regulation of ermD, a macrolide-lincosamide-streptogramin B resistance element from Bacillus licheniformis.* Mol Gen Genet, 1984. 194(3): p. 349-56.
39. Horinouchi, S. and B. Weisblum, *Posttranscriptional modification of mRNA conformation: mechanism that regulates erythromycin-induced resistance.* Proc Natl Acad Sci U S A, 1980. 77(12): p. 7079-83.
40. Takyar, S., R.P. Hickerson, and H.F. Noller, *mRNA helicase activity of the ribosome.* Cell, 2005. 120(1): p. 49-58.
41. Sorensen, M.A., C.G. Kurland, and S. Pedersen, *Codon usage determines translation rate in Escherichia coli.* J Mol Biol, 1989. 207(2): p. 365-77.
42. Dubnau, D., *Translational attenuation: the regulation of bacterial resistance to the macrolide-lincosamide-streptogramin B antibiotics.* CRC Crit Rev Biochem, 1984. 16(2): p. 103-32.
43. Horinouchi, S., W.H. Byeon, and B. Weisblum, *A complex attenuator regulates inducible resistance to macrolides, lincosamides, and streptogramin type B antibiotics in Streptococcus sanguis.* J Bacteriol, 1983. 154(3): p. 1252-62.
44. Mayford, M. and B. Weisblum, *The ermC leader peptide: amino acid alterations leading to differential efficiency of induction by macrolide-lincosamide-streptogramin B antibiotics.* J Bacteriol, 1990. 172(7): p. 3772-9.
45. Mayford, M. and B. Weisblum, *ermC leader peptide. Amino acid sequence critical for induction by translational attenuation.* J Mol Biol, 1989. 206(1): p. 69-79.
46. Yao, S., J.B. Blaustein, and D.H. Bechhofer, *Erythromycin-induced ribosome stalling and RNase J1-mediated mRNA processing in Bacillus subtilis.* Mol Microbiol, 2008. 69(6): p. 1439-49.
47. Mao, J.C. and E.E. Robishaw, *Effects of macrolides on peptide-bond formation and translocation.* Biochemistry, 1971. 10(11): p. 2054-61.
48. Menninger, J.R. and D.P. Otto, *Erythromycin, carbomycin, and spiramycin inhibit protein synthesis by stimulating the dissociation of peptidyl-tRNA from ribosomes.* Antimicrob Agents Chemother, 1982. 21(5): p. 811-8.
49. Tenson, T., M. Lovmar, and M. Ehrenberg, *The mechanism of action of macrolides, lincosamides and streptogramin B reveals the nascent peptide exit path in the ribosome.* J Mol Biol, 2003. 330(5): p. 1005-14.

50. Lovmar, M., et al., *The molecular mechanism of peptide-mediated erythromycin resistance.* J Biol Chem, 2006. 281(10): p. 6742-50.
51. Leclercq, R. and P. Courvalin, *Bacterial resistance to macrolide, lincosamide, and streptogramin antibiotics by target modification.* Antimicrob Agents Chemother, 1991. 35(7): p. 1267-72.
52. Allen, N.E., *Macrolide resistance in Staphylococcus aureus: inducers of macrolide resistance.* Antimicrob Agents Chemother, 1977. 11(4): p. 669-74.
53. Pestka, S., et al., *Induction of erythromycin resistance in Staphyloccus aureus by erythromycin derivatives.* Antimicrob Agents Chemother, 1976. 9(1): p. 128-30.
54. Schlunzen, F., et al., *Structural basis for the interaction of antibiotics with the peptidyl transferase centre in eubacteria.* Nature, 2001. 413(6858): p. 814-21.
55. Ono, H., et al., *Drug resistance in Staphylococcus aureus. Induction of macrolide resistance by erythromycin, oleandomycin and their derivatives.* Jpn J Microbiol, 1975. 19(5): p. 343-7.
56. Clarebout, G. and R. Leclercq, *Fluorescence assay for studying the ability of macrolides to induce production of ribosomal methylase.* Antimicrob Agents Chemother, 2002. 46(7): p. 2269-72.
57. Vazquez-Laslop, N., et al., *Role of antibiotic ligand in nascent peptide-dependent ribosome stalling.* In press, 2011.
58. Tu, D., et al., *Structures of MLSBK antibiotics bound to mutated large ribosomal subunits provide a structural explanation for resistance.* Cell, 2005. 121(2): p. 257-70.
59. Vazquez-Laslop, N., et al., *The key function of a conserved and modified rRNA residue in the ribosomal response to the nascent peptide.* EMBO J, 2010. 29(18): p. 3108-17.
60. Harms, J.M., et al., *Alterations at the peptidyl transferase centre of the ribosome induced by the synergistic action of the streptogramins dalfopristin and quinupristin.* BMC Biol, 2004. 2: p. 4.
61. Hansen, J.L., et al., *The structures of four macrolide antibiotics bound to the large ribosomal subunit.* Mol Cell, 2002. 10(1): p. 117-28.
62. Bayfield, M.A., J. Thompson, and A.E. Dahlberg, *The A2453-C2499 wobble base pair in Escherichia coli 23S ribosomal RNA is responsible for pH sensitivity of the peptidyltransferase active site conformation.* Nucleic Acids Res, 2004. 32(18): p. 5512-8.
63. Hesslein, A.E., et al., *Exploration of the conserved A+C wobble pair within the ribosomal peptidyl transferase center using affinity purified mutant ribosomes.* Nucleic Acids Res, 2004. 32(12): p. 3760-70.
64. Cruz-Vera, L.R., et al., *Features of ribosome-peptidyl-tRNA interactions essential for tryptophan induction of tna operon expression.* Mol Cell, 2005. 19(3): p. 333-43.
65. Lawrence, M.G., L. Lindahl, and J.M. Zengel, *Effects on translation pausing of alterations in protein and RNA components of the ribosome exit tunnel.* J Bacteriol, 2008. 190(17): p. 5862-9.
66. Barta, A., et al., *Identification of a site on 23S ribosomal RNA located at the peptidyl transferase center.* Proc Natl Acad Sci U S A, 1984. 81(12): p. 3607-11.
67. Yang, R., L.R. Cruz-Vera, and C. Yanofsky, *23S rRNA nucleotides in the peptidyl transferase center are essential for tryptophanase operon induction.* J Bacteriol, 2009. 191(11): p. 3445-50.
68. Berisio, R., et al., *Structural insight into the role of the ribosomal tunnel in cellular regulation.* Nat Struct Mol Biol, 2003. 10(5): p. 366-370.
69. Seidelt, B., et al., *Structural insight into nascent polypeptide chain-mediated translational stalling.* Science, 2009. 326(5958): p. 1412-5.
70. Cruz-Vera, L.R., R. Yang, and C. Yanofsky, *Tryptophan inhibits Proteus vulgaris TnaC leader peptide elongation, activating tna operon expression.* J Bacteriol, 2009. 191(22): p. 7001-6.
71. Roberts, M.C., et al., *Nomenclature for macrolide and macrolide-lincosamide-streptogramin B resistance determinants.* Antimicrob Agents Chemother, 1999. 43(12): p. 2823-30.
72. Murphy, E., L. Huwyler, and C. de Freire Bastos Mdo, *Transposon Tn554: complete nucleotide sequence and isolation of transposition-defective and antibiotic-sensitive mutants.* Embo J, 1985. 4(12): p. 3357-65.
73. Murphy, E., *Nucleotide sequence of ermA, a macrolide-lincosamide-streptogramin B determinant in Staphylococcus aureus.* J Bacteriol, 1985. 162(2): p. 633-40.
74. Clarebout, G., E. Nativelle, and R. Leclercq, *Unusual inducible cross resistance to macrolides, lincosamides, and streptogramins B by methylase production in clinical isolates of Staphylococcus aureus.* Microb Drug Resist, 2001. 7(4): p. 317-22.
75. Subramanian, S., H. Ramu, and A.S. Mankin, *Inducible resistance to macrolide antibiotics.* . In Antibiotic Drug Discovery and Development, Dougherty TJ, Pucci, M. J. (ed). New York, NY: Springer Publishing Company, In press., 2011.

76. Seppala, H., et al., *A novel erythromycin resistance methylase gene (ermTR) in Streptococcus pyogenes.* Antimicrob Agents Chemother, 1998. 42(2): p. 257-62.
77. Schmitz, F.-J., et al., *Structural Alterations in the Translational Attenuator of Constitutively Expressed erm(A) Genes in Staphylococcus aureus.* Antimicrob. Agents Chemother., 2001. 45(5): p. 1603-1604.
78. Min, Y.H., et al., *Molecular analysis of constitutive mutations in ermB and ermA selected in vitro from inducibly MLSB-resistant enterococci.* Arch Pharm Res, 2008. 31(3): p. 377-80.
79. Min, Y.H., et al., *Heterogeneity of macrolide-lincosamide-streptogramin B resistance phenotypes in enterococci.* Antimicrob Agents Chemother, 2003. 47(11): p. 3415-20.
80. Docherty, A., et al., *Naturally occurring macrolide-lincosamide-streptogramin B resistance in Bacillus licheniformis.* J Bacteriol, 1981. 145(1): p. 129-37.
81. Hue, K.K. and D.H. Bechhofer, *Regulation of the macrolide-lincosamide-streptogramin B resistance gene ermD.* J Bacteriol, 1992. 174(18): p. 5860-8.
82. Kwak, J.H., E.C. Choi, and B. Weisblum, *Transcriptional attenuation control of ermK, a macrolide-lincosamide-streptogramin B resistance determinant from Bacillus licheniformis.* J Bacteriol, 1991. 173(15): p. 4725-35.
83. Kwon, A.R., et al., *ErmK leader peptide : amino acid sequence critical for induction by erythromycin.* Arch Pharm Res, 2006. 29(12): p. 1154-7.
84. Roberts, M.C., *Update on macrolide-lincosamide-streptogramin, ketolide, and oxazolidinone resistance genes.* FEMS Microbiology Letters, 2008. 282(2): p. 147-159.
85. Kamimiya, S. and B. Weisblum, *Induction of ermSV by 16-membered-ring macrolide antibiotics.* Antimicrob Agents Chemother, 1997. 41(3): p. 530-4.
86. Shimizu, Y., et al., *Cell-free translation reconstituted with purified components.* Nat Biotechnol, 2001. 19(8): p. 751-5.
87. Hartz, D., et al., *Extension inhibition analysis of translation initiation complexes.* Methods Enzymol, 1988. 164: p. 419-25.
88. Varshney, U., C.P. Lee, and U.L. RajBhandary, *Direct analysis of aminoacylation levels of tRNAs in vivo. Application to studying recognition of Escherichia coli initiator tRNA mutants by glutaminyl-tRNA synthetase.* J Biol Chem, 1991. 266(36): p. 24712-8.
89. Schagger, H. and G. von Jagow, *Tricine-sodium dodecyl sulfate-polyacrylamide gel electrophoresis for the separation of proteins in the range from 1 to 100 kDa.* Anal Biochem, 1987. 166(2): p. 368-79.
90. Douthwaite, S., et al., *Defining the structural requirements for a helix in 23 S ribosomal RNA that confers erythromycin resistance.* J Mol Biol, 1989. 209(4): p. 655-65.
91. Asai, T., et al., *Construction and initial characterization of Escherichia coli strains with few or no intact chromosomal rRNA operons.* J Bacteriol, 1999. 181(12): p. 3803-9.
92. Zaporojets, D., S. French, and C.L. Squires, *Products transcribed from rearranged rrn genes of Escherichia coli can assemble to form functional ribosomes.* J Bacteriol, 2003. 185(23): p. 6921-7.
93. Sato, N.S., et al., *Comprehensive genetic selection revealed essential bases in the peptidyl-transferase center.* Proceedings of the National Academy of Sciences, 2006. 103(42): p. 15386-15391.
94. Ohashi, H., et al., *Efficient protein selection based on ribosome display system with purified components.* Biochem Biophys Res Commun, 2007. 352(1): p. 270-6.
95. Matsuoka, M., et al., *Cloning and sequences of inducible and constitutive macrolide resistance genes in Staphylococcus aureus that correspond to an ABC transporter.* FEMS Microbiology Letters, 1999. 181(1): p. 91-100.
96. Kamimiya, S. and B. Weisblum, *Translational attenuation control of ermSF, an inducible resistance determinant encoding rRNA N-methyltransferase from Streptomyces fradiae.* J Bacteriol, 1988. 170(4): p. 1800-11.
97. Shine, J. and L. Dalgarno, *The 3'-terminal sequence of Escherichia coli 16S ribosomal RNA: complementarity to nonsense triplets and ribosome binding sites.* Proc Natl Acad Sci U S A, 1974. 71(4): p. 1342-6.
98. McLaughlin, J.R., C.L. Murray, and J.C. Rabinowitz, *Unique features in the ribosome binding site sequence of the gram-positive Staphylococcus aureus beta-lactamase gene.* J Biol Chem, 1981. 256(21): p. 11283-91.
99. Chang, B., S. Halgamuge, and S.L. Tang, *Analysis of SD sequences in completed microbial genomes: non-SD-led genes are as common as SD-led genes.* Gene, 2006. 373: p. 90-9.
100. Heurgue-Hamard, V., et al., *Origins of minigene-dependent growth inhibition in bacterial cells.* EMBO J, 2000. 19(11): p. 2701-9.

101. Cooper, A.J., N.B. Shoemaker, and A.A. Salyers, *The erythromycin resistance gene from the Bacteroides conjugal transposon Tcr Emr 7853 is nearly identical to ermG from Bacillus sphaericus.* Antimicrob Agents Chemother, 1996. 40(2): p. 506-8.
102. Monod, M., S. Mohan, and D. Dubnau, *Cloning and analysis of ermG, a new macrolide-lincosamide-streptogramin B resistance element from Bacillus sphaericus.* J Bacteriol, 1987. 169(1): p. 340-50.
103. Madsen, C.T., et al., *Methyltransferase Erm(37) slips on rRNA to confer atypical resistance in Mycobacterium tuberculosis.* J Biol Chem, 2005. 280(47): p. 38942-7.
104. Morris, R.P., et al., *Ancestral antibiotic resistance in Mycobacterium tuberculosis.* Proceedings of the National Academy of Sciences of the United States of America, 2005. 102(34): p. 12200-12205.
105. Ramu, H., et al., *Nascent Peptide in the Ribosome Exit Tunnel Affects Functional Properties of the A-Site of the Peptidyl Transferase Center.* Mol Cell, 2011.
106. Douthwaite, S., *Structure-activity relationships of ketolides vs. macrolides.* Clin Microbiol Infect, 2001. 7 Suppl 3: p. 11-7.
107. Schmeing, T.M., et al., *The crystal structure of the ribosome bound to EF-Tu and aminoacyl-tRNA.* Science, 2009. 326(5953): p. 688-94.
108. Mankin, A.S., *Nascent peptide in the "birth canal" of the ribosome.* Trends Biochem Sci, 2006. 31(1): p. 11-3.
109. Bailey, M., T. Chettiath, and A.S. Mankin, *Induction of erm(C) Expression by Noninducing Antibiotics.* Antimicrob Agents Chemother, 2008. 52(3): p. 866-74.
110. Weisblum, B., *Macrolide resistance.* Drug Resist Updat, 1998. 1(1): p. 29-41.
111. Memili, E. and B. Weisblum, *Essential role of endogenously synthesized tylosin for induction of ermSF in Streptomyces fradiae.* Antimicrob Agents Chemother, 1997. 41(5): p. 1203-5.
112. Madsen, C.T., L. Jakobsen, and S. Douthwaite, *Mycobacterium smegmatis Erm(38) is a reluctant dimethyltransferase.* Antimicrob Agents Chemother, 2005. 49(9): p. 3803-9.
113. Ounissi, H. and P. Courvalin, *Nucleotide sequence of the gene ereA encoding the erythromycin esterase in Escherichia coli.* Gene, 1985. 35(3): p. 271-8.
114. Muto, H. and K. Ito, *Peptidyl-prolyl-tRNA at the ribosomal P-site reacts poorly with puromycin.* Biochem Biophys Res Commun, 2008. 366(4): p. 1043-7.
115. Bonnefoy, A., et al., *Ketolides lack inducibility properties of MLS(B) resistance phenotype.* J Antimicrob Chemother, 1997. 40(1): p. 85-90.
116. Green, R., C. Switzer, and H.F. Noller, *Ribosome-catalyzed peptide-bond formation with an A-site substrate covalently linked to 23S ribosomal RNA.* Science, 1998. 280(5361): p. 286-9.
117. Yap, M.N. and H.D. Bernstein, *The plasticity of a translation arrest motif yields insights into nascent polypeptide recognition inside the ribosome tunnel.* Mol Cell, 2009. 34(2): p. 201-11.
118. Tanner, D.R., et al., *Genetic identification of nascent peptides that induce ribosome stalling.* J Biol Chem, 2009.
119. Fahlman, R.P. and O.C. Uhlenbeck, *Contribution of the Esterified Amino Acid to the Binding of Aminoacylated tRNAs to the Ribosomal P- and A-Sitesâ€* Biochemistry, 2004. 43(23): p. 7575-7583.
120. Bashan, A., et al., *Structural basis of the ribosomal machinery for peptide bond formation, translocation, and nascent chain progression.* Mol Cell, 2003. 11(1): p. 91-102.
121. Voorhees, R.M., et al., *Insights into substrate stabilization from snapshots of the peptidyl transferase center of the intact 70S ribosome.* Nat Struct Mol Biol, 2009. 16(5): p. 528-533.
122. Whitford, P.C., et al., *Accommodation of aminoacyl-tRNA into the ribosome involves reversible excursions along multiple pathways.* RNA, 2010. 16(6): p. 1196-204.
123. Fulle, S. and H. Gohlke, *Statics of the ribosomal exit tunnel: implications for cotranslational peptide folding, elongation regulation, and antibiotics binding.* J Mol Biol, 2009. 387(2): p. 502-17.

VITA

NAME: Haripriya Ramu

EDUCATION: B.Pharmacy, J.S.S. College of Pharmacy, affiliated to the Tamil Nadu Dr. M.G.R Medical University, Chennai, Tamil Nadu, India, 2001

M.S., Pharmacognosy, University of Illinois at Chicago, Chicago, Illinois, 2005

Ph.D., Pharmacognosy, Univeristy of Illinois at Chicago, Chicago, Illinois, 2011

AWARDS: Chicago Biomedical Consortium Scholar, 2010

Best Poster Award, American Society for Biochemistry and Molecular Biology, 2009

van Doren Scholar Award for Best Graduate Student, 2009

PUBLICATIONS: Maguire, B.A., Beniaminov, A.D., Ramu, H., Mankin, A.S., and Zimmermann, R.A. (2005). A protein component at the heart of an RNA machine: the importance of protein l27 for the function of the bacterial ribosome. Mol Cell *20*, 427-435.

Ramu, H., Mankin, A., and Vazquez-Laslop, N. (2009). Programmed drug-dependent ribosome stalling. Mol Microbiol *71*, 811-824.

Ramu, H., Vazquez-Laslop, N., Klepacki, D., Dai, Q., Piccirilli, J., Micura, R., and Mankin, A.S. (2011). Nascent peptide in the ribosome exit tunnel affects functional properties of the A-site of the peptidyl transferase center. Mol Cell *41*, 321-330.

Vazquez-Laslop, N., Ramu, H., Klepacki, D., Kannan, K., and Mankin, A.S. (2010). The key function of a conserved and modified rRNA residue in the ribosomal response to the nascent peptide. EMBO J *29*, 3108-3117.

Vazquez-Laslop, N., Klepacki, D., Mulhearn, D., Ramu, H., Krasnykh, O., Franzblau, S., and Mankin, A. (2011). Role of antibiotic ligand in nascent peptide-dependent ribosome stalling. In press.

Vazquez-Laslop, N., Ramu, H., and Mankin, A.S. (2011). Nascent peptide-mediated ribosome stalling promoted by antibiotics (SpringerWien, NewYork). In press.

Subramanian, S., Ramu, H., and Mankin, A.S. (2011). Inducible resistance to macrolide antibiotics. In Antibiotic Drug Discovery and Development, Dougherty TJ, Pucci, M. J. (ed). New York, NY: Springer Publishing Company, In press.